Microbial-based Bioremediation of an Exemplar Organophosphorus Chemical Warfare Agent.

by

Alaa Hassan Radhi Al-Farttoosy

A thesis submitted to the University of Sheffield in fulfilment of the requirement for the degree of Doctor of Philosophy in Chemical and Biological Engineering

The University of Sheffield

Faculty of Engineering

Department Chemical and Biological Engineering

July 2020

DECLARATION OF AUTHENTICITY

I, Alaa Hassan Radhi Al-Farttoosy declare that this thesis is my own work and effort, which was conducted at the University of Sheffield, U.K. This work has not been submitted anywhere for any other degree of qualification.

Alaa Hassan Radhi Al-Farttoosy
July 2020

Acknowledgements

I would like to express my deep thanks and appreciation to both my supervisors Dr Jags Pandhal and Dr Mark D Ogden for their expertise, understanding and patience as well as their huge support and dedication to my project.

I would also like to thanks, Andrew Fairburn, Mark Jones, and James Grinham, Josie-May Whitnear, Duncan Schofield for their assistance and for teaching me nearly all the lab techniques regarding GC-FID. In addition, it is my pleasure to thanks Dr Esther Karunakaran, and Dr Annette F. Taylor in the CBE, and Dr Gabriella Kakony in Kroto Institute-Environmental Engineering Labs. Also many thanks for Dr Joy Mukherjee for helping me in TECAN usage, in addition Dr Seham Moussa for lab help, and James P. Bezzina for his help in kinetic and isotherm study.

I would also like to thank Iraqi Cultural Attaché in London, and Iraqi Ministry of High Education and Scientific Research in Baghdad-Iraq, and the University of Basrah all of those who helped me during my 4 years of study.

Many thanks for my wife Dr. Jenan Al-Sadoon and my lovely daughters Sara and Sally, the love of my life, for her endless patience, love and a huge steadfast support.

Finally, big thanks for my family in Iraq, dad, mom, my siblings, and my grandpa soul for their love and support even from afar.

List of abbreviations and acronyms

iii | P a g e

A.P.G = Arabian-Persian Gulf

Ach = Acetylcholine

Ache = Acetyl cholinesterase

ALE = Adaptive laboratory evolution experiment

AMPP = Aminopeptidase P

ANOVA= Analysis of Variance

BR = bioremediation

BTEX = Xylene

CEC = cation exchange capacity

CNS = Central nervous system

CPDs= Cyclobutane-pyrimidine dimers

CWA = Chemical warfare agents

CWC = Chemical Weapons Convention

DEClP = Diethyl chlorophosphate

DECnP = diethyl pyrophosphate

DEMP = Diethyl methyl phosphonate

DFP = Diisopropylfluorophosphatase

DMMP = Dimethyl methyl phosphonate

DNA = Deoxyribonucleic acid

EMPA= Ethyl methyl Phosphonic acid

EMS = Ethyl methane sulfonate

EPA= Environmental Protection Agency

Eq = Equation

EthBr = Ethidium bromide

EU = European Union

FID = Flame Ionisation Detector

FTIR = Fourier-transform infrared spectroscopy

GA = Tabun

GB = Sarine

GC-FID = Gas chromatography -Flame Ionisation Detector= FID

GC-MS = Gas chromatography mass spectrometry

iii | P a g e

GD = Soman

GE = Ethylsarin OPNAs

GEM = Genetic engineering application of microorganisms

HD = sulfur mustard

HPLC = High performance liquid chromatography

i.m = intramuscular

ICWT = International Chemical Weapons Treaty

L = Lewisite

LB = Luria-Bertani medium

LB = Luria-Bertani

MPD = Mevalonate pyrophosphate decarboxylase

MPH = methyl parathion hydrolase

MPn = Methyl phosphonate

MSM = Mineral Salt Medium

MTBE = Methyl-tertbutyl ether

NAs = Nerve agents

NATO = North Atlantic Treaty Organization

NCBI = National Centre for Biotechnology Information

NTG = N-Nitrosoguanidine

OC = organic content

OPAA = Organophosphorus acid a hydrolase enzyme

OPD = O-phenylene diamine dihydrochloride

Opd = Organophosphorus degrading

OpdA = Organophosphorus acid a hydrolase

OPEs = OP esters

OPH = Organophosphorus hydrolase

OPNAs = Organophosphorus nerve agents

OPs = Organophosphorus compounds or Organophosphates

PAH = Polyaromatic hydrocarbons

PCBs = polychlorinated biphenyls

PCBs = Poly chlorinated biphenyls

PCE = Perchloroethylene

PCP = Pentachlorophenol

PCR = Polymerase chain reaction

PFO = Pseudo first order

PNP = P-nitrophenoyl

POPs = Persistence Organic Pollutants

PSO = Pseudo second order

PTEs = Phosphotriesterase

PTEs = Phosphotriesterase

R2A = Reasoner's 2A agar

RNA = Ribonucleic acid

SDZ = sulfadiazine

SMX = Sulfamethoxazole

SPE = Solid phase extraction

SPME = Solid phase micro extraction

TBP = tributyl phosphate

TCE = trichloroethylene

TEPO = triethyl phosphine-oxide

TNT = trinitrotoluene

UK = United Kingdom

UVR = Ultraviolet radiation

VC = Vinyl chloride

VR = nerve agent (Russian VX, Soviet V-gas, Substance 33, R-33, Agent "November")

VX = nerve agent a neurotoxic chemical warfare agent

WWI = First World War

WWII = Second World War

List of contents

List of Figures

List of Tables

List of Schemes

Abstract

A variety of chemical warfare agents (CWAs) and pesticides are organophosphorus compounds with high levels of toxic activity. Organophosphorus compounds (OPs) are characterised by a C-P bond that makes them hydrolytically stable and chemically inert; therefore their use in the environment leads to contaminated soils and aquatic systems. This study focused on developing a bioremediation strategy to address the detoxification of an exemplar organophosphorus compound, Diethyl methyl phosphonate (DEMP). Initially, an assessment of DEMP stability in soil and water was undertaken. DEMP behaviour in soil was subjected to a pseudo-second order with a rate constant of 1.04 min^{-1}. The Langmuir model KL 0.14 L g^{-1} of DEMP data was a better fit than the Freundlich model in the soil column. This suggested that DEMP was adsorbed by a saturated monolayer of soil. The hydrolysis mechanism of DEMP in buffer solutions suggested that DEMP was pH and temperature dependent, where the half-life decreased by increasing the temperature and pH. A bacterial consortium was enriched from soil where organophosphorus compounds have regularly been used, and it was adapted long-term to use DEMP as a carbon and phosphorus source. The results suggested that the long-term adaptation enhanced bacterial growth by 250%. After 21 days, the consortium could degrade 100 mg L^{-1} DEMP by 93.4% in Minimal Salts Medium and 85.7% in the Minimal Salts Medium without phosphorus, compared to 55.4% DEMP hydrolysis. Three bacterial isolates with DEMP degradation capability were identified from the consortia as *Bacillus cereus, Micrococcus luteus,* and *Dermacoccus nishinomiyaensis*. Moreover, both *B. cereus* and *M. luteus* were shown to be able to degrade two different OPs compounds: triethyl phosphine-oxide, and tributyl phosphate. Over 21 days, the *B.* cereus reduced 100 mg L^{-1} TEPO to 6.33 mg L^{-1}, and 100 mg L^{-1} TBP to 5.66 mg L^{-1}, while the *M. luteus* reduced 100 mg L^{-1} TEPO and TBP into 7.33 and 4.33 mg L^{-1} respectively. *B cereus* was exposed to random mutagenesis and selection, showing an improved growth rate to 0.38 $days^{-1}$ compared to 0.32 $days^{-1}$ of the wild-type strain (WT), and achieved a higher DEMP degradation rate over 12 days 95.1%, compared to 91.6% in the wild type.

Chapter I

1. Introduction

This chapter introduces chemical warfare agents in terms of historical use and the associated environmental consequences. It then discusses the different applications that have been used to dispose of CWA munitions, as well as their concentrations in water and soil. Finally, the aims and structure of the thesis are given.

1.1 Organophosphorus compounds

Chemical warfare agents (CWAs) are a type of OPs compounds with high levels of toxic activity (Gao et al. 2013). They represent the most significant group of weapons of mass destruction, utilised for their properties to kill, incapacitate or injure enemies during fighting. In recent years, the use of CWAs in wars and terrorist attacks has been widely documented across the world (Chauhan et al. 2008).

1.2 Historical Overview

Chemical warfare agents have been produced for over 100 years. Historically, a team at the Catholic University in Washington, DC produced the first blister agent called Lewisite (L) in 1918. It has a fast effect compared to the blister agent sulphur mustard gas (HD). However, since 1918, evidence has indicated the use of chemical warfare during military fighting, for example, phosgene ($COCl_2$) and HD were sent from Britain in 1919 to use along India's borders (Coleman, 2005). Of further historical importance is that chlorine (Cl_2), phosgene ($COCl_2$) and HD were the first CWAs used in the First World War (WWI).

Despite the pledge by many countries in the Geneva Protocol of 1925, not to use these substances, (Department of Defense, 1998), except for scientific research, countries did not stop their use and many lethal agents were developed by German scientists during the Second World War (WWII). In 1936, a German scientist discovered the first nerve agent, Tabun (GA). By WWII, Germany had developed CWAs to include the G-group and the V-group. The former, called nerve agents (NAs), includes Tabun (North Atlantic Treaty Organization [NATO] that designed GA) and sarin (GB), Soman (GD) while, the V-group includes VX and VR (Benschop and De Jong, 1988; Talbot et al. 2008).

The Italians used HD during the war between 1936 and 1937 on the Abyssinians in Ethiopia. Additionally, it was used in 1963-1967 during the civilian war in Yemen. Furthermore, many allegations showed that HD was extensively used in South East Asian conflicts (D'Agostino and Chenier, 2006). During the Iran-Iraq war in the 1980s, HD and GA were also used (Balali-Mood and Saber, 2012). Then, 100,000 soldiers were injured and more than 5,000 were killed. In addition, Halabja is an Iraqi Kurdish village that was exposed to a chemical attack at the end of 1988. This caused many deaths, approximately 10% of the population.

CWAs have not only been used in military operations, but also in the terrorist attacks. The Aum Shinrikyo cult used GB on Japan's Tokyo subway system in 1995 (Tu, 1996). In the modern era, OP nerve agents (OPNAs) were used in Syria in 2013 (Pita and Domingo, 2014), and more recently the Novichok agent was used in the UK in an alleged attempted political assassination of the Russian dissident Sergei Skripal and his daughter Yulia in 2018 (Chai et al. 2018).

1.3 General Introduction

Synthetic OPs have a similarity with CWAs in the chemical structure and functional group. This facilitates their use in different fields, such as pesticides in agriculture (Grey et al. 2006), medicine as ophthalmic agents (isoflurophate, echothiophate) and moreover, in the detergent and air-fuel industries owing to their physical and biological characteristics (Adelowo, 2012). Furthermore, there is global use of OP esters (OPEs), in particular, triesters which are flame-retardants, plasticizers and to produce or enhance textiles, furniture, plastics, and other materials. This extensive usage resulted from the increasing bans on brominated diphenyl ethers as flame-retardants, and their problems due to being spread in air, water, and airborne particulate matter (Reemtsma et al. 2008).

CWAs represent a huge group of chemicals with a stockpile that is estimated at 200,000 tons (Singh, 2009). In the US alone, there are 28,000 tons with a stockpile of OPs CWAs, mostly GB, VX, and HD (Blackwood, 1998). Based on the International Chemical Weapons Treaty (ICWT), these munitions must be destroyed within 10 years (Singh and Walker, 2006). The disposal of these banned chemicals has been undertaken using *Ex*-situ techniques, such as incineration (Leung, 2004) or dumped in the Baltic Sea after WWII (Glasby, 1997; Pearson and Magee, 2002). However, these methods have implications for air pollution and cost. Meanwhile the disposal of CWAs concentrations from the environment by using various applications, for instance phytoremediation or bioremediation methods (Zhang et al., 1999; Koptsik, 2014).

The first important step in evaluating the fate of OP xenobiotics in the environment is to determine the hydrolysis rate. This step mainly depends on the pH of water, which plays a major role in the OPs breakdown (Thuyet et al. 2012). The hydrolysis reactions result in various metabolite products that can be degraded by different microorganisms. For this reason, bioremediation (BR) using microorganisms, can be more favourable, cheaper, more effective,

and an even a faster method compared to chemical and physical applications in the degradation of these different substances (Bonaventura and Johnson, 1997).

Many studies have reported the importance of BR in removing pollutants from the environment. BR has been significant in cleaning soil contaminated with trinitrotoluene (TNT), pesticides, or radioactive compounds such as uranium (Glick, 2003). A number of studies were carried out to remove CWAs from soil and water (Yang et al. 1992; Raber and McGuire, 2002).

An organism, identified as *Klebsiella aerogenes* by Imazu et al. (1998), has the ability to degrade several substances like methyl phosphonate or amino methyl phosphonate to gain a phosphorus source. The study of biodegradation focuses on the enzymatic degradation (Cheng et al, 1993). In this field, Hoskin et al., (1995) and Ohmori et al., (2013) revealed that the enzyme organophosphorus hydrolase (*oph*) degraded VX and GB, which are sourced from *Pseudomonas diminuta* and *Sphingobium fuliginis*, respectively. Other studies have found that organophosphorus acid anhydrase (*opaa*), which is released from *Alteromonas sp*. and *A. haloplanktis*, can degrade cyclo-sarin (GF) (Harvey et al. 2005). In addition, *A. undina* can degrade GA and GD (Cheng et al. 1993).

Diethyl methyl phosphonate (O, O-diethyl methyl phosphonate, DEMP) is an OP compound that can simulate the nerve gas sarin (Garach-Domech et al. 2002) (Fig. 1-1). This compound is therefore used as an exemplar CWA in this thesis, where the methodology to discover and optimise the biodegradation capability of environmental microbes is demonstrated. There is no information on the fate or biodegradation of DEMP therefore, this study is considered the first report of its biodegradation.
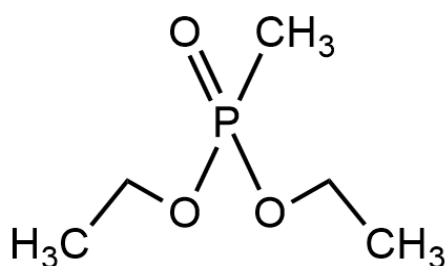
Fig. 1-**1** Chemical structure of Diethyl methyl phosphonate (DEMP).

To date, there is very little information available on DEMP in terms of chemical degradation. Neither is the information available specifically on the environmental fate or biodegradation. An approach to tackle this challenging problem is presented within this thesis, where the aim is to develop a strategy to isolate, optimise and utilise a novel soil microorganism that is capable of rapidly destroying DEMP, thereby demonstrating how the same methodology could be applied to target real CWAs. To achieve this, the environmental fate of DEMP is investigated through abiotic methods, such as chemical behaviour in soil relevant parameters, and hydrolysis in aqueous. Once 'benchmarked', a methodology is applied to degrade DEMP biologically.

1.4   Thesis Objectives

This research seeks to demonstrate how microorganisms with the native capability to degrade OP compounds can be isolated from the environment, and subsequently optimised through strain engineering. To achieve this, an exemplar OP called DEMP was used and initially its chemical degradation characterised. Therefore, the research can be considered as being divided into two distinct parts: chemical process characterisation and biological process characterisation.

1.4.1 Chemical Process Characterisation

The aims of this section are to determine the potential behaviour of DEMP in soil and water, and to estimate the time required for its degradation. The specific objectives are to:-

1. Investigate the adsorption behaviour of DEMP in soil to evaluate whether DEMP will be adsorbed onto the surface of soil, affecting bacterial biodegradation rates. Moreover, these parameters provide information about potential rates of ground-water contamination.

2. Determine the reaction rate of DEMP hydrolysis in aqueous samples in order to characterise the breakdown mechanisms and rates. This analysis provides a benchmark for comparing biological routes to degradation.

1.4.2 Biological Process Characterisation

This part of the thesis presents work with the aim of identifying and characterising microbial based biodegradation of DEMP. The specific objectives are to:-

1. Enrich DEMP-degrading microorganisms present within soil samples as a consortium and also as individual isolates. The objective is obtaining organisms (mostly bacteria) that can utilise DEMP as a source of carbon and/or phosphorus.
2. Characterise the kinetic biodegradation rates of DEMP using bacterial isolates and a consortium, including the impact of additional carbon and phosphorus sources.
3. Characterise DEMP-degrading isolate growth rates (individual isolates and as a community matrix).
4. Assess the capability of bacterial isolates to degrade different OP compounds, triethyl phosphine-oxide (TEPO) and tributyl phosphate (TBP), which have a different structure to DEMP. This should facilitate understanding of whether the feature of biodegradation can be extended to include other OPs.
5. Apply strain engineering by random mutagenesis to increase rates of DEMP degradation.
6. Identify the gene encoding for the OP-degrading enzyme in the bacterial strains capable of DEMP-degradation.
7. Design a Morbidostat device to use in the optimisation of bacterial consortia or individual bacteria for DEMP degradation. This device provides all the necessary circumstances to evolve bacteria to ascertain the real time when bacteria start to resist the certain compound, which allows raising the concentration to keep bacteria under the enforced environmental pressure.

1.5 Chapter Outlines

This thesis has seven chapters.

- Chapter 2 is a literature review that aims to define the importance of OP compounds, particularly chemical warfare agents in the environment, in terms of their toxicity, spread, classification and how to remove them from the environment by using chemical, physical and biological applications. In addition, it seeks to determine their different pathways under different environmental conditions.

- Chapter 3 focuses on the sorption behaviour of DEMP in local soil using the soil column. Additionally, this chapter is an investigation into the chemical processes which are able to degrade DEMP under different temperatures and pH conditions. This chapter is a benchmark to demonstrate the importance of developing a biological strategy for degradation of DEMP.

- Chapter 4 reports on utilising soil, which historically has high levels of OP compounds and enriching it with bacteria capable of using DEMP as a carbon or phosphorus source. Further adaptation in the presence of DEMP in the mineral salt media is then undertaken to further refine the bacterial community. Then, this study investigates the capability of the bacterial community to use DEMP as a carbon and phosphorus source. Consequently, this step leads to identifying which microorganisms are in the community, and their ability to use DEMP, whether they are used as an individual organism or as consortia. To extend the study, the ability of individual organisms to degrade two different OP compounds, TEPO and TBP, is examined, which have different chemical bonds compared to DEMP.

- Chapter 5 aims to increase the bacterial performance in DEMP degradation through exposing the wild-type bacterium to the random mutagenesis, which are UV radiation (UVR) as a physical factor as well as chemical factors like ethidium bromide (EthBr), followed by selecting a superior mutant strain that utilises DEMP as a sole carbon and/or phosphorus form.

- Chapter 6 reports on constructing the device called 'Morbidostat' in order to use it in the adaptation process of bacteria versus chemical compounds. This device enables

researchers to ascertain the exact point at which bacteria start to become resistant to the chemical substance to increase the chemical concentration to keep bacteria under the biochemical pressure. Moreover, this device could be used to monitor bacterial growth via computer software called 'CoolTerm'.

- Chapter 7 is the final chapter that will summarise this thesis and offer suggestions for future work.

1.6 References

Adelowo, F. E. (2012) 'Synthesis , Characterization and Fungicidal Activity of Some Dialkyl Alkylphosphonates and Dialkyl Phenylphosphonates', *Ijrras*, 12(July), pp. 107–114.

Balali-Mood, M. and Saber, H. (2012) 'Recent advances in the treatment of organophosphorous poisonings', *Iranian Journal of Medical Sciences*, 37(2), pp. 74–91.

Benschop, H. P. and De Jong, L. P. A. (1988) 'Nerve Agent Stereoisomers: Analysis, Isolation, and Toxicology', *Accounts of Chemical Research*, 21(10), pp. 368–374.

Blackwood Jr, M. E. (1998) 'Beyond the chemical weapons stockpile: {The} challenge of non-stockpile materiel', *Arms Control Today*, 28(5), pp. 10–15.

Bonaventura, C. and Johnson, F. M. (1997) 'Healthy environments for healthy people: Bioremediation today and tomorrow', *Environmental Health Perspectives*, 105(SUPPL. 1), pp. 5–20.

Chai, P. R., Hayes, B. D., Erickson, T. B., Boyer, E. W. (2018) 'Novichok agents: a historical, current, and toxicological perspective', *Toxicology Communications*. Taylor & Francis, 2(1), pp. 45–48.

Chauhan, S., Chauhan, S., D'Cruz, R., Faruqi, S., Singh, K.K., Varma, S., Singh, M., Karthik, V. (2008) 'Chemical warfare agents', *Environmental Toxicology and Pharmacology*, 26(2), pp. 113–122.

Cheng, T. C., Harvey, S. P. and Stroup, A. N. (1993) 'Purification and properties of a highly active organophosphorus acid anhydrolase from Alteromonas undina', *Applied and Environmental Microbiology*, 59(9), pp. 3138–3140.

Coleman, K. (2005). A History of Chemical Warfare. Antony Rowe Ltd, Chippenham and Eastbourne, PP: 198.

D'Agostino, P. a. and Chenier, C. L. (2006) 'Analysis of Chemical Warfare Agents: General Overview , LC-MS Review , In- House LC-ESI-MS Methods and Open Literature Bibliography', (March), pp. 1–76.

Department of Defense (1998) 'The Militarily Critical Technologies List', This document was prepared by the Office of the Under Secretary of Defense for Acquisition and Technology Washington, D.C. MCTL Internet Home *Page: http://www.dtic.mil/mctl*, (February), PP. II-D-5

Gao, X., Lin, H., Ray, R., Ray, P. (2013)Toxicogenomic studies of human neural cells following exposure to organophosphorus chemical warfare nerve agent VX', *Neurochemical Research*, 38(5), pp. 916–934.

Garach-Domech, A., Rock, D., Sandhu, G., Russel, J., McHugh, M.A., MacIver, B.K. (2002) 'Phase behavior of diethyl methylphosphonate and 2-chloroethyl methyl sulfide in supercritical carbon dioxide', *Journal of Chemical and Engineering Data*, 47(4), pp. 984–986.

Glasby, G. P. (1997) 'Disposal of chemical weapons in the Baltic Sea', *Science of the Total Environment*, 206(2–3), pp. 267–273.

Glick, B. R. (2003) 'Phytoremediation: Synergistic use of plants and bacteria to clean up the environment', *Biotechnology Advances*, 21(5), pp. 383–393.

Grey, C. N. B., Nieuwenhuijsen, M. J. and Golding, J. (2006) 'Use and storage of domestic pesticides in the UK', *Science of the Total Environment*, 368(2–3), pp. 465–470.

Harvey, S. P., Kolakowski, J. E., Cheng, T. C., Rastogi, V. K., Reiff, L. P., DeFrank, J. J., Raushel, F. M., Hill, C. (2005) 'Stereospecificity in the enzymatic hydrolysis of cyclosarin (GF)', *Enzyme and Microbial Technology*, 37(5), pp. 547–555.

Hoskin, F. C., Walker, J. E., Dettbarn, W. D., Wild, J. R. (1995) 'Hydrolysis of tetriso by an enzyme derived from Pseudomonas diminuta as a model for the detoxication of O-ethyl S-(2-diisopropylaminoethyl) methylphosphonothiolate (VX)', *Biochemical Pharmacology*, 49(5), pp. 711–715.

Imazu, K., Tanaka, S., Kuroda, A., Anbe, Y., Kato, J., Ohtake, H. (1998) 'Enhanced utilization of phosphonate and phosphite by Klebsiella aerogenes', *Applied and Environmental Microbiology*, 64(10), pp. 3754–3758.

Koptsik, G. N. (2014) 'Problems and prospects concerning the phytoremediation of heavy metal polluted soils: A review', *Eurasian Soil Science*, 47(9), pp. 923–939.

Leung, M. (2004) 'Bioremediation: techniques for cleaning up a mess', *Journal of Biotechnology*, 2, pp. 18–22. Available at: http://bioteach.ubc.ca/Journal/V02I01/bioremediation.pdf.

Ohmori, T., Kawahara, K., Nakayama, K., Shioda, A., Ishikawa, S., Kanamori-Kataoka, M., Kishi, S., Komano, A., Seto, Y. (2013) 'Decontamination of nerve agents by immobilized organophosphorus hydrolase', *Forensic Toxicology*, 31(1), pp. 37–43.

Pearson, G. S., and Magee, R. S. (2002). Working party on evaluation of proven chemical weapon destruction, Critical Evaluation of proven chemical weapon destruction technologies (IUPAC Technical Report). Pure Appl. Chem., Vol. 74, No. 2, pp. 187–316.

Pita, R. and Domingo, J. (2014) 'The Use of Chemical Weapons in the Syrian Conflict', *Toxics*, 2(3), pp. 391–402.

Raber, E. and McGuire, R. (2002) 'Oxidative decontamination of chemical and biological warfare agents using L-Gel', *Journal of Hazardous Materials*, 93(3), pp. 339–352.

Reemtsma, T., García-López, M., Rodríguez, I., Quintana, J. B., Rodil, R. (2008) 'Organophosphorus flame retardants and plasticizers in water and air I. Occurrence and fate', *TrAC - Trends in Analytical Chemistry*, 27(9), pp. 727–737.

Singh, B. K. (2009) 'Organophosphorus-degrading bacteria: ecology and industrial applications.', *Nature Reviews Microbiology*, 7(2), pp. 156–164.

Singh, B. K. and Walker, A. (2006) 'Microbial degradation of organophosphorus compounds', *FEMS Microbiology Reviews*, 30(3), pp. 428–471.

Talbot, T. B., Lukey, B. and Platoff, G. E. (2008) 'Chapter 01: Introduction to the Chemical Threat', *Medical Aspects of Chemical Warfare*, pp. 1–8.

Thuyet, D. Q., Watanabe, H., Takagi, K., Yamazaki, K., Nhung, D. T. T. (2012) 'Behavior of nursery-box-applied imidacloprid in micro paddy lysimeter', *Journal of Pesticide Science*, 37(1), pp. 20–27.

Tu, A. T. (1996) 'Biological Mass Spectrometry. Basic Information on Nerve Gas and the Use of Sarin by Aum Shinrikyo. Plenary Lecture at the Biological Mass Spectrometry Conference Seto, Aichi, Japan July 3-6, 1995.', *Journal of the Mass Spectrometry Society of Japan*, pp. 293–320.

Yang, Y. C., Baker, J. A. and Ward, J. R. (1992) 'Decontamination of Chemical Warfare Agents', *Chemical Reviews*, 92(8), pp. 1729–1743.

Zhang, Y., Autenrieth, R. L., Bonner, J. S., Harvey, S. P., Wild, J. R. (1999) 'Biodegradation of neutralized sarin', *Biotechnology and Bioengineering*, 64(2), pp. 221–231.

2. Literature Review

This chapter is a literature review, which looks at the importance of organophosphorus compounds, their structure, mechanism of toxicity, health effects, classification, elimination from the environment, and the challenge of measuring organophosphorus compound degradation kinetics in soil.

2.1 Introduction

OPs are a large synthetic group of chemicals resulting from alcohol and phosphoric acid reaction. In the 1930s, OPs were used as insecticides for crop protection and public health before the German military developed them in WWI as chemical warfare agents (CWAs) (neurotoxins) (Ghorab and Khalil, 2015) to inhibit the acetylcholine esterase (AchE) in mammals (Banks and Lein, 2012). It has been estimated that more than 100,000 CWAs are controlled by the Chemical Weapons Convention (CWC), while the database indicates that the actual number is in thousands (Ganesan and Vijayaraghavan, 2010). In contrast, the number of OP insecticides sales was approximately 34% of global OP sales (Singh and Walker, 2006).

The general structure consists of an active group of phosphorus that is connected by a double bond with terminal oxygen or sulphur atoms to form the phosphoryl group (Fig. 2-1). R1 and R2 represent an aryl or alkyl group. They are lipophilic groups and directly bonded to phosphorus atoms forming phosphinates or to oxygen or sulphur atoms forming phosphates or phosphorothioates. In addition, the X group is called a leaving group; it leaves as a result of hydrolysis of its ester bonds (Elersek and Filipic, 2011).

OPs compounds are related to the pentavalent group. Therefore, they could be used as CWAs like nerve gas agents, which include Tabun (GA), sarin (GB), soman (GD), and VX (Fig. 2-2); botch or blister agents, such as Lewisite (L) and mustard gas (HD) (Fig. 2-3) (Abou-Donia 2003). Additionally, OPs can be applied as pesticides, for example, chlorpyrifos, diazinon, parathion, and dimethoate (Fig. 2-4). The physicochemical features of OPs are viscous oils, which can be soluble in organic solvents and tend to be steady in high air temperatures (Feng, 2012).
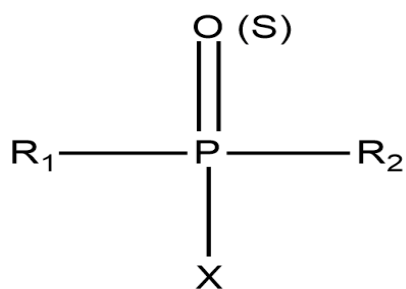
Fig. 2-**1** The general structure of OPs compounds.

(GA)

(GB)

(GD)

(VX)
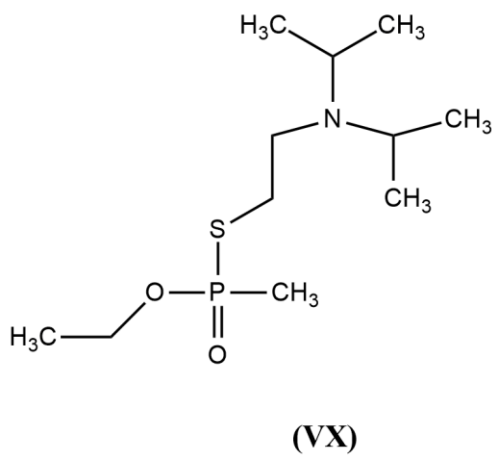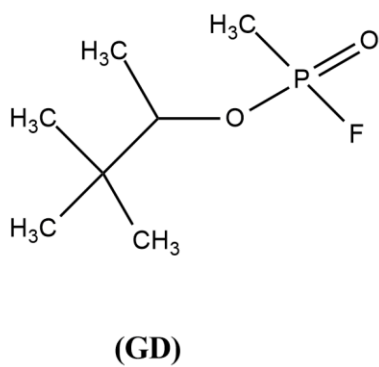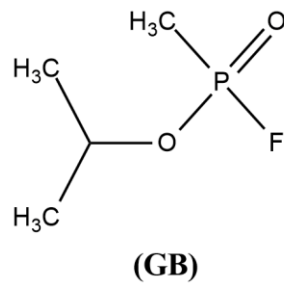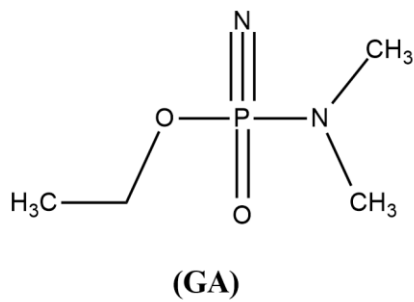
Fig. 2-2 The chemical structure of nerve gas.

(L)

(HD)
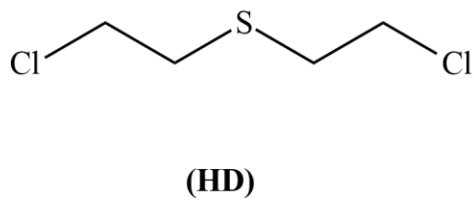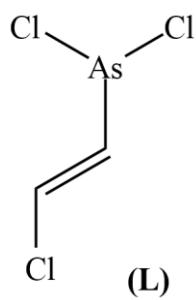
Fig. 2-3 The chemical structure of blister agents.
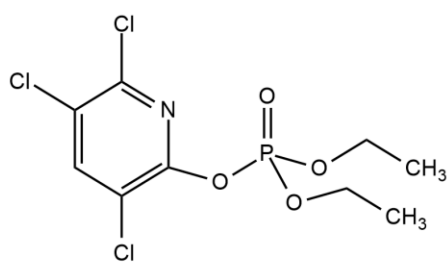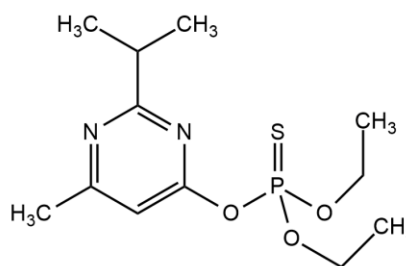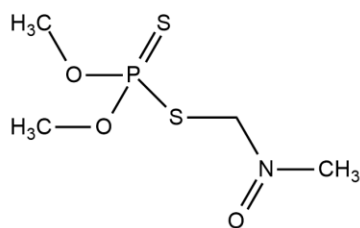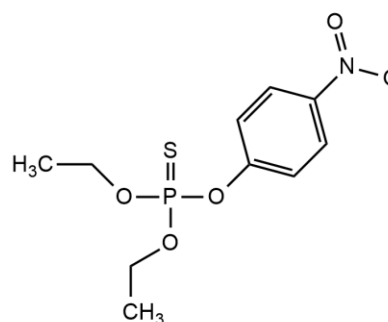
Fig. 2-4 Four examples of OPs pesticides.

2.1.1 Chemical warfare agents and their classification

CWAs possess various features being classified into different classes of substances. They are classified based on their chemical structure into OPs, organoflur, organofluorine compounds, and arsenicals. The second classification relies on their persistence in the environment. This includes persistent agents (non-volatile) like VX and HD; non-persistent agents (volatile) such as chlorine, phosphogen and hydrogen cyanide. The volatile agents tend to evaporate quickly and disperse compared to non-volatile agents (López-Muñoz et al., 2008).

In addition, CWAs are also classified according to their physiological effects on humans. Trap and Van Der Schans (2007) and Smart (1997) divided CWAs used in warfare as follows: nerve agents (e.g. sarin, soman, tabun and VX), vesicants or blistering agents (e.g. mustard gas, Lewisite), blood agents (e.g. carcinogens), choking agents (e.g. pulmonary), riot-control agents (tear gases), psychomimetic agents, and toxins.

The main problem with using OPs is soil, groundwater and sediment pollution. Furthermore, CWAs represent the current challenge to our communities due to the increased use of these toxic compounds by terrorist groups (Worek et al., 2016).

2.2 Organophosphorus compounds

2.2.1 Importance of Phosphorus atom

There are two useful roles for a phosphorus atom. Firstly, it can contribute to forming new compounds, owing to its ability to bond with various elements (Fig. 2-5). Secondly, phosphorus has an empty d-orbital, which easily receives electrons of ideal donors (Haddon, 1985). Consequently, OPs can be divided into many groups: phosphates, phosphonates, phosphinates, phosphorothioates, phosphorodithioates, phosphorotrithioates, and phosphoroamidothioates (Gupta, 2006).
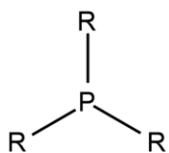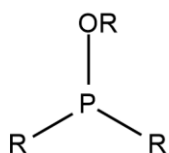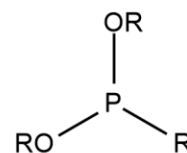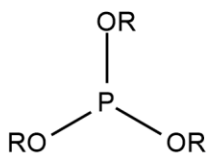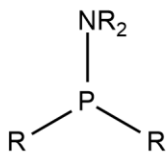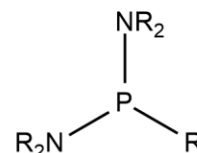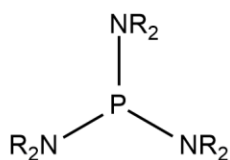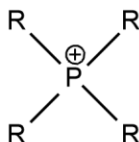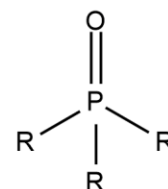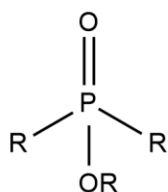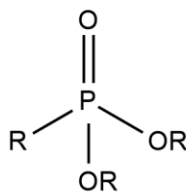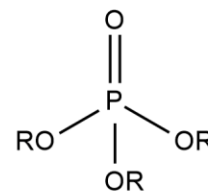
Fig. 2-5 Various example of OPs compound chemical structures (Gupta, 2006).

2.2.2 Toxicity and health effect of OPs to human

Toxicity is the ability of a chemical substance to cause an inherent toxic reaction or illness or death. This parameter can be evaluated in toxicological laboratories, using the common quantitative expression called lethal concentration or lethal dose (LC_{50} or LD_{50}), which kills 50% of testing animals (Frank and Ottobni, 2011). The observation of chemical toxicity could be performed through the examining the capability of a substance during the accidental exposure, studying in vivo and in vitro using cells or animals (Parasuraman, 2011).

Humans are exposed to OPs through three routes; inhaled, absorption by the skin and ingestion. Exposure is considered deleterious and can cause illness or very often death. Perhaps the most serious effects of these chemical compounds on human health are: teratogenic, delayed neuropathic, mutagenic, carcinogenic, cytogenetic effects, immune toxicity, and immune suppression, they can also affect lipid metabolism (De Meyer and De Plaen, 1984; Ghorab and Khalil, 2015).

However, the exposure period of the empirical animals to chemical substances can be categorised into four groups: acute, subacute, chronic, and subchronic. Acute toxicity can occur during inhalation, leading to the death within less than 24 hours, usually 4 hours, while subacute takes 1 month or less. However, subchronic and chronic, require 1-3 months and more than 3 months, respectively (Klaassen, 2019).

Accordingly, it is important to determine the toxicity of chemical substances to understand their mode of action and hazards (Arome and Chinedu, 2014). This is because the toxicity of a chemical in the environment not only depends on concentrations, but also on its bioavailability (Ali and Khan 2017). Although CWAs have not long persisted in the environment, they are highly poisonous. Hence, many studies have been carried out to determine their toxicity to humans using rats as animal models.

Bide et al. (2005) examined the toxicity of GB on humans via inhalation using exposure periods ranging from 1-30 mins, and the concentration (LCt_{01}, LCt_{05}, LCt_{50} and LCt_{95}). The study revealed that the toxicity of GB to a 70 kg human breathing 15 min^{-1} for LCt_{01}, LCt_{05}, LCt_{50}

and LCt_{95} and exposure time of 2, 10, and 30 mins were 11, 16, 36 and 83; 18, 25, 57 and 132 and 24, 34, 79 and 182 mg min m^{-3} respectively. Misik et al. (2015) studied the acute toxicity of CWAs in rats using a median lethal dose (LD_{50}, mg kg^{-1}). The results were the LD_{50} of VX toxicity between 0.0082 to 1.402 mg kg^{-1} via an intramuscular (i.m.). Furthermore, the LD_{50} of soman (GF) was 0.069 mg kg^{-1}, and sarin GB 117.9 mg kg^{-1} i.m. Li et al. (2016) reported that Arsenicals (a type of CWAs) is a toxic compound that can cause acute and chronic toxicity. Moreover, the exposure to Lewisite (L), which is a synthetic chemical weapon used during WWI, led to blistering damage to the skin, lungs, and eyes with painful inflammation.

Consequently, most recent studies have focused on reducing the use of organophosphorus compounds, whether as CWAs or pesticides, as a result of their acute toxicity. Furthermore, the CWC bans the usage of CWAs due to the high risks generated from their distribution in the environment, or that might be accumulated in humans. Thus, the current study aims to demonstrate a strategy for developing a bioremediation process of an exemplar OP compound called DEMP.

2.2.3 Mechanism of OPs toxicity

Neurotransmission is an essential process occurring in the central nervous system (CNS) in both invertebrates and mammals. This process occurs at the site called synapses, where the pre-synaptic terminal and the post-synaptic dendrite or cell body connect. In the exocytosis process, the pre-synaptic vesicles release neurotransmitters into the synaptic cleft due to chemical, electrical, or physical triggers. Eventually, the infused neurotransmitter blocks the postsynaptic receptors in the synaptic cleft, delivering the information to the target tissue or organ (Bean, 2007).

Colovic et al. (2013) define neurotransmission as the process of hydrolysing the Acetylcholine (Ach) into acetic acid and choline. This process is crucial since it permits neurotransmission in the central nervous system of humans and mammals (Eq. 2-1).

$$H_3C\overset{\underset{\displaystyle CH_3}{\big|}}{\overset{\displaystyle \overset{CH_3}{\big|}}{N^+}}\!-\!CH_2CH_2O\overset{O}{\overset{\|}{C}}CH_3 \xrightarrow[\;H_2O\;]{AchE} H_3C\overset{\underset{\displaystyle CH_3}{\big|}}{\overset{\displaystyle \overset{CH_3}{\big|}}{N^+}}\!-\!CH_2CH_2OH \; + \; CH_3\overset{O}{\overset{\|}{C}}\!-\!OH$$

Acetyl choline (Ach) Choline Acetic acid
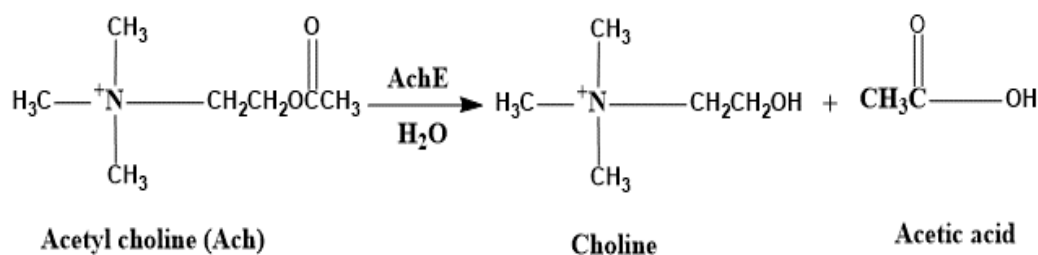
Eq. 2.1.

Acetylcholine Esterase (AchE) is a biological enzyme that exists in the brain of humans and mammals. Additionally, the membranes of red blood cells that are available in various forms enable it to catalyse the Ach (Krsti et al., 2013). This enzyme suffers from inhibition (Fig. 2-6) because Oxon OPs bind the site of action of the AchE, which leads to accumulating the neurotransmission Ach at cholinergic receptor sites (Bocquené and Galgani 1998; Apilux et al. 2015), thereby resulting in strong hyper-stimulation of muscles (Topczewski and Quinn, 2013; Dianyi, 2010).

Furthermore, another impact on the inhibition of AchE is that Ach accumulates in the ganglion of the autonomic nervous system, adrenal medulla, the sympathetic nervous system, skeletal neuromuscular junctions, and the synapses of the brain (Kamanyire and Karalliedde, 2004). Likewise, GA, GB, GD, and VR have a fundamental toxicity for mammals, resulting from their chemical isopropyl-containing oxons and physically volatile properties (Lee, 2003).

However, pentavalent, tetra coordinates compounds act as anticholinesterase organophosphates, which involves an oxygen atom and three singly bonded substituents. It can bond to the central phosphorus atom of the nerve agents. Consequently, they are inhibited in the serine proteases and serine esterases. In addition, they highly resemble AchE (Chambers and Oppenheimer 2004).

ENZ Active Enzyme + OP with leaving group (-X) → Inactive organophosphorylated enzyme → ageing, H₂O

Hydrolysis → ENZ reactivated enzyme
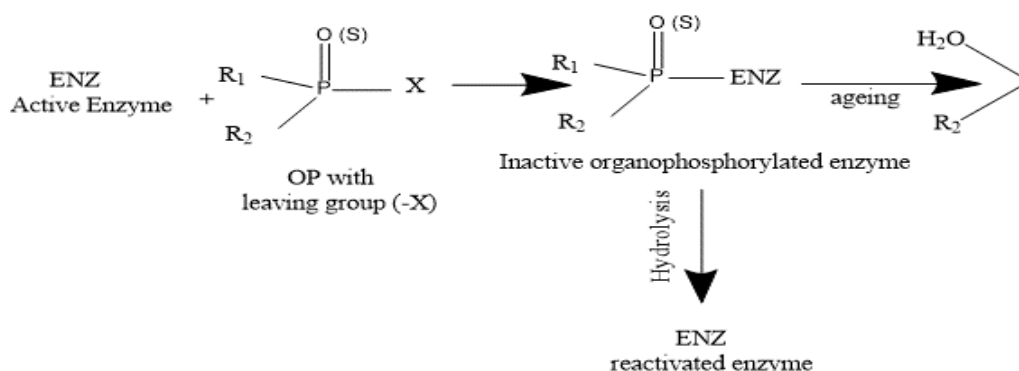
Fig. 2-6 Inhibition of acetyl cholinesterase by OPs compounds.

2.3 Remediation of OPs

To clean the environment from persistent compounds, two different remediation approaches have been used, *Ex-situ* and *In-situ*. The former could be applied through the extraction of polluted media (e.g. soil or water) and then transferred to a treatment plant. The *In-situ* remediation option can be implemented on the same lands or aquifers that are contaminated. In this case, the method does not need the contaminants to be extracted and transported to another location for treatment, potentially reducing costs.

However, both methods have advantages and disadvantages. *In-situ* downsides are that it is less efficient with respect to removing the pollutants compared with the *Ex-situ*. However, *In-situ* has been more widely applied than *Ex-situ* due to *Ex-situ* increasing the cost of remediation owing to the extraction process of the polluted soil and the exposure of workers to the deleterious effects of extracting contaminants (Leung, 2004; Kuppusamy et al., 2016). Moreover, implementation of the *In-situ* approach is easier in terms of adding the necessary nutrients to stimulate the indigenous organisms to utilise the compounds that exist at the site and achieve great progress (McLean and Bledsoe, 1992).

2.3.1 Physical and chemical treatment

Persistent organic pollutants (POPs), are contaminants that can spread, persist, and biomagnify in the food chain, human bodies, and wildlife animal tissue. Additionally, their potential toxicity has resulted in many countries banning their use or production (Ee et al., 2005). However, some POPs, like CWAs or pesticides, are still used and found in the environment. This leads to more harmful effects not only for humans or animals, but also to other biota (Romeh and Hendawi, 2014).

A common physical treatment is incineration. It provides a combustion chamber, which is able to completely destroy pollutants. This room is supplied with electrostatic filters and scrubbers to reduce the harmful emissions, which must not exceed 180 milligrams per Dry Standard Cubic Meter (mg/DSCM) (Ferguson and Wilkinson, 1984).

The incineration process essentially depends on heat and oxygen to generate combustion, resulting in oxidising the compounds. This treatment has been extensively applied to remediate

pesticides (Nadeau et al., 1993). The incineration process involves using high temperatures, for example, to 1315.5°C, and between 982.2-1093.3°C in the combustion room and 1093.3-1260°C for a short time (Lauer, 1964) to destroy the pollutant entirely. At the end of this process, an ash will be produced.

Incineration is an important procedure that can be used to dispose of pollutants in landfill, particularly in the European Union (EU). Moreover, it has been considered a good option regardless of the high costs (Rabl and Spadaro, 2008). However, it was uncontrolled in the 1990s, despite the numerous strict measures that were set to reduce air pollution from emissions, in the EU and the UK. Nevertheless, continued concerns and public health risks as the result of emissions have resulted in the search for an alternative method (Ashworth et al., 2013).

The other technique used is dig and dump sites. In this method, a site containing concrete or plastic within it is used to absorb the evaporation of the chemical compounds. This method replaced incineration, used by the US army in the 1970s, to dispose of the munitions of all types of CWAs (Singh and Walker, 2006). However, this technique is unsafe and has caused contamination of rivers, lakes and groundwater. Due to the risks arising from exposure to the deleterious emissions from landfill, and the incineration, these techniques are not convenient methods to dispose of pollutants (Department for Environment, 2013).

In contrast, a chemical treatment is a process targeting pollutants by adding a chemical reagent. This works to reduce the toxicity, waste volume and the mobility (Evangelista, 1993). The common chemical method used to remove soil pollutants is soil chemical oxidation, which is known as 'chemox'. This method includes insertion of chemical oxidants in water and soil to break down the pollutants and has been widely used. Furthermore, this method works to reduce the oxidation state of a compound through accepting an electron to oxidise certain substances, leading to the removal of the original pollutant's toxicity (Hueling and Pivetz, 2006). It is efficient in the degradation of a wide various group of organic solvents, such as polyaromatic hydrocarbons (PAH), vinyl chloride (VC), trichloroethylene (TCE), perchloroethylene (PCE), methyl-tert-butyl-ether (MTBE), xylene (BTEX), toluene, ethylbenzene, and benzene (Block et al., 2004).

The drawbacks of the oxidants are rapid reaction rate, leading to short-term persistent problems related to the safety and health issues of using powerful oxidants, and moreover the possibility of pollutants' movements exists (Hueling and Pivetz, 2006). All these drawbacks necessitate the development of effective biological tools.

2.3.2 Phytoextraction

Decontamination of environmental sites from CWAs is considered a major challenge. Given this, using plants is interesting and likely to be increased due to their potential capacity to uptake toxic substances (Ramacharyulu et al., 2014). Phytoremediation or phytoextraction refers to the capability of plants to take up contaminants by the roots and translocate them to above ground shoots or leaves (Chang and Corapcioglu, 1998; Kamath et al., 2004).

Phytoremediation has many advantages. For instance, it does not affect the soil structure or texture. Furthermore, it depends on sunlight for energy and produces high levels of biomass (Glick, 2003). In this scope, a study by Zakharova et al. (2000) proved the plant-effectiveness of oats *Avena sativa* L. to remediate yperite (a CWA product) from contaminated soil.

The disadvantages of phytoremediation are that it relies on the pollutant's solubility and bioavailability. Furthermore, the plant roots should be deep in the soil for effective uptake. Additionally, it takes a prolonged time to remediate. Whilst it is appropriate for use in some areas that have low population density, it relies on seasonal and climatic conditions and if non-native plants are used, it might be affected by the local ecology and adversely impact biodiversity (Koptsik, 2014). As such, the interesting challenge is to search for an alternative method, which should be safe, efficient and cheaper than others in its application to completely degrade organic pollutants into non-toxic components. This method is called bioremediation (Zhang et al., 2004).

2.3.3 Bioremediation

Bioremediation (BR) is the application of microbes to break down or reduce the POPs level. It can be used to reduce their toxicity in soil, sludge, solids, and groundwater (Kumar et al. 2011). The process mainly uses the native soil organisms or their enzymes to convert complex organic

compounds into simple inorganic compounds in a process called mineralisation, to provide energy or nutrient sources (Singh, 2009; Vidali, 2001).

Bacteria, fungi, and yeast are common microorganisms that can be used in bioremediation. These organisms would interact with exudates of plant roots, which results in decontamination and determines the fate of the contaminants (Chatterjee et al., 2008). As previously stated, BR mainly relies on the presence of microorganisms, which can attack the contaminant with their enzymes, converting it into less or non-toxic substances (Karigar and Rao, 2011).

The use of aerobic bacteria in BR is a promising strategy because of the low cost, eco-friendliness and high reduction of pollutants, in addition to the abundance of microorganisms in the soil (Drzyzga et al., 1998). The essential feature of BR is minimising the cost compared to other techniques, like incineration, phytoremediation or even dig and dumping (Perelo, 2010). Consequently, the importance of BR is that it can achieve the mineralisation of the contaminants entirely. Moreover, it is friendly to ecosystems and has the ability to remove low concentrations of pollutants.

Successful bioremediation mainly relies on the use of individual microbes that have been completely adapted to target the pollutant. Meanwhile, their efficiency depends on the ability to avoid local predators, and compete with indigenous microbes, as well as different abiotic factors like the physicochemical conditions or the concentration of contaminants and the chemical structure (Adams et al., 2015). Therefore, BR can be grouped into three classifications and used *In-situ* or *Ex-situ* as follows:

1. Enzymatic biotransformation, in which the molecules of the chemical compound is transformed into a less or non-toxic compound (Asha and Vidyanathi, 2009).
2. Biodegradation, when a chemical compound is broken down by various soil microorganisms (Leung, 2004).

3. Mineralisation is the process in which a cell protein, like microorganisms, can complete degradation of complex organic pollutants into simpler organic compounds, inorganic compounds, CO_2, and H_2O (Das and Chandran, 2011).

Nevertheless, BR has certain drawbacks. For instance, it takes a long time and is difficult to predict its efficiency compared to the chemical or physical processes. BR technology has been

globally applied to decontaminate OPs pesticides such as triclopyr (butoxyethylester) and chlorpyrifos, as well as crude oil and heavy metals, because it adheres to the laws and regulations relating to food safety and preserving human health (Milic et al., 2009; Massiha et al., 2011).

Today, the challenge facing scientists is how to tackle water or land contaminated with POPs by applying an inexpensive method, in a safer, and most importantly, an environmentally sound approach with rational cost implications.

2.4 Bioremediation strategies

There is a BR wider strategy available for decontaminating most pollutants from groundwater (EPA, 2013). It can be used individually or combined with others. Such strategies essentially depend on the microbes, electron donors and acceptors.

2.4.1 Aerobic and anaerobic treatment

This strategy has been widely implemented for a variety of chemicals, including vinyl chloride (Davis and Carpenter, 1990), acetone solvent (Pielech-Przbylska et al., 2006), atrazine and 2, 4-dichlorophenoxy acetic acid (Carboneras et al., 2017), and (E)-phytol [3,7,11,15-tetramethylhexadec-2(E)-en-1-ol] (Rontani et al., 1999).

Aerobic conditions increase the biodegradation rate, reducing pollutants compared to anaerobic circumstances. For that reason, the introduction of oxygen to anaerobic environments increases the aerobic microorganism activity (EPA, 2013).

Pseudomonas, *Alcaligenes*, *Sphingomonas*, *Rhodococcus* and *Mycobacterium* revealed their capability in the degradation of pesticides and hydrocarbons, in addition to alkanes and polyaromatic compounds to utilise as a source of carbon in the presence of oxygen (Kensa, 2011). Using a microbubble suspension in the limited oxygen circumstances can improve the biodegradation of phenanthrene (Choi et al., 2009).

2.4.2 Anaerobic Reduction and Co-metabolism

Anaerobic reduction of OPs occurs in the absence of oxygen, usually reducing sulfates and nitrates, as well as dechlorination reduction. In this reaction, the electron acceptor might be organic compounds, sulfates, carbon dioxide or nitrates, which would oxidize materials instead of oxygen (International Centre for Soil and Contaminated Sites, 2006). Anaerobic reduction has been used in the BR of chloroform, dechlorination of the solvent trichloroethylene (TCE) and polychlorinated biphenyls (PCBs) in river sediments (Kensa, 2011).

In contrast, during co-metabolism, bacteria can degrade the contaminants via a side reaction, and not as a source of carbon or energy (International Centre for Soil and Contaminated Sites, 2006). For that reason, co-metabolism is often indistinct biochemically (Wackett, 1996), however, co-metabolism can be more effective in degrading very low concentrations of some contaminants (Prasad et al., 2012).

2.5 DEMP

DEMP is an OP compound. It is used to synthesise (i) phosphonylated peptides, (ii) gem-difluroalkenyphosphonate by its reaction with alpha-trifluromethylstyrene, (iii) pyridone alkaloids with neuritogenic activity and (iv) lipophilic meropenem-derived prodrugs, fluoroalkyl alpha- and beta-aminophosphonates (https://www.alfa.com/en/catalog/A14772/). The toxicity of phosphonates, especially aromatic and aliphatic versions, ranges between moderate to high toxicity. Their toxicity increases with benzene rings and halogen or nitro group substitution (Material Safety Data Sheet, 2010).

DEMP is considered a simulant of the nerve agent sarin (Chaudot et al., 2000). Simulants are similar in both their structure and presence of functional groups, e.g. phosphoryl groups (p=o), and therefore make good exemplars for research and development testing. Simulant OPs molecules have one or more extra functional groups. They include four main groups: isopropyl groups, esters, P-CH$_3$ bonds and P-X bonds (Uzarski, 2009). The chemical and physical properties of DEMP are shown in Table 2-1.

Table 2-1 The physical and chemical properties of DEMP (Material Safety Data Sheet, 2010).

State	Liquid
Boiling point	194°C [381.2 °F]
Density (Relative vapor density(air=1)	> 1(1.052 g.mL^{-1}) at 25°C
Flash point and Specific gravity	75°C [168.008°F], 1.041 respectively.
Linear Formula	CH3P(O)(OC$_2$H$_5$)$_2$
Molecular weight	152.13 g. mol^{-1}
Solubility in water and Reactivity	Partly miscible g.L^{-1}, and Stable under normal conditions.
LD50	2240 mg. kg^{-1} Intraperitoneal (mouse)

2.6 Chemical elimination of DEMP

The hydrolysis reaction is one of the most common degradation pathways that DEMP can undergo, since it has a site susceptible to nucleophile attack (by H$_2$O, acid or base). It was expected that DEMP hydrolysis pathways might resemble those of esters of carboxylic acids, as esters' hydrolysis pathways proceed through a tetrahedral transition state. The degradation pathways for DEMP can be predicted through the simulation of the ester hydrolysis mechanism in the environment (Larson and Weber, 1994) as detailed in the following paragraphs.

2.6.1 Acid hydrolysis pathways

The first step is that a proton H$^+$ attaches itself to oxygen in P=O, resulting in an increase in the positivity of the phosphorus atom and enhances the attack of the nucleophile (H$_2$O) on P atom. Meanwhile, P-O cleaves and the rearrangement occurs to produce phosphonic acid and an ethanol molecule, eventually regenerating H$^+$ as an acid catalysed scheme (2-1).
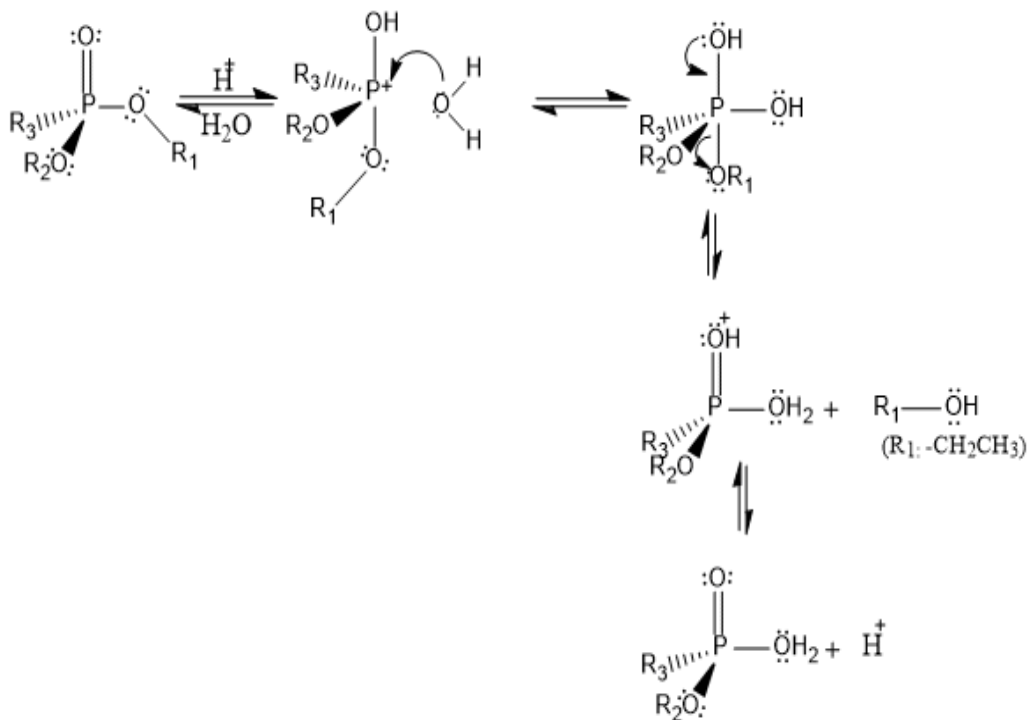
Scheme 2-1 Acidic hydrolysis of DEMP.

Acid catalyse rate = kA [H+] [ester].

KA is the second order rate constant (M-1s-1).

$-\dfrac{d[DEMP]}{dt} = $ KA [H+][DEMP]

The hydrolysis of DEMP in acid can proceed via bimolecular mechanism.

Situation 1. [A]≠ [B]

$$kt = \frac{1}{[B]_0 - [A]_0} \ln \frac{[B]_0[A]}{[A]_0[B]}$$

$$kt = \frac{1}{[H^+] - [DEMP]_0} \ln \frac{[H_0^+][DEMP]}{[DEMP]_0[H^+]}$$

Situation 2. [A] = [B]

Since A and B react with 1:1 stoichiometry, [A] = [A]o –x & [B] = [B]o –x

At any time, [A] = [B] and the rate law will be:

$rate = k[A][B] = K[A][A], \dfrac{-d[A]}{dt} = $ K [A]^2, $\dfrac{1}{[A]} = \dfrac{1}{[A]_0} + 2kt$

2.6.2 Base enhanced

Scheme 2-2 displays the base hydrolysis mechanism. The nucleophile OH⁻ (Base) will attack the phosphorus atom, resulting in the cleavage of a P-O bond and the production of phosphoric acid owing to the strong base of RO⁻. It grabs proton H⁺ from phosphoric acid to produce finally:
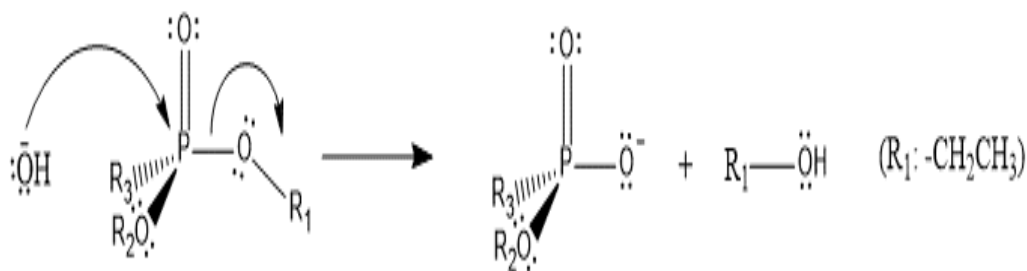
Scheme 2-2 Base hydrolysis of DEMP.

Rate = kB [OH-] [DEMP]

$$\frac{-d[DEMP]}{dt} = \text{KB [OH-] [DEMP].}$$

2.6.3 Neutral hydrolysis of DEMP

A nucleophile is a water molecule that attacks electrophiles, especially C. In this reaction, the water molecule kicks the C-O bond and cleaves it. Furthermore, the leaving group is the Phosphonate anion that forms Phosphonic anion and ethanol alcohol.
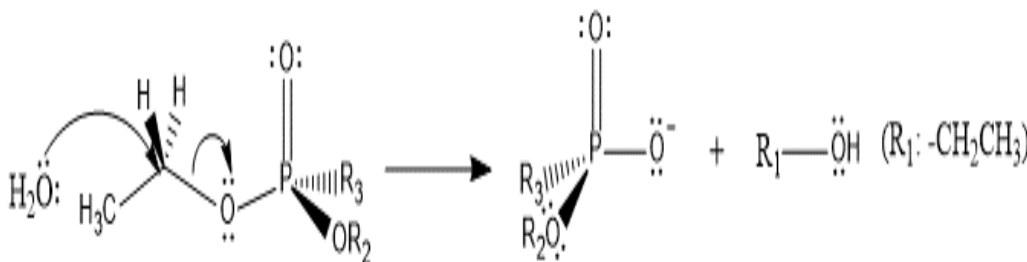
Scheme 2-3 Neutral hydrolysis of DEMP.

2.6.4 Pseudo-first order reaction

The kinetic study of DEMP hydrolysis or degradation can be evaluated using a pseudo first order reaction (PFO). This reaction occurs when in a bimolecular reaction that one of the reactants is present in great excess or is maintained at a constant concentration compared with the other reactant. Therefore, the reaction rate depends on the concentration of the changeable concentration reactant (D'Ottone et al., 2018). Hence, the PFO was used to monitor the changes in the concentration of DEMP during the reaction time. The DEMP hydrolysis reaction is similar to ester hydrolysis that converts into a carboxylic acid in water (Larson and Weber, 1994). It can be described as follows:

$$Rate = -\frac{d[DEMP]}{dt} = k_h \, [DEMP]$$

K_h: the constant rate for the overall pseudo-first order hydrolysis (s⁻).

The hydrolysis of DEMP can proceed via three distinct bimolecular mechanisms: acid catalysed, neutral and base enhanced.

Acid catalysed rate = $K_A[H^+]$ [DEMP]

Base catalysed rate = $k_B[OH^-]$ [DEMP]

H_2O catalysed rate = K_{H2O} [H_2O] [DEMP]

K_A, K_{H2O} and K_B are the second order constant ($M^{-1}s^{-1}$).

The overall rates will be the sum of three individual rates.

Rate (overall) = {$k_A [H^+] + k_{H2O} [H_2O] + k_B[OH^-]$} [DEMP].

Since the concentration of water in aqueous solution is still constant $\approx$ 55.5 M, the value for K_{H2O} [H2O] will replaced by KN.

Consequently,

Kh = kA [H+] +KN+ kB [OH⁻]

If the experiment was carried out at high pH, the KB [OH]$>> Kn$

Then, kh$\approx$ kB [OH⁻]

Rate = kB [OH-] [DEMP]

Rate = kh [DEMP]

This will be the pseudo-first order reaction.

$$ln\frac{[DEMP]t}{[DEMP]o} = -kt$$

Through the plot ln [DEMP] versus time will provide a slop that equals –kh.

$Kh = kB [OH-]$...............1

Repeat the same experiment as neutral pH (6 or 7) will provide kh value which is equal to:

$Kh = KB [OH-] + KN$.........2

By substituting the value of KB [OH] from Equation 1, and the kh value extracted from the repeat experiment at pH 6 in Equation 2, KN value is obtained.

2.7 Enzymatic degradation

Bacteria can produce many different types of enzymes to break down the different substances and gain energy. This biotic factor leads to rapid hydrolysing and decreasing the toxicity in a process called 'detoxification' of OPs (Scheme 2-4). As a consequence, this process could occur under three different conditions, which are acid, base, and neutral conditions (Elersek and Filipic, 2011).
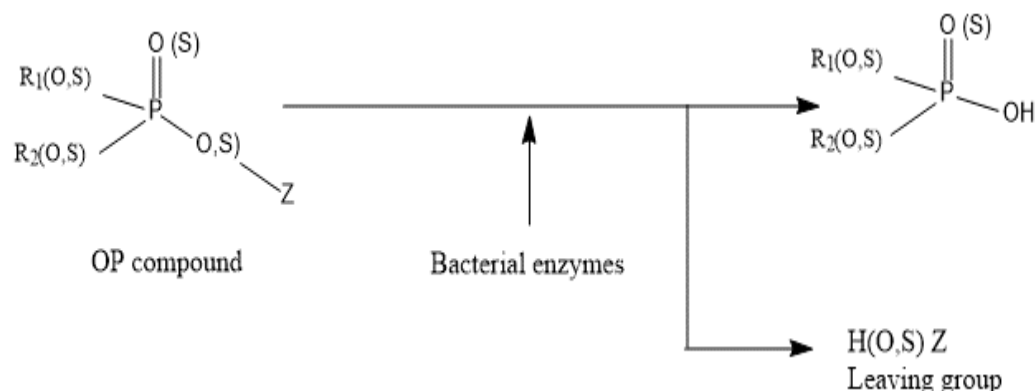
Scheme 2-**4** The general hydrolysis of the OPs compounds.

A major challenge is to determine whether bacteria can be isolated and which are able to degrade the OPs compound of interest (in this case DEMP), as individual strains or communities. This activity will depend on a number of enzymes that can actively target the OPs substrate:

1. Phosphotriesterases (PTEs) are known for their ability to hydrolyse the OPs esters, particularly NAs (Raushel, 2002; Tsai et al., 2012). Several microbes have been isolated from soil. They are capable of using different OPs substances as a result of the presence

of OPs hydrolase (*oph*) that is encoded in the *opd* gene cluster, such as, *Pseudomonas putida*, *Flavobacterium* and *Arthrobacter* (Zheng et al., 2013). This enzyme has proved its various capabilities to break down the P-O, P-S and P-F bonds (Singh and Walker, 2006).

Oph is referred to by various names in academic research, for instance, Phosphotriesterase (PTE), *opd* hydrolases, organophosphate-degrading enzymes, or parathion hydrolases. It has proven its capability in the hydrolysis of NAs (Raushel 2002). The *oph* has a broad substrate requirement and is able to break down the OPs, mostly P–O, P–CN, and P–F bonds, being the only enzyme known to cleave to the P–S bond in the NAs, particularly the V-type (Cheng and De Frank, 2000; Lai et al., 1995). Moreover, it is a member of the amide hydrolase superfamily that has urease (Holm and Sander, 1996), but *oph* is unable to degrade the p-nitrophenol (PNP), therefore, it was used as the surface-expressed method on *P. putida* in order to improve degradation of OP NAs and PNP simultaneously. This approach with a single organism has the ability to efficiently degrade these compounds at the same time (Lei et al., 2005).

2. Another enzyme called OPs acid, a hydrolase (*opaa*) that is encoded in the *opaa* gene isolated from *Alteromonas haloplanktis* and *A. undina,* can detoxify NAs (Cheng et al., 1993). Theriot and Grunden (2011) revealed that the future applications of *oph* and *opaa* are important, not only because of cost-effectiveness compared to a physical method, like incineration, but also their effectiveness in reaction with OPs, in addition to their forming environmentally friendly products. Another study improved the hydrolysis of VR by engineering a modified version of the *opaa* enzyme in *Escherichia coli* (Daczkowski et al., 2015).

Additionally, a study by Ali et al. (2012) demonstrated that using different metals, involving Mg^{2+}, Mn^{2+}, Zn^{2+}, and Co^{2+} can affect the activity of the *opda*. The enzyme activity was enhanced 4.84 ± 0.39-fold in the presence of Mn^{2+}. The *opda* enzyme isolated from *A. radiobacter* has 90% similarity to *oph* in function, but the main difference lies in the structure (Raushel, 2002), as well as in the presence of Arg at positions 254 and Tyr at positions 257, instead of His in PTE (Nakayama et al., 2014). PTE has a high activity in degrading NAs, such as GA, GB, and ethyl sarin (GE), although it was comparatively inefficient in GD degrading (Dawson et al., 2008).

3. Aminopeptidase P (*ampp*) can hydrolyse a range of OPs triesters. It can cleave to an amino-terminal x-pro peptide bond (Jao et al., 2004) and has many similarities with the *opaa* enzyme.

4. Other studies have proven that some bacteria have methyl parathion hydrolase (*mph*). This enzyme was encoded as *mpd* and found in a variety of soil bacteria, for instance, *Bacillus thuringiensi* and *Chromobacterium violaceum* (Singh, 2009).

Andrew et al. (2014) found some enzymes have a similar function with *oph* including: OPs acid hydrolase (*opaA*), methyl parathion hydrolase (*mph*), Diisopropylfluorophosphatase (*dfp*), and paraoxonase. All these enzymes interact with P-O. Further studies have been carried out to identify the role of enzymes in catalysing the OPs compounds such as, O-phenylenediamine dihydrochloride (*opd*), methyl parathion hydrolase (*mph*) mevalonate pyrophosphate decarboxylase (*mpd*) (Zheng et al., 2013). Subsequently, they have isolated the gene responsible for these enzymes. This gene was then cloned, identified and purified in several organisms. The function of enzymes is to attack the bond P-O or P-S (Sogorb and Vilanova, 2002).

However, Lei et al. (2005) isolated *P. putida* JS444 from soil contaminated by PNP. This bacterium underwent genetic modification, which resulted in a raised OPs degradation rate of methyl parathion, paraoxon, and parathion into 1.53, 7.90, and 3.54, and μmol h^{-1} mg^{-1} dry weight respectively. Moreover, Iyer and Iken (2013) identified *Senotrophomonas maltophilia* and *Exiguobacterium indicum* and showed their capability to remediate a broad spectrum of OPs compounds, particularly methyl parathion, due to having the *mpd* gene.

In an organism identified as *P. putida* by Walker and Keasling (2002), they modified the *oph* gene and measured its activity, after catalysing the OPs parathion into new products, p-nitrophenol, and diethyl thiophosphate. It succeeded in degrading parathion, but failed to degrade these new products. Consequently, they cloned a tac promoter to improve expression and therefore activity.

Fungal enzymes have also been isolated and shown to degrade OPs. *A-oph* is a novel OPs degrading enzyme, isolated from *Aspergillus niger*. It could catalyse the P-S bond (Liu et al.,

2001). *A. penicillium oph* (*p-oph*) enzyme was isolated from *Penicillium lilacinum* that can cleave to a range of OPs, specifically the bonds of P-O and P-S (Liu et al., 2004).

2.7.1 Microbial degradation of CWAs

Many different tools have been suggested to remediate soil polluted by CWAs. The most recent efforts have focused on using microorganisms that are capable of degrading CWAs, owing to having a reduced negative impact on the environment. Many microorganisms have been isolated that degrade OPs compounds and identification of their enzymes shows their capability to utilise them as a C or P source (Table 2-2).

Subsequently, a study by Attaway et al. (1987) shed light on the possibility of eighteen isolates of bacteria gram-negative, which can utilise the analogue structure of GB and GD, diisopropyl fluorophosphates. Other studies have focused on the ability of soil microbes to use phosphonate as a source of phosphorus through the fission of the C-P bond. In addition, *Rhodobacter capsulatuscan* uses 2-aminoethylphosphonate and alkylphosphonates (Schowanek and Verstraete, 1990).

Additionally, the bacterium *Klebsiella aerogenes* has shown ability in the biodegradation of various OPs phosphonate, in particular aminomethyl phosphonate, methyl phosphonate (MPn), and phosphonoacetate, and inorganic phosphate to take advantage of phosphorus (Imazu et al., 1998). Hence, there is the potential capability for DEMP degradation due to the P-O bond or P-C bond, which are degradable by various bacterial enzymes.

Table 2-**2** CWAs and their degradation by various microorganisms.

CWAs	Microorganisms (Bacteria)	Enzyme	Function	Reference
GA	*Alteromonas undina*	OPAA	It can also hydrolyse the P-C bond of GA to N,N-dimethylethylphosphoramidate	(Cheng et al., 1993).
GB	*Sphingobium fuliginis*	OPH	It could hydrolyse the GB, GA, GD, and GF, with high activities, but not VX.	(Ohmori et al., 2013).
GD	*Alteromonas strain & A. undina*	OPAA	the hydrolysis of the P-F bond in GB, GD, and GF.	(Cheng et al., 1993).
GF	*Alteromonas sp. A. haloplanktis*	OPAA, PTE	The hydrolysis of the (+) GF isomer.	(Harvey et al., 2005).
VX	*Pseudomonas diminuta*	OPH	It can hdyrolyse VX, VX analogue. Additionally, it can degrade GD, DFP and O,O-diisopropyl S-(2-diisopropylaminoethyl) phosphorothiolate (Tetriso).	(Hoskin et al., 1995)

2.8 Random mutagenesis to improve strain function

In molecular evolution studies, the term mutation refers to a process resulting from an error in the DNA sequences (a genetic system) or it means a permanent alteration in the sequence of nitrogenous bases of a DNA molecule. The main reasons for the mutation are the cellular processes, for instance oxidative damage in DNA, or as a result of mutagens, i.e. radiation and chemicals (Gregory, 2009; Najafi and Pezeshki, 2013).

However, the mutation could occur by a series of processes called mutagenesis, with tools used called mutagens. The organisms that undergo the mutations are called mutants, whilst the strain that is not exposed to the mutagens is called the wild type (Snyder and Champness, 2017).

Therefore, using the mutation rate is necessary to estimate the rate of mutation per nucleotide, generation, or the whole genome in order to determine beneficial, non-beneficial or neutral (most commonly) mutations (Martínez and Baquero, 2000).

2.9 Types of Mutation

There are two different types of bacterial mutations: spontaneous mutation and induced mutation. The former can happen without intervention. It has often happened as a result of errors in DNA through replication. For example, during the synthesis of a new DNA strand by DNA pol III, occasionally a new nucleotide will be added or omitted. This process results in the mutation occurring.

Ultimately, this mechanism of spontaneous mutation of the errors in the replication of DNA contributes to adding or deleting the erroneous nucleotides from template nucleotides. It can occur as follows:

T – A --> Tautomerization --> T' – A --> replication 1 --> T' – G and A –T,
T – G --> Replication 2 --> T – A and G – C, (enol form of thymine indicated as T').

Conversely, the 'Induction' mutation can be performed by exposing microorganisms to chemical, physical or even biological mutagens. These tools act directly on the nucleotides of DNA and can bring damage to the DNA. This damage causes errors through DNA replication and produces the mutation (Watford and Warrington, 2018).

2.9.1 How does ultraviolet irradiation light cause mutations in bacteria?

The exposure of microorganisms to UV or chemical agents results in either death or mutation. Irradiation is one of the multiple types of mutagen agents that has been used to bring about mutations in microorganisms. In the past, the use of the high-energy irradiation like x-rays, and gamma rays often required costly devices to be used, in addition to having safety issues. Moreover, they can produce wide damage in the chromosomal, which is difficult for the

microorganism to repair. However, UV radiation light, particularly 250 nm, can influence the microorganism.

The basic impact of the UV produces bonds between the adjacent pyrimidine to compose the pyrimidine dimers (Fig. 2-7). These structures distort the formation of bacterial DNA resulting in the inhibition of the replication of bacterial DNA, in addition to their transcription (Dale and Park, 2014). Therefore, UV has become a common mutagen due to its ability to ionise, despite its energy being very weak. It can change DNA structure and cause breakage of the DNA strand. Oller et al., (1992) revealed that UV light can affect bacterial DNA at adjacent pyrimidines of *E. coli*. This induced mutation is almost the same as DNA absorption, which is around 255 nm (Al-Xiang et al., 2017).
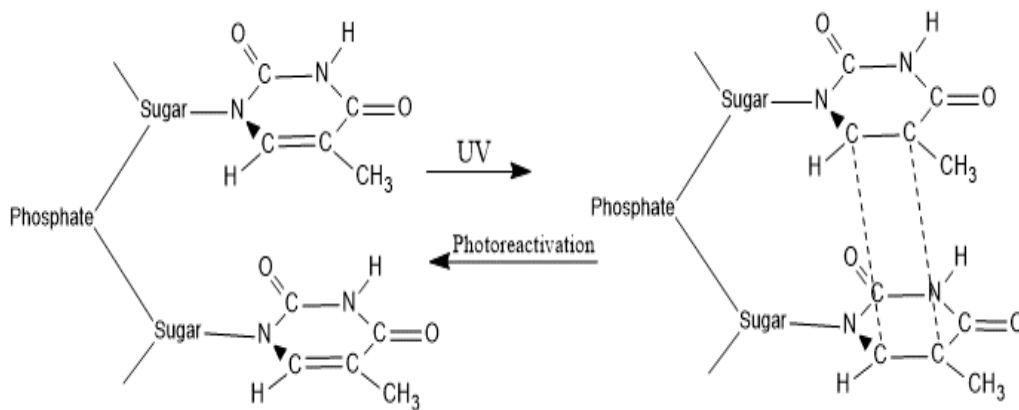
Fig 2-7 Structure of thymine dimers.

2.9.2 How do chemical agents cause mutations in bacteria?

Many chemical agents have interacted with bacterial DNA or during its replication. This reaction produces a new DNA sequence, for example, ethidium bromide EthBr (Fig. 2-8) and acridine orange. These molecules have intercalated mechanisms. EthBr and acridine orange include a flat ring structure and can be inserted between the adjacent bases of the double helix. Consequently, this process leads to the addition or deletion of a single base during the replication of DNA, resulting in a frameshift mutation (Dale and Park, 2014).
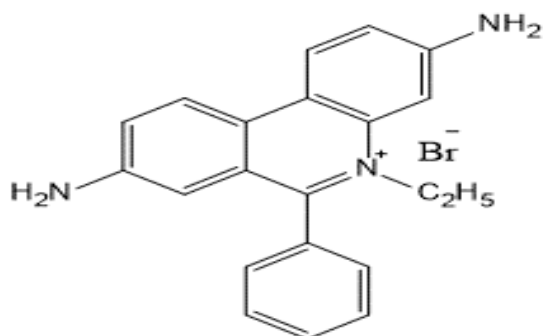
Fig 2-**8** The chemical structure of the ethidium bromide.

2.10 Challenges in studying DEMP kinetics in the soil

Soils are considered a complicated environment. Most organic compounds, like CWAs, have undergone an important process called adsorption, meaning the accumulation of substances in the soil interfacial layer, while the term 'desorption' indicates a reverse operation (Dąbrowski, 2001). These substances usually accumulate either on the interface where they are called adsorbate or on the surface where they are termed adsorbents (Al-Anber, 2011).

The kinetics reactions of the CWAs through the soil have not been extensively studied, meaning that little data is available on the fate of CWAs. Jonas et al., (1975) studied the effect of temperature on predictive equations dimethyl methyl phosphonate (DMMP) adsorption using activated carbon. They found that a small amount of DMMP can be adsorbed by carbon at 25°C. Nowack and Stone (1999) noted that both phosphonates and phosphate were greatly adsorbed on the surface depending on each other. Likewise, the results reported that phosphonates could minimise phosphate adsorption by between 10-35%.

Additionally, Michalkova et al. (2004) studied the GB and GD adsorbed on the surface of the octahedral and tetrahedral structure. They found out that optimal adsorption occurred with the octahedral rather than the tetrahedral.

Furthermore, Saxena et al. (2005) analysed the DMMP, diethyl chlorophosphate (DEClP), diethyl pyrophosphate (DECnP) and nerve agents, like GB, with different kinds of carbon at the surface. They conducted the experiments so that all these compounds underwent the

pseudo-first order reaction and that the half-life of degradation was 1.5, 7.9, 1206 and 20 minutes for DECnP, DEClP, DMMP and GB respectively.

Schuldt (2007) studied the effect of activated sludge on the adsorption of the hydrolysis product of VX ethyl methylphosphonic acid (EMPA) in the bioreactors to simulate a municipal wastewater treatment system. The study revealed that EMPA can pass through the activated sludge, and that only 28% of the compound was degraded. Recently, Morrissey et al. (2012) concluded that VX is subjected to rapid sorption in less than 15 minutes. There is also a reaction between VX and clay.

As such, it is necessary to understand the fate of DEMP in the soil for many reasons. First, no study has yet been performed. Secondly, and most significantly, is that DEMP might suffer mobility in the soil. This makes the study of adsorption and desorption essential to predict groundwater contamination.

2.10.1 Sorption isotherm

CWAs are man-made chemicals that can reach directly into soil, causing a harmful effect to the ecosystem. The adsorption-desorption process is the most important parameter for risk assessment. It can be defined as a relationship between two variables at a constant temperature, for instance, the relationship between an organic adsorbate on the adsorbent surface and the concentration of liquid or pressure (Pennington et al., 2006). The basic concept of this process is the balance between the adsorbed concentration and the concentration in the adsorbent or bulk fluid at constant temperature (Dąbrowski, 2001)

For this reason, two mathematical equations' modelling, the Freundlich and Langmuir isotherms (Ismail et al., 2013) are often used to determine the potential of chemicals for the movement in soil. Many studies have examined the sorption of pesticides in soil, yet few studies have focused on the CWAs sorption in soil. As an example, Soltani et al. (2018) studied the effect of fullerene in the sorption of sarin, chlorosoman, chlorosarin, and soman.

Consequently, the current project examines DEMP movement through the soil using two different models. First, a Freundlich isotherm, an experimental model is used to study the non-

ideal sorption on a heterogeneous surface, using (Eq. 2-1) because the application of these models is important to understand DEMP behaviour in soil (Ho et al., 2002).

$$q_e = af C_e^{bf} \dots\dots\dots\dots(2.1).$$

Where: -

qe: solid phase metal ion concentration at equilibrium, mmolg^{-1}, af: Freundlich isotherm constant, dm^3 mmolg^{-1}, Ce Solution phase metal ion concentration at equilibrium, mmol dm^{-3}.

However, the Langmuir isotherm model (Eq. 2-2), derived from the kinetic mechanism, also could be applied to estimate the behaviour of DEMP in the environment (Ho et al., 2002). It is expressed as:

$$q_e = \frac{K_L C_e}{1 + a_L C_e} \dots\dots\dots\dots(2.2).$$

Where: - qe: solid phase metal ion concentration at equilibrium, mmolg^{-1}, K$_L$: Langmuir isotherm constant, dm^3 g^{-1}, Ce Solution phase metal ion concentration at equilibrium, mmol dm^{-3} , and aL: Langmuir isotherm constant, dm^3 mmolg^{-1}.

2.11 Challenge of chemical analysis technique used in thesis

2.11.1 Solid phase extraction (SPE)

SPE defines an extraction procedure that uses the liquid or solid phase to isolate the analyte of interest from a matrix which includes urine, blood, water, soil, plant or animal tissues as well as beverages. This process is normally used to clean and concentrate the sample before using it in any chromatography method aiming to measure the amount of analyte in the sample (Żwir-Ferenc and Biziuk, 2006).

Saçmaci et al. (2011) pinpointed the advantages of this method, as it being simple, fast, environmental, and sensitive and could be used with CWAs. The majority of CWAs are volatile and have polarity, furthermore, the matrices of CWAs contain dangerous components

(Vanninen, 2017). The sample preparation procedure is influenced by various factors, such as the kind of sample, the interest analyte and their concentrations in the sample.

In contrast, SPE was developed for solid phase microextraction, (SPME) by using fibre for the extraction of organic and inorganic pollutants with a small amount of solvents and time (Liu et al., 2003). The use of fibre can increase the capacity for the extraction of organic pollutants based on the porous structure. Liu et al. (2003) prepared a novel coating by using Sol-gel and cross-linking methods in the SPME of phosphate and methyl phosphonate. This gave sensitivity and high selectivity compared to the commercial SPME fibre.

2.11.2 Analysis of CWAs by Gas Chorography

Gas Chorography (GC) is an instrument or a physical method capable of separating and identifying mixtures and compounds effectively to determine the quality of CWAs in the different environmental matrices (Trap and Van Der Schans, 2007). This technology was used to verify GA, GB, VX, and GD in water samples contaminated by these pollutants (Degenhardt-Langelaan and Kientz 1996). Various types of detectors are used, such as the Flame Ionisation Detector (FID) to detect the small concentrations of chemicals ranging between (10^{-9} -10^{-12}) (D'Agostino and Chenier, 2006). Tandem, GC, Mass Spectrophotometry was utilised to identify most contaminants. Rohloff (2015) shows that GC-MS is an accurate technique used particularly with volatile compounds. Therefore, using this technology can have many advantages, for instance sensitivity, which is able to determine the smallest number of compounds in the pictograms in less than 30 minutes. Furthermore, the cost is reasonable compared to other analysis tools. Moreover, it is able to achieve a high separation power. In terms of the sensitive detecting systems, it has detectors that are fast to respond, having high and efficient sensitivity. Additionally, it is characterised by the ease of recording or outputting huge data by computer. Eventually, it could be used to monitor the substances that require periodic detection. In addition, it is easy to apply and does not need experts (Matei et al., 2018). Furthermore, the simulants of nerve agent such as DMMP, DECIP, DECnP and GB have been extensively studied In-situ degradation, by GC-FID (Saxena et al., 2005). Despite the accuracy of GC-FPD in the analysis of OPs substances, GC-FID has also proved that it is capable of determining these substances, whether in terms of quantity or quality.

2.12 Conclusions

Based on the information provided in the literature review, the study of biodegradation of anthropogenic toxic, organic compounds, is an important area of research. This is due to their health impact and implications including mortalities in humans and animals. Hence, many areas of research have been applied to remove a variety of chemical pesticides, but there are relatively few studies focussed on the biodegradation of CWAs from contaminated soil, surface water, and groundwater. Moreover, there are reports of high amounts of CWAs used in Iraq between 1980-1988 (Talabani et al., 2018; Riedel, 2004) and chlorine in Anbar Province in 2007 during the Iraq war (Polat et al., 2018). Therefore, increased attention to is required to assist in environmental detoxification efforts. There have previously been efforts to isolate microorganisms from soils contaminated with organic compounds, then reusing them in the biodegradation process. In this study, we build on this approach by designing a methodology to enrich functionally relevant microbes and aim to improve their biodegradation capability using tools such as adaptation and mutagenesis. The exemplar OP compound is DEMP, and currently there is no study about the fate and kinetics of DEMP in an aquatic or soil environment. Thus, this study will begin by addressing important environmental parameters, such as kinetic behaviour, adsorption, and DEMP hydrolysis reaction. This information is required to benchmark the rate of DEMP breakdown in the environment, in order to evaluate how efficient a bioremediation approach would need to be.

2.13 References

Abou-Donia, M. B. (2003) 'Organophosphorus ester-induced chronic neurotoxicity', *Archives of Environmental Health*, 58(8), pp. 484–497.

Adams, G. O., Prekeyi, T. F., Samson, E. O., Igelenyah, E. (2015) 'Gogoi B , Dutta N , Goswami P , Mohan T .. A case study of bioremediation of petroleum-hydrocarbon contaminated soil at a crude oil spill site . Adv Environ', *International Journal of Environmental Bioremediation & Biodegradation*, 3(August 2016), pp. 28–39.

Ai-Xiang, W., Kai-jian, H., Hong-jiang, W., Ai-qing, Z., and Ying, Y. (2017) 'Effect of ultraviolet mutagenesis on heterotrophic strain mutation and bioleaching of low grade copper ore', *Journal of Central South University*, 24(10), pp. 2245–2252.

Al Hattab T., M. and E. Ghaly, A. (2012) 'Disposal and Treatment Methods for Pesticide Containing Wastewaters: Critical Review and Comparative Analysis', *Journal of Environmental Protection*, 03(05), pp. 431–453. doi: 10.4236/jep.2012.35054.

Al-Anber, M. A. (2011) 'Thermodynamics Approach in the Adsorption of Heavy Metals', *J. Intech open*, pp. 737–764.

Ali, H. and Khan, E. (2017) 'Environmental chemistry in the twenty-first century', *Environmental Chemistry Letters*. Springer International Publishing, 15(2), pp. 329–346.

Ali, M., Naqvi, T. A., Kanwal, M., Rasheed, F., Hameed, A., Ahmed, S. (2012) 'Detection of the organophosphate degrading gene opdA in the newly isolated bacterial strain Bacillus pumilus W1', *Annals of Microbiology*, 62(1), pp. 233–239.

Andrews, L. D., Zalatan, J. G. and Herschlag, D. (2014) 'Probing the origins of catalytic discrimination between phosphate and sulfate monoester hydrolysis: Comparative analysis of alkaline phosphatase and protein tyrosine phosphatases', *Biochemistry*, 53(43), pp. 6811–6819.

Apilux, A.,Isarankura-Na-Ayudhya, Ch., Tantimongcolwat, T.Prachayasittikul, V. (2015) 'Paper-Based Acetylcholinesterase Inhibition Assay Combining a Wet System for Organophosphate and Carbamate Pesticides Detection', *Excli Journal*, 14, pp. 307–319.

Arome, D. and Chinedu, E. (2014) 'The importance of toxicity testing', *Journal of Pharmaceutical and BioScience*, 4(2013), pp. 146–148.

Asha, S. and Vidyavathi, M. (2009) 'Cunninghamella - A microbial model for drug metabolism studies - A review', *Biotechnology Advances*. Elsevier B.V., 27(1), pp. 16–29.

Ashworth, D. C., Fuller, G. W., Toledano, M. B., Font, A., Elliott, P., Hansell, A. L., de Hoogh, K. (2013) 'Comparative assessment of particulate air pollution exposure from municipal solid waste incinerator emissions', *Journal of Environmental and Public Health*, 2013, pp. 560342.

Attaway, H., Nelson, J. O., Baya, A. M., Voll, M. J., White, W. E., Grimes, D. J., Colwell, R. R. (1987) 'Bacterial detoxification of diisopropyl fluorophosphate.', *Applied and Environmental Microbiology*, 53(7), pp. 1685–1689.

Banks, C. N. and Lein, P. J. (2012) 'A review of experimental evidence linking neurotoxic organophosphorus compounds and inflammation', *NeuroToxicology*, 33(3), pp. 575–584.

Bean, A. (2007) *Protein Trafficking in Neurons. The University of Texas Health Science Center at Houston Houston, Texas* Elsevier Academic Press. PP:448.

Bide, R. W., Armour, S. J. and Yee, E. (2005) 'GB toxicity reassessed using newer techniques for estimation of human toxicity from animal inhalation toxicity data: New method for estimating acute human toxicity (GB)', *Journal of Applied Toxicology*, 25(5), pp. 393–409.

Block, P. a, Brown, R. a and Robinson, D. (2004) 'Novel Activation Technologies for Sodium Persulfate', *In Situ*, Monterey,(May), pp. 2A – 05. Available at: http://www.envsolutions.fmc.com/Portals/fao/Content/Docs/Novel.

Bocquené, G. and Galgani, F. (1998) 'Biological effects of contaminants: Cholinesterase inhibition by organophosphate and carbamate compounds', *ICES Techniques in Marine Environmental Sciences*, 22(22), PP. 1-19.

Carboneras, B., Villaseñor, J. and Fernandez-Morales, F. J. (2017) 'Modelling aerobic biodegradation of atrazine and 2,4-dichlorophenoxy acetic acid by mixed-cultures', *Bioresource Technology*. Elsevier Ltd, 243, pp. 1044–1050.

Chambers, J. E. and Oppenheimer, S. F. (2004) 'Organophosphates, serine esterase inhibition, and modeling of organophosphate toxicity', *Toxicological Sciences*, 77(2), pp. 185–187.

Chang, Y.-Y. and Corapcioglu, M. Y. (1998) 'Plant-Enhanced Subsurface Bioremediation of Nonvolatile Hydrocarbons', *Journal of Environmental Engineering*, 124(2), pp. 162–169.

Chatterjee, S., Chattopadhyay, P., Roy, S., Sen, S. K. (2008) 'Bioremediation: a tool for cleaning polluted environments', *Journal of Applied Biosciences*, 11, pp. 594–601.

Chaudot, X., Tambuté, A. and Caude, M. (2000) 'Selective extraction of hydrocarbons,

phosphonates and phosphonic acids from soils by successive supercritical fluid and pressurized liquid extractions', *Journal of Chromatography A*, 866(2), pp. 231–240.

Cheng TC, and De Frank, J. J. (2000) 'Hydrolysis of Organophosphorus Compounds by Bacterial Prolidases. In: Zwanenburg B, Mikolajczyk M, Kielbasinski P (eds) Enzymes in action green solutions for chemical problems, vol 33. Kluwer Academic, Dordrecht, pp 243 – 261.

Cheng, T. C., Harvey, S. P. and Stroup, A. N. (1993) 'Purification and properties of a highly active organophosphorus acid anhydrolase from Alteromonas undina', *Applied and Environmental Microbiology*, 59(9), pp. 3138–3140.

Choi, Y. J., Kim, Y. J. and Nam, K. (2009) 'Enhancement of aerobic biodegradation in an oxygen-limiting environment using a saponin-based microbubble suspension', *Environmental Pollution*. Elsevier Ltd, 157(8–9), pp. 2197–2202.

Colovic, M.B., Krstic, D. Z., Lazarevic-Pasti, T. D., Bondzic, A. M., Vasic, V. M. (2013) 'Acetylcholinesterase Inhibitors: Pharmacology and Toxicology', *Current Neuropharmacology*, 11(3), pp. 315–335.

D'Agostino, P. a. and Chenier, C. L. (2006) 'Analysis of Chemical Warfare Agents: General Overview , LC-MS Review , In- House LC-ESI-MS Methods and Open Literature Bibliography', (March), pp. 1–76.

D'Ottone, L. and Ochonogor. (2018). 'Error Analysis of Absolute Rate Coefficient Extrapolated under *Pseudo*-First Order Conditions'. Journal of the Turkish Chemical Society, Section A: Chemistry 5(1):29–40.

Dąbrowski.A (2001) 'Adsorption - from theory to practice', *Advances in Colloid and Interface Science*, 93, pp. 135–224.

Daczkowski, C. M., Pegan, S. D. and Harvey, S. P. (2015) 'Engineering the Organophosphorus Acid Anhydrolase Enzyme for Increased Catalytic Efficiency and Broadened Stereospecificity on Russian VX', *Biochemistry*, 54(41), pp. 6423–6433.

Dale J. W. and Park S. F. (2014) *Molecular Genetics of Bacteria.* 5th Editio. *University of Surrey, UK,* Wiley-Blackwell, A John Wiley & Sons, Ltd., Publication. pp: 388

Das, N. and Chandran, P. (2011) 'Microbial Degradation of Petroleum Hydrocarbon Contaminants: An Overview', *Biotechnology Research International*, 2011, pp. 1–13.

Davis, J. W. and Carpenter, C. L. (1990) 'Aerobic biodegradation of vinyl chloride in groundwater samples', *Applied and Environmental Microbiology*, 56(12), pp.

3878–3880.

Dawson, R.M., Pantelidis, S., Rose, H.R., Kotsonis, S.E. (2008) 'Degradation of nerve agents by an organophosphate-degrading agent (OpdA)', *Journal of Hazardous Materials*, 157(2–3), pp. 308–314.

De Meyer, R. and and De Plaen, J. (1984) 'United States . (Received 20 April 1984 ; in final form 1 June 1984) Biochemical Study of Teratogenic Substances', *Life Sciences*, 3(7), pp. 709–713.

Degenhardt-Langelaan, C. E. A. M. and Kientz, C. E. (1996) 'Capillary gas chromatographic analysis of nerve agents using large volume injections', *Journal of Chromatography A*, 723(1), pp. 210–214.

Department for Environment, F. & R. A. (Defra) (2013) *Incineration of Municipal Solid Waste*, *Waste Management*. Available at: https://www.gov.uk/government/publications/incineration-of-municipal-solid-waste. PP:1-48.

Dianyi Yu, M. (2010) 'Agency for Toxic Substances and Disease Registry Case Studies in Environmental Medicine (CSEM) Ethylene Glycol and Propylene Glycol Toxicity', *Environmental Medicine*, pp. 1–65.

Drzyzga, O., Bruns-Nagel, D., Gorontzy, Th., Blotevogel, K. H., Gemsa, D., Von Löw, E. (1998) 'Mass balance studies with 14C-labeled 2,4,6-trinitrotoluene (TNT) mediated by an Anaerobic Desulfovibrio species and an Aerobic Serratia species', *Current Microbiology*, 37(6), pp. 380–386.

Ee, L. A., Zhao, H. and Obbard, J. P. (2005) 'Recent advances in the bioremediation of persistent organic pollutants via biomolecular engineering', *Enzyme and Microbial Technology*, 37(5), pp. 487–496.

Elersek, T. and Filipic, M. (2011) 'Organophosphorous Pesticides - Mechanisms of Their Toxicity', *Pesticides - The Impacts of Pesticides Exposure*. doi: 10.5772/14020.

EPA (2013) 'Introduction To in Situ Bioremediation of Groundwater', United States Environmental Protect Agency, Office of Solid Waste and Emergency Response 542-R-13-018, pp.1-86.

Evangelista, R. (1993) 'Physical and Chemical on site remediation processes Presented at the HazMat 93 Spring Conference , Long Beach , CA', *Presented at the HazMat 93 Spring Conference, Long Beach, CA.*, pp. 20.

Feng, G. (2012) 'The Synthesis and Characterization of Phosphonic Acids for the Surface Modification Study on Indium Tin Oxide the Synthesis and Characterization of

Phosphonic Acids for the Surface Modification Study on Indium', *Master of Science in the School of Chemistry and Biochemistry, Georgia Institute of Technology.*, (August), p. 60.

Ferguson, T. L. and Wilkinson, R. R. (1984). "Incineration of Pesticide Wastes," Treatment and Disposal of Pesticide Wastes, ACS Symposium Series, Vol. 259, pp. 181- 191.

Frank, P. and Ottoboni, M. A. 2011. The Dose Makes the Poison. A Plain-Language Guide to Toxicology. 3rd Edition. John Wiley & Sons, Inc., Hoboken, New Jersey.p-262.

Ganesan K. and Vijayaraghavan R. (2010) 'Chemical warfare agents.', *J Pharm Bioallied Sci.*, 2(3), pp. 166–178.

Ghorab, M. A. and Khalil, M. S. (2015) 'Toxicological Effects of Organophosphates Pesticides', *International Journal of Environmental Monitoring and Analysis*, 3(4), p. 218.

Glick, B. R. (2003) 'Phytoremediation: Synergistic use of plants and bacteria to clean up the environment', *Biotechnology Advances*, 21(5), pp. 383–393.

Gregory, T. R. (2009) 'Understanding Natural Selection: Essential Concepts and Common Misconceptions', *Evolution: Education and Outreach*, 2(2), pp. 156–175.

Gupta, R. C. (2006) *Toxicity of Organophosphate & Carbamate Compounds*. Elsevier Academic Press.PP. 763.

Haddon, R. C. (1985) 'Theoretical Study of the Cyclotriphosphazenes. Importance of phosphorus d orbitals', Chemical Physical Letters, Vol 120 (4,5): 372-374.

Harvey, S. P., Kolakowski, J. E., Cheng, T. Ch., Rastogi, V. K., Reiff, L. P., DeFrank, J. J., Raushel, F. M., Hill, Craig (2005) 'Stereospecificity in the enzymatic hydrolysis of cyclosarin (GF)', *Enzyme and Microbial Technology*, 37(5), pp. 547–555.

Ho, Y. S., Porter, J. F. and McKay, G. (2002) 'Equilibrium isotherm studies for the sorption of divalent metal ions onto peat: Copper, nickel and lead single component systems', *Water, Air, and Soil Pollution*, 141(1–4), pp. 1–33.

Holm, L. and Sander, C. (1996) 'An evolutionary treasure - Vast set of amido hydrolases related to urease', *Proteins*, 82(061/20), pp. 72–82.

Hoskin F. C. G., Walker J. E., Dettbarn W. D., and W. J. R. (1995) 'Hydrolysis of Tetriso By an Enzyme Derived From : Pseudomonas Diminuta As a Model for the Detoxication of O-Ethyl', *Biochemical Pharma*, 49(5), pp. 711–715.

Huling, S. and Pivetz, B. (2006) 'Engineering Issue Paper: In-Situ Chemical Oxidation', Engineering, pp. 1–60. Available at: http://scholar.google.com/scholar?hl=en&btnG=Search&q=intitle:Engineering+Is

sue+In-Situ+Chemical+Oxidation#3%5Cnhttp://scholar.google.com/scholar?hl=en&btnG=Search&q=intitle:Engineering+Issue+Paper:+In-Situ+Chemical+Oxidation#0.

Imazu, K., Tanaka, Sh., Kuroda, A., Anbe, Y., Kato, J., Ohtake, H. (1998) 'Enhanced utilization of phosphonate and phosphite by Klebsiella aerogenes', *Applied and Environmental Microbiology*, 64(10), pp. 3754–3758.

International Centre for Soil and Contaminated Sites (2006) 'Manual for Biological for Biological Remediation Techniques', *ICSS at the German Federal Environmental Agency POB 14 06 06813 Dessau GERMANY Source:*, pp. 81.

Ismail, M. G., Chan, N. W. and Rahman, H. A. (2013) 'Freundlich Isotherm Equilibrium Equations in Determining Effectiveness a Low Cost Absorbent to Heavy Metal Removal In Wastewater (Leachate) at Teluk Kitang Landfill, Pengkalan Chepa, Kelantan, Malaysia', *Journal of Geography and Earth Science*, 1(June), pp. 1–8.

Iyer, R. and Iken, B. (2013) 'Identification of water-borne bacterial isolates for potential remediation of organophosphate contamination', 2013(February), pp. 146–152.

Jao, Sh. Ch., Huang, L. F., Tao, Y. Sh., Li, W. Sh. (2004) 'Hydrolysis of organophosphate triesters by Escherichia coli aminopeptidase P', *Journal of Molecular Catalysis B: Enzymatic*, 27(1), pp. 7–12.

Jonas, L. A., Boardway, J. C. and Meseke, E. L. (1975) 'Prediction of adsorption behavior of activated carbons', *Journal of Colloid And Interface Science*, 50(3), pp. 538–544.

Kamanyire, R. and Karalliedde, L. (2004) 'Organophosphate toxicity and occupational exposure', *Occupational Medicine*, 54(2), pp. 69–75.

Kamath, R., Rentz, J.A., Schnoor, J.L., Alvarez, P.J.J. (2004) 'Chapter 16 Phytoremediation of hydrocarbon-contaminated soils: principles and applications', in *Petroleum Biotechnology: Developments and Perspectives Studies in Surface Science and Catalysis*, pp. 447–478.

Karigar, C. S. and Rao, S. S. (2011) 'Role of microbial enzymes in the bioremediation of pollutants: A review', *Enzyme Research*, pp.1-11.

Kensa V. M. (2011) 'Bioremediation - An overview', *Journal of Industrial Pollution Control*, 27(2), pp. 161–168.

Klaassen, C. D. (2019). Toxicology the Basic Science of Poisons. Casarett & Doull's. 6th Edition. P-1620.

Koptsik, G. N. (2014) 'Problems and prospects concerning the phytoremediation of heavy metal polluted soils: A review', *Eurasian Soil Science*, 47(9), pp. 923–939.

Krsti, D. Z., Lazarevi, T. D., Bond, A. M., Vasi, V. M. (2013) 'Acetylcholinesterase Inhibitors : Pharmacology and Toxicology', Current Neuropharmacology 11(3) 315-335.

Kumar, A., Bisht, B.S., Joshi, V. D., Dhewa, T (2011) 'Review on Bioremediation of Polluted Environment : A Management tool', *International journal of environmental science*, 1(6), pp. 1079–1093.

Kuppusamy, S., Palanisami, Th., Megharaj, M., Venkateswarlu, K., Naidu, R. (2016) *Ex-Situ Remediation Technologies for Environmental Pollutants : A Critical Perspective*. Reviews of Environmental Contamination and Toxicology Vol. 236: pp 117-192.

Lai K., Stolwich N. J., and W. J. R. (1995) 'Characterization of P-S Bond Hydrolysis in Organophosphorothioate Pesticides by Organophosphorus Hydrolase.', *Archives of Biochemistry and Biophysics*, 318(1), pp. 59–64.

Larson, R. A. and Weber, E. J. (1994) *Reaction Mechanisms in Environmental Organic Chemistry, Lewis Publishers is an imprint of CRC Press LLC*. PP: 433.

Lauer, J. L. (1964) 'Incinerator Temperature Measurement How , What and Where', *National Incinerator Conference*, pp. 165–169.

Lee, E. C. (2003) 'Clinical manifestations of sarin nerve gas exposure. A review of nerve agent exposure for the critical care physician', *Crit Care Med,* 290(5), pp. 659–662.

Lei, Y., Mulchandani, A. and Chen, W. (2005) 'Improved degradation of organophosphorus nerve agents and p-nitrophenol by Pseudomonas putida JS444 with surface-expressed organophosphorus hydrolase', *Biotechnology Progress*, 21(3), pp. 678–681.

Leung, M. (2004) 'Bioremediation: techniques for cleaning up a mess', *Journal of Biotechnology*, 2, pp. 18–22. Available at: http://bioteach.ubc.ca/Journal/V02I01/bioremediation.

Li, C., Srivastava, R. K. and Athar, M. (2016) 'Biological and environmental hazards associated with exposure to chemical warfare agents: arsenicals', *Annals of the New York Academy of Sciences*, 1378(1), pp. 143–157.

Liu, M., Zeng, Z., Wang, C., Tan, Y., Liu, H. (2003) 'Solid-phase microextraction of phosphate and methylphosphonate using novel fibers coated with a sol-gel-derived silicone divinyl benzene co-polymer', *Chromatographia*, 58(9–10), pp. 597–605.

Liu, Y. H., Chung, Y. C. and Xiong, Y. (2001) 'Purification and Characterization of a Dimethoate-Degrading Enzyme of Aspergillus niger ZHY256, Isolated from Sewage', *Applied and Environmental Microbiology*, 67(8), pp. 3746–3749.

Liu, Y., Liu, Y., Chen, Z., Lian, J., Huang, X., Chung, Y. (2004) 'Purification and

characterization of a novel organophosphorus pesticide hydrolase from Penicillium lilacinum BP303', *Enzyme and Microbial Technology*, 34(3–4), pp. 297–303.

López-Muñoz, F., Álamo, C., Guerra, J., García-García, P. (2008) 'Desarrollo de agentes neurotóxicos como herramientas de guerra química durante el período nacionalsocialista alemán', *Revista de Neurologia*, 47(2), pp. 99–106.

Martínez, J. L. and Baquero, F. (2000) 'MINIREVIEW Mutation Frequencies and Antibiotic Resistance', *Antimicrobial Agents and Chemotherapy*, 44(7), pp. 1771–1777.

Massiha, A., Pahlaviani, M. and Issazadeh, K. (2011) 'Microbial degradation of pesticides in surface soil using native strain in Iran', *International Conference on Biotechnology and Environment Management*, 18, pp. 76–81. Available at: http://www.ipcbee.com/vol18/16-ICBEM2011M10013.pdf.

Matei, V., Iulian C., Anca-Florentina, B. (2018) 'Stationary Phases', Advanced Gas Chromatography – Progress in Agricultural, Biomedical and Industrial 28 Applications. Petroleum and Gas University of Ploieşti,Romania, *Intech open*, 2, pp. 64.

Material Safety Data Sheet '(2010)'. Diethyl methylphosphonate sc-252711. P:1-8.

Mclean, J. E. and Bledsoe, B. E. (1992) 'Ground Water Issue: Behavior of Metals in Soils', *Regional Superfund Ground-Water Forum*, pp. 1–25.

Michalkova, A., Gorb, L., Ilchenko, M., Zhikol, O., Shishkin, O.,Leszczynski, J. (2004) 'Adsorption of Sarin and Soman on Dickite : An ab Initio ONIOM Study', Journal of Physical Chemistry B, 08(6) 1918-1930.

Milic, J., Beskoski, V., Ilic, M., Ali, S., Gojgic-Cvijovic, G., Vrvic, M. (2009) 'Bioremediation of soil heavily contaminated with crude oil and its products: Composition of the microbial consortium', *Journal of the Serbian Chemical Society*, 74(4), pp. 455–460.

Misik, J, Pavlikova, R., Cabal, J., and Kuca, K. (2015) 'Acute toxicity of some nerve agents and pesticides in rats', *Drug and Chemical Toxicology*, 38(1), pp. 32–36.

Morrissey, K. M., Schenning, A. M. and Cheicante, R. L. (2012) 'Sorption of Vx To Clay Minerals and Soils : Thermodynamic and Kinetic Studies', Edgewood Chemical Biological Center U.S Army Research, Development and Engineering Command, (December), pp. 92.

Nadeau, R., Singhvi, R., Ryabik, J., Lin, Y., Syslo, J. (1993) 'Monitoring for bioremediation efficacy: The Marrow Marsh experience', *International Oil Spill Conference Proceedings*, 1993(1), pp. 477–485.

Najafi, M. B.H. and Pezeshki, N. P. (2013) 'Bacterial Mutation; Types, Mechanisms and Mutant Detection Methods: a Review', *European Scientific Journal*, 4(December), pp. 1857–7881.

Nakayama, K., Ishikawa, S., Kawahara, K., Ohmori, T., Seto, Y. (2014) 'Improvement of organophosphorus hydrolase activity toward nerve agents by amino acid substitutions', *Forensic Toxicology*, 32(2), pp. 203–213.

Nowack, B. and Stone, A. (1999) 'Adsorption of Phosphonates onto the Goethite-Water Interface.', *Journal of colloid and interface science*, 214(1), pp. 20–30.

Ohmori, T., Kawahara, K., Nakayama, K., Shioda, A., Ishikawa, S., Kanamori-Kataoka, M., Kishi, S., Komano, A., Seto, Y. (2013) 'Decontamination of nerve agents by immobilized organophosphorus hydrolase', *Forensic Toxicology*, 31(1), pp. 37–43. doi: 10.1007/s11419-012-0162-5.

Oller, A. R., Fijalkowska, I. J., Dunn, R. L., Schaaper, R. M. (1992) 'Transcription-repair coupling determines the strandedness of ultraviolet mutagenesis in Escherichia coli.', *Proceeding of the National Academy of Science of the United States of America. United States,* (89), pp.11036-11040.

Parasuraman, S. (2011) 'Toxicological screening', *Journal of Pharmacology and Pharmacotherapeutics*, 2(2), pp. 74–79.

Pennington, J., Jenkins, T., Ampleman, G., Thiboutot, S., Brannon, J., Lynch, J., Ranney, T., Start, J., Walsh, M., Lewis, J., Hayes, C., Mirecki, J., Hewitt, A., Perron, N., Lambert, D., Clausen, J., Delfino, J. (2006) 'Distribution and Fate of Energetics on DoD Test and Training Ranges: Final Report', (March), pp. 1–165.

Perelo, L. W. (2010) 'Review: In situ and bioremediation of organic pollutants in aquatic sediments', *Journal of Hazardous Materials*. Elsevier B.V., 177(1–3), pp. 81–89. doi: 10.1016/j.jhazmat.2009.12.090.

Pielech-Przybylska, K., Ziemiński, K. and Szopa, J. S. (2006) 'Acetone biodegradation in a trickle-bed biofilter', *International Biodeterioration and Biodegradation*, 57(4), pp. 200–206.

Polat, S., Gunata, M. and Parlakpinar, H. (2018) 'Chemical warfare agents and treatment strategies', *Annals of Medical Research*, 25(4), p. 776.

Prasad, M., Garg, A. and Maheshwari, R. (2012) 'Decontamination of Polluted Water Employing Bioremediation Processes ':, *International Journal of Life Sciences*

Biotechnology and Pharma Research, 1(3), pp. 11–21.

Rabl, A. and Spadaro, J. V (2008) 'published in Waste Management & Research, vol.26, 147-162 (2008)', pp. 1–26.

Ramacharyulu, P. V. R. K., Kumar, J. P.,Prasad, G. K., and Dwivedi, K. (2014) 'Photoassisted remediation of toxic chemical warfare agents using titania nanomaterials', *Journal of Scientific and Industrial Research*, 73(5), pp. 308–312.

Raushel, F. M. (2002) 'Bacterial detoxification of organophosphate nerve agents', *Current Opinion in Microbiology*, 5(3), pp. 288–295. doi: 10.1016/S1369-5274(02) 00314-4.

Riedel, S. (2004) 'Biological Warfare and Bioterrorism: A Historical Review', *Baylor University Medical Center Proceedings*, 17(4), pp. 400–406.

Rohloff, J. (2015) 'Analysis of phenolic and cyclic compounds in plants using derivatization techniques in combination with GC-MS-based metabolite profiling', *Molecules*, 20(2), pp. 3431–3462.

Romeh, A. A. and Hendawi, M. Y. (2014) 'Bioremediation of certain organophosphorus pesticides by two biofertilizers, Paenibacillus (Bacillus) polymyxa (Prazmowski) and Azospirillum lipoferum (Beijerinck)', *Journal of Agricultural Science and Technology*, 16(2), pp. 265–276.

Rontani, J. F., Bonin, P. C. and Volkman, J. K. (1999) 'Biodegradation of free phytol by bacterial communities isolated from marine sediments under aerobic and denitrifying conditions', *Applied and Environmental Microbiology*, 65(12), pp. 5484–5492.

Sacmaci, S., Kartal, S., Sacmaci, M., Soykan, C. (2011) 'Novel solid phase extraction procedure for some trace elements in various samples prior to their determinations by FAAS', *Bulletin of the Korean Chemical Society*, 32(2), pp. 444–450.

Saxena, A., Sharma, A., Singh, B., Venkata, M., Suryanarayana, S., Mahato, T. H., Sharma, M., Semwal, R. P. (2005) 'Kinetics of In-situ Degradation of Nerve Agent Simulants and Sarin on Carbon with and without Impregnants', 6(3), pp. 158–165.

Schowanek, D. and Verstraete, W. (1990) 'Phosphonate utilization by bacterial cultures and enrichments from environmental samples', *Applied and Environmental Microbiology*, 56(4), pp. 895–903.

Schuldt S. J. (2007) *Biodegradation of Organophosphate Chemical Warfare Agents By Activated Sludge.*, *Virtualization Technology Applied to Rootkit Defense*. PP:38.

Singh, B. K. (2009) 'Organophosphorus-degrading bacteria: ecology and industrial

applications.', *Nature Reviews Microbiology*, 7(2), pp. 156–164.

Singh, B. K. and Walker, A. (2006) 'Microbial degradation of organophosphorus compounds', *FEMS Microbiology Reviews*, pp. 428–471.

Smart, J. K. (1997) 'History of chemical and biological warfare: an american perspective', *Medical Aspects of Chemical and Biological Warfare*, pp. 9–86.

Snyder L, and Champness, W. (2017) *Molecular Genetic Bacteria*. Third edit, *ASM WASHINGTON, d.c.* Third edit. pp-739.

Sogorb, M., and Vilanova, E. (2002) 'Enzymes involved in the detoxi cation of organophosphorus, carbamate and pyrethroid insecticides through hydrolysis', *Toxicology Letters*, 128, pp. 215–228.

Soltani, A., Bezi, J., Baei, M.T., and Azmoodeh, Z. (2018) 'Adsorption of chemical warfare agents over C24 fullerene: Effects of decoration of cobalt', *Journal of Alloys and Compounds*. Elsevier B.V, 735, pp. 2148–2161.

Talabani, J.M., Ali, A.I., Kadir, A.M., Rashid, R., Samin, F., Greenwood, D., Hay, A.W.M. (2018) 'Long-term health effects of chemical warfare agents on children following a single heavy exposure', *Human and Experimental Toxicology*, 37(8), pp. 836–847.

Theriot, C. M. and Grunden, A. M. (2011) 'Hydrolysis of organophosphorus compounds by microbial enzymes', *Applied Microbiology and Biotechnology*, 89(1), pp. 35–43.

Topczewski, J. J. and Quinn, D. M. (2013) 'Kinetic assessment of N-methyl-2-methoxypyridinium species as phosphonate anion methylating agents', *Organic Letters*, 15(5), pp. 1084–1087.

Trap, H. C. and Van Der Schans, M. (2007) 'Gas chromatographic techniques for the analysis of chemical warfare agents', *LC-GC Europe*, 20(4), pp. 202–207. Available at: http://www.scopus.com/inward/record.url?eid=2-s2.0-34047214276&partnerID=40&md5=0c10e5e28ececa419512cea3165a3641.

Tsai P.-Ch. , BigleyA., Li Y., Ghanem E. , Cadieux C. L. , Kasten Sh. A., Reeves T. E. , Cerasoli D. M., and R. F. M. (2012) 'Stereoselective Hydrolysis of Organophosphate Nerve Agents by the Bacterial Phosphotriesterase.', *Biochemistry.*, 1(3), pp. 233–245.

Uzarski J. (2009) 'Reflection Absorption Infrared Spectroscopic Studies of Surface Chemistry Relevant to Chemical and Biological Warfare Agent Defense'. *Dissertation submitted to the faculty of the Virginia Polytechnic Institute and State University in partial fulfillment of the requirements for the degree of Doctor of Philosophy In*

Chemistry.pp:246.

Vanninen, P. (2017). Recommended Operating Procedures for Analysis in the Verification of Chemical Disarmament. The Ministry for Foreign Affairs of Finland, University of Helsinki. PP:809.

Vidali, M. (2001) *Bioremediation. An overview*, *Pure and Applied Chemistry. Pure Appl. Chem.*, Vol. 73, No. 7, pp. 1163–1172.

Wackett, L. P. (1996) 'Co-metabolism: is the emperor wearing any clothes?', *Current opinion in biotechnology*. England, 7(3), pp. 321–325.

Walker, A. W. and Keasling, J. D. (2002) 'Metabolic engineering of Pseudomonas putida for the utilization of parathion as a carbon and energy source', *Biotechnology and Bioengineering*, 78(7), pp. 715–721.

Watford S. and Warrington S. J. (2018) *Bacterial DNA Mutations.*, *The National Library of Medicine, National Institutes of Health.pp:1-6. Last access 08-08,2019.*

Worek, F., Wille, T., Koller, M., Thiermann, H. (2016) 'Toxicology of organophosphorus compounds in view of an increasing terrorist threat', *Archives of Toxicology*. Springer Berlin Heidelberg, 90(9), pp. 2131–2145. doi: 10.1007/s00204-016-1772-1.

Zakharova, E. A., Kosterin, P. V., Brudnik, V. V., Shcherbakov, A. A., Ponomaryov, A. A.Shcherbakova, L. F., Mandich, V. G., Fedorov, E. E., Ignatov, V. V. (2000) 'Soil phytoremediation from the breakdown products of the chemical warfare agent, Yperite', *Environmental Science and Pollution Research*, 7(4), pp. 191–194.

Zhang, J., Lan, W., Qiao, Ch., Jiang, H., Mulchandani, A., Chen, W. (2004) 'Bioremediation of organophosphorus pesticides by surface-expressed carboxylesterase from mosquito on Escherichia Coli', *Biotechnology Progress*, 20(5), pp. 1567–1571.

Zheng, Y., Lifang, L., Yuanyuan, F., Jianping, G., Jianping, F., Weibin, J. (2013) 'A review on the detoxification of organophosphorus compounds by microorganisms', *African Journal of Microbiology Research*, 7(20), pp. 2127–2134.

Żwir-Ferenc A. and Biziuk M. (2006) 'Solid Phase Extraction Technique--Trends, Opportunities and Applications.', *Polish Journal of Environmental Studies*, 15(5), pp. 677–690

Chapter III

Determining the hydrolysis of DEMP in aqueous solutions and the soil surface

Chapter three highlights the investigation of DEMP's kinetic behaviour in soil for the adsorption process. Additionally, how DEMP behaves in aqueous solutions under various environmental conditions to evaluate the hydrolysis degradation-mechanisms is discussed. Furthermore, it gives a benchmark parameter for the biological study in the next chapters.

3.1 Abstract

DEMP kinetic experiments were carried out using a soil column, which is widely used to monitor and evaluate the behaviour and mobility of pollutants. The sorption process of DEMP examined the pseudo-first order, pseudo-second order, the distribution coefficient Kd, power function equation, and Freundlich and Langmuir models. The study also included DEMP hydrolysis using three different temperatures 25°C, 30°C 35°C and buffer aqueous solutions with pH levels of 6.0, 7.0, 10.0. The DEMP kinetic results revealed that the pseudo-second order (PSO) model was the best fit with the current empirical results. The rate constant for DEMP sorption was 1.04 min^{-1}. This result indicates that there might be more than two factors playing a role in DEMP sorption for example, soil, DEMP, and the liquid solution used. The linear distribution coefficient Kd was 0.95 mL g^{-1}, and the DEMP power function model was 3.47 min^{-1} (SE=0.219), indicating that DEMP sorption has affinities to the soil. DEMP fitted the Langmuir better than the Freundlich model and the value of KL was 0.14 L g^{-1}, suggesting that the adsorption increased with the time increase. The hydrolysis rates of DEMP were stable when acidic at 25°C and neutral buffer solutions at 30°C. The rate of DEMP hydrolysis was 0.01 min^{-1} and 0.03 min^{-1} under pH 6.0 (25°C) and pH 7.0 (30°C) respectively. The results indicate that increasing the temperature and the pH accelerate DEMP hydrolysis rate. This suggests that DEMP hydrolysis is dependent and temperature-dependent together, and the pH or temperature alone cannot be used as a parameter to predict the DEMP hydrolysis. The higher activation energy of DEMP kinetic hydrolysis were ordered based on the pH value studies into pH 7.0, which were 150.9 KJ mol^{-1}, pH 6.0 149.9 KJ mol^{-1}, and lastly pH 10.0 was 102.3 KJ mol^{-1}. This suggests that the Ea is pH-independent.

3.2 Introduction

The sorption of chemical substances is an important process to understand the fate of chemical compounds in the environment. Soil pollution by CWAs is linked to their usage in military and terrorist activities, or due to their disposal if unused (Rearden and Harrington 2005). Sorption is classified into positive and negative sorption (Calvet 1972). This process is influenced by soil characteristics, involving, cation exchange capacity (CEC), pH, texture, organic content (OC), and metal ions (Hu et al. 2019). Meanwhile, the examination of pollutants' sorption in soil is quite complex (Lambert 1967) because soil is characterised by heterogeneous compositions, and due to surface activity, there can be adsorption of chemical compounds essentially minimising their bioavailability (Torrents and Jayasundera 1997).

Two different mathematical models, Freundlich and Langmuir, can represent the sorption process equation (Jeppu and Clement 2012). Therefore, the objective of this experiment was to determine DEMP sorption behaviour to assess its availability in the soil and understand whether bioremediation is a feasible option for its decontamination.

In the aqueous environment, hydrolysis is a key process in which OP reacts with water by several reactive centers (Florian and Warshel 1998). The nucleophilic substitution and a direct displacement pathway are the significant reactions of OPs (Scheme 3.1) (Knowles 1980).

Many experiments were performed and are reported on in this chapter to estimate and understand DEMP hydrolysis, due to it containing an electrophile (a carbon or phosphorus atom), which can be attacked by a nucleophile (H_2O or OH^-) (Yang et al. 2006). This process is impacted by the presence of specific or general acid-base catalysis or metal ions catalysis (Larson and Weber 1994).

addition - elimination pathway

$$\left[\underset{R_2 \quad R_1}{OH\text{-}\text{-}\overset{\overset{\displaystyle X}{\|}}{P}\text{-}Z} \right]^{\ddagger \ominus} \longrightarrow \left[\underset{R_2 \quad R_1}{OH\text{-}\text{-}\overset{\overset{\displaystyle X}{\|}}{P}\text{-}Z} \right]^{\ominus} \longrightarrow \left[\underset{R_2 \quad R_1}{OH\text{-}\text{-}\overset{\overset{\displaystyle X}{\|}}{P}\text{-}Z} \right]^{\ddagger \ominus}$$

direct-displacement pathway

$$\underset{R_2 \quad R_1}{OH^-\text{+} \overset{\overset{\displaystyle X}{\|}}{P}\text{-}Z} \longrightarrow \left[\underset{R_2 \quad R_1}{OH\text{-}\text{-}\overset{\overset{\displaystyle X}{\|}}{P}\text{-}Z} \right]^{\ddagger \ominus} \longrightarrow \underset{R_2 \quad R_1}{OH\text{-}\overset{\overset{\displaystyle X}{\|}}{P}\text{+}} \quad Z^-$$
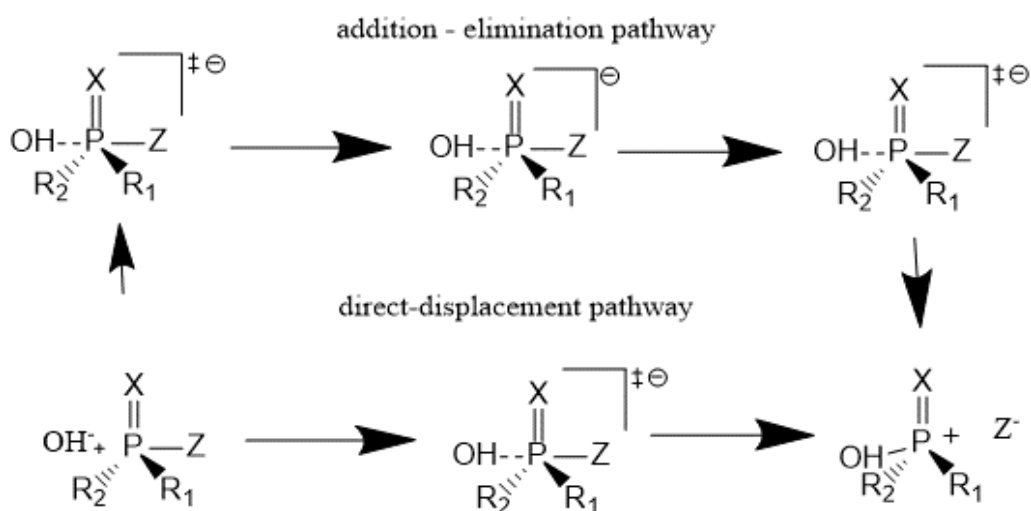
Scheme 3-1: Nucleophilic substitution variants at the phosphorus centre.

Hence, the aim of the current experiment was to: (i) determine the time required to break down DEMP itself under three different buffer solutions to characterise the hydrolysis mechanism of DEMP. (ii) To study the effect of activation energy using the Arrhenius equation to determine the energy required to initiate DEMP hydrolysis. The results of this chapter are a benchmark to the next chapter, in particular, to assess microbial based DEMP degradation.

3.3 Methodology

3.3.1 Reagents and soil properties

Analytical grade DEMP (purifying 96/9%) was purchased from Acros Organics, Geel, Belgium. All the solvents and chemicals were obtained from Sigma-Aldrich, whereas the flasks (100, 250 and 500 mL) used during the experiments were Erlenmeyer. Soil was collected from Wise Warren at Spen Farm, Tadcaster, England, which has no history of DEMP exposure, but is exposed to many OP pesticides. Prior to carrying out experiments, soil properties were determined. The physical and chemical characteristics of the soils are given in Appendix (3).

3.3.2 Sorption soil column

This experiment was conducted by a batch equilibrium method using a soil column. The soil was autoclaved three times at 121°C for 15 minutes to confirm that every microorganism was killed. 80 g of dried soil was packed in a 10cm plastic column and 4.5 dimeters with a filter paper in the bottom. 50 mL of 0.01M $CaCl_2$ was used to allow the soil to reach maximum capacity (saturating =1.6 mmol g^{-1}) and was kept for 24 hours to reach equilibrium. The plastic soil columns were put in the incubator shaker's holder using a blue tissue to tide it strongly at 30°C and 120 RPM for 24 hours. After equilibrium, 20 mL of 10 mg L^{-1} DEMP was passed through the column to measure DEMP concentrations by taking 1 mL effluent every 15 minutes by beakers and then transferred into Eppendorf. This elution was centrifuged at 14,000 rpm for 15 minutes, and filtered by a 0.22 μm syringe before the GC-FID analysis (Nur et al, 2014).

3.3.3 Buffered solution and temperature effect

Buffered solutions were prepared by following the proportions given in Appendix (4). For the study of DEMP hydrolysis influenced by the temperatures, three different temperatures were investigated, 25°C, 30°C, and 35°C. All flasks were incubated at 120 rpm and samples were withdrawn regularly to extract DEMP and injected in the GC-FID. The experiment was designed as follows: three 250 mL flasks containing 100 mL buffer solutions for the pH 6.0, 7.0, and 10.0, plus 5 mg L^{-1} DEMP with three replicates. Additionally, three 250 mL flasks containing 100 mL buffer solutions for the 0.02 M $CaCl_2$ plus 5 mg.L^{-1} DEMP were incubated under 30°C with three replicates.

3.3.4 Hydrolysis study and batch extraction

The hydrolysis of DEMP was studied by using buffered solutions at pH 6.0, pH 7.0, and pH 10.0. Three flasks for each buffered solution contained 5 mg L^{-1} DEMP in acetone. After the evaporation of acetone by N_2, the flasks were filled with 100 mL buffered solutions. Then, the flasks were covered with aluminium foil to avoid photolysis of DEMP and were kept under three different temperatures 25°C, 30°C and 35°C in an incubator. The concentrations of DEMP were measured every two days.

Samples of DEMP were withdrawn and extracted using DSC-18 SPE (1 mL, 100 mg of solid phase). 1 mL of the sample was taken out by micropipette. Then the sample was passed through an SPE cartridge. The adsorbed compounds were eluted with 2 mL of acetone. The organic solution was collected in a 4-mL vial. Finally, 1μL of the extract was injected into the GC-FID to measure the concentration of DEMP in the various buffer solutions over the period of the study.

3.3.5 DEMP analysis

Samples were analysed at the Kroto Research Institute using Gas Chromatography–Flame Ionization Detector (GC-FID) (Thermo Scientific Trace 1300 GC) and equipped by the column type and temperature: Chrompack capillary column CP-Sil 24CB, 30m 0.25mm. The analysis conditions were as follows: The FID (front) settings: Temperature = 250ºC, Ignition threshold= 0.5pA, Gas flow: Air = 330.0 mL min^{-1}, Hydrogen = 35.0 mL min^{-1}, Makeup gas = 40.0 mL min^{-1}, S/SL front Settings, S/SL mode, Split less, Inlet: Temperature = 200ºC, Split flow 50.0 mL min^{-1}, Split ratio = 0, Split less time = 1.00 min, Surge pressure = 0.725 psi, Surge duration = 0.00 min, Septum purge: Purge flow = 5.0 mL min^{-1}, Stop purge for = 0.00, Carrier mode: constant flow, Carrier flow, Flow = 1.500 mL min^{-1}, Carrier options: Gas saver flow = 20.0 mL min^{-1}, Gas saver time = 2.00 min. The oven run time of the data acquisition was 9:00 minutes at maximum temperature = 350.0 ºC, prep-run timeout = 999.99 min, Equilibration time = 0.50 min, Ready delay = 0.00 min.

3.4 Results and Discussion

3.4.1 Adsorption kinetics of DEMP

DEMP sorption process data were evaluated by following pseudo-first order (PFO) and pseudo-second order (PSO) models. The PFO equation was used by applying Eq. (3.1) (Tseng et al 2010).

$$ln\ (qe - qt) = ln\ qe - k_1 t \dots\dots\dots\dots\dots\dots\dots\dots\dots\dots\dots\dots\dots\dots \text{(3.1)}.$$

Where: - k_1 = is the equilibrium rate constant of the PFO sorption (min⁻¹), t = the time (min), qe = is the initial concentration of DEMP (mol L⁻¹) and qt = the amount adsorbed of DEMP (mol g⁻¹) at time t. Thus, the K_1 was calculated from the plot of (qe-qt) versus t.

The data of DEMP kinetic in this experiment did not display a linear trend. Thus, data will be fitted to the PSO model using Eq. (3.2) (Bezzina et al., 2018).

$$q_e = \frac{k_2 q_e^{2} t}{1 + k_2 q_e^{t}} \dots\dots\dots\dots\dots\dots\dots\dots\dots\dots\dots\dots\dots\dots\dots\dots \text{(3.2)}.$$

The equation above can be converted to linear form through applying Eq. (3.3).

$$\frac{t}{qt} = \frac{1}{k_2 q_e^2} + \frac{t}{q_e} \dots\dots\dots\dots\dots\dots\dots\dots\dots\dots\dots\dots\dots\dots\dots\dots \text{(3.3)}.$$

Where: - qe, qt, t = above described. K_2= equilibrium rate constant of the PSO sorption (min⁻¹). According to this equation, the PSO rate reaction of DEMP (K_{2nd}) and equilibrium sorption (qe) will be generated via the plotting of $\frac{t}{qt}$ versus a time (t).

The outcomes also enable determining the initial rate of DEMP reaction (ho) by applying Eq. (3.4) (Bezzina et al., 2018).

$$ho = kq_e^2 \dots\dots\dots\dots\dots\dots\dots\dots\dots\dots\dots\dots\dots\dots\dots\dots\dots \text{(3.4)}.$$

In consequence, DEMP fitted better to PSO than PFO, with the rate constant of the reaction being 1.04 min^{-1} (Fig.3.1).
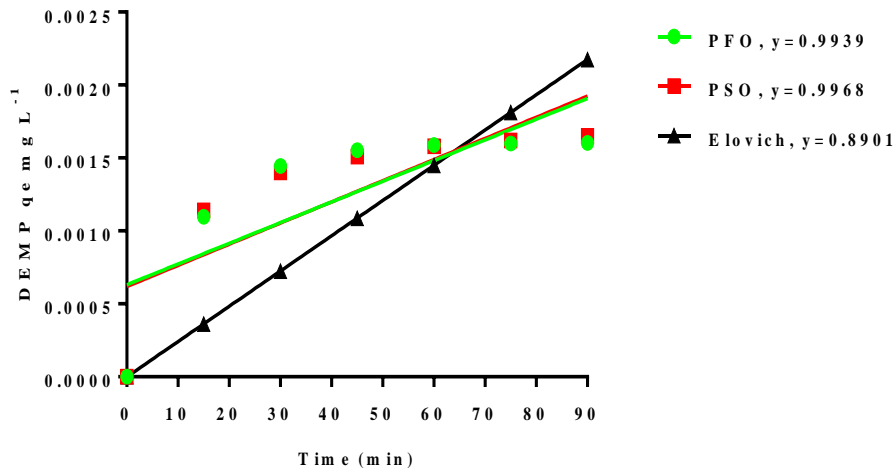
Fig. 3-1 Evaluating DEMP sorption under pseudo-first and pseudo-second order.

The soil column method is more suitable to study the breakthrough curve than the desorption model. Thus, this study was carried out to investigate the ability of DEMP to breakthrough soil using the Thomas model (Bhuvaneshwari and Sivasubramanian, 2014).

To calculate Thomas constant K_{Th} (L min^{-1} mg^{-1}) and q_0, using linear least square regression analysis of Eq. 3-6 by the plotting of $\ln\left(\frac{C_0}{C_t} - 1\right)$ vs time (t) and an adsorption column was expressed using nonlinear Thomas model by applying Eq. (3-5).

$$\ln\left(\frac{C_0}{C_t} - 1\right) = K_{Th}q_0 \, {}^M\!/_Q - K_{Th}C_0 t \dots\dots\dots\dots\dots\dots\dots\dots\dots\dots\dots\dots\dots\dots\dots\dots\dots\dots \text{(3-5).}$$

Where: - K_{Th} = Thomas rate constant (mL min^{-1} mg^{-1}), q_0 = equilibrium DEMP adsorbed per g of soil (mg.g^{-1}), C_0 = initial DEMP concentration (mg.L^{-1}), C_t= DEMP concentration at time t (mg L^{-1}), M= mass of soil (g), Q= filtration velocity mL.min^{-1} and t= time (min), and V= the flow rate (mL min^{-1}). This model allows the generation of a nonlinear plot by plotting $\ln\left(\frac{C_0}{C_t} - 1\right)$ vs time (t) (Fig. 3-2A).

$$\frac{C0}{Ct} = \frac{1}{1 + e^{\left(\frac{Kth}{Q}\right)}(q_m m - CiVef)} \dots\dots\dots\dots\dots\dots\dots\dots\dots\dots\dots\dots\dots\dots\dots\dots\dots\dots\dots\dots \text{(3-6).}$$

K_{Th}, q_0, C_0, C_t, M, Q, t as described above, and *Vef is* the effluent volume (mL) (Amphlett *et al.*, 2018). By plotting $\frac{C_0}{C_t}$ versus t, a nonlinear regression model can be generated (Fig. 3-2B).
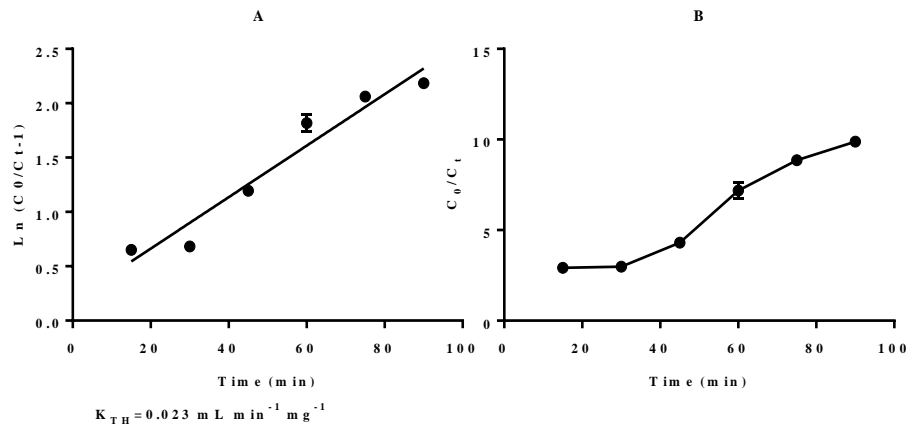
Fig. 3-2 Breakthrough curve of DEMP based on Thomas model.

3.4.2 Distribution coefficient Kd and Power Function

The value of Kd can be directly calculated using a batch experiment. This experiment involves mixing the mass of soil (g) in a soil column with 0.01M of $CaCl_2$ (mL) to minimise disruption of the soil mineral balance. Then the initial concentration Ci of DEMP is recorded in the liquid phase after 24 hours. The liquid is then analysed for equilibrium concentration Ce of DEMP in aqueous solution. The Kd sorption constant is then measured using Eq. (3-7). Kd is a ratio of the solid phase to solute concentration (Technical Report 123, 2019).

The Kd coefficient is a crucial parameter used to understand the chemicals' mobility in the ecosystem and their distribution between soil, sediment and water compartments (OECD, 2000). This is widely used because of its simplicity, hence DEMP sorption was expressed by a linear relationship of the distribution coefficient's Eq. (3.7). It supposes that DEMP concentrations held by the soil matrix, qe to the DEMP concentrations in the soil solution Ce.

$$Kd = {}^{qe}/_{Ce} \ldots\ldots\ldots\ldots\ldots\ldots\ldots\ldots\ldots\ldots\ldots\ldots\ldots \text{(3.7)}.$$

Where the Kd is the partition coefficient of DEMP sorption constant, qe = the DEMP concentrations in the soil (mg g^{-1}), and Ce is the concentrations of DEMP (mg L^{-1}) during the equilibrium. The qe is calculated via Eq. (3.8).

$$qe = \frac{(Ci-Ce)\,Vaq}{m} \dots\dots\dots\dots\dots\dots\dots\dots\dots\dots\dots\dots\dots\dots\dots\dots\dots\dots (3.8).$$

Ci = the concentration of DEMP used mg L^{-1}, Ce = previously described, Vaq is volume analysed (mL) and m= the mass of soil used (g).

The kd value of DEMP was 0.95 mL g^{-1}, which showed that DEMP moderately distributes and is adsorbed to soil, similarly also that DEMP can move to reach water. The high values of Kd in sulfadiazine (SDZ) (1.54 -3.41) L Kg^{-1} were compared to sulfamethoxazole (SMX), which ranged between (1.13-2.41) L Kg^{-1} in the soil. This indicated that SDZ has a higher affinity for soil adsorption compared to the SMX (Hu et al., 2019).

The power function equation is used to describe the sorption of DEMP from the soil. It can be measured by using Eq. (3.9) (Shariff, 2012).

$$Ln\,(C_t) = ln\,C_0 - klnt \dots\dots\dots\dots\dots\dots\dots\dots\dots\dots\dots\dots\dots\dots\dots\dots (3.9).$$

Where Ct= DEMP amount that was released at time t. By plotting Ln, Ct against Ln t, a straight line was generated with a slope K and intercept is Ln C$_0$. The value of DEMP-sorption power function was 3.47 min^{-1} (SE=0.219) (Fig. 3-3).

Power function = 3.47 min^{-1}, SE = 0.219, R^2 = 0.85
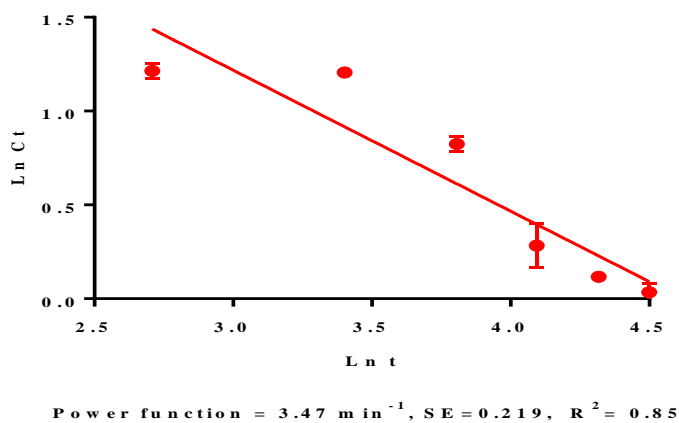
Fig. 3-3 Power function of DEMP behaviour in soil.

3.4.3 Freundlich and Langmuir models

DEMP concentrations were evaluated to the Freundlich sorption coefficient by using Eq. (3.10).

$$qe = aF C_e^{bF}$$ …………………………………………………………..…..……… (3.10).

Where qe: DEMP concentration adsorbed per unit mass of soil, bF, aF are Freundlich isotherm constants, and Ce mol L^{-1} is the equilibrium DEMP concentration in the solution. The plotting of Ln (qe) versus Ln (Ce) will provide the linear form of the Freundlich constant model.

Data of DEMP from batch sorption will confirm to the Langmuir model by applying Eq. (3.11).

$$q_e = \frac{qm\, K_L C_e}{1 + a_L C_e}$$……………………………………………….…………….… (3.11).

Where: -

qe: DEMP concentration adsorbed per unit mass of soil, KL: Langmuir isotherm constant, Ce is DEMP concentration at equilibrium, aL: Langmuir isotherm constant (Ho et al., 2002). The value of K$_L$ obtained by applying the linear form of the Langmuir through the plotting of the Ce/Cs versus Ce will generate a straight line (Fig. 3-4).
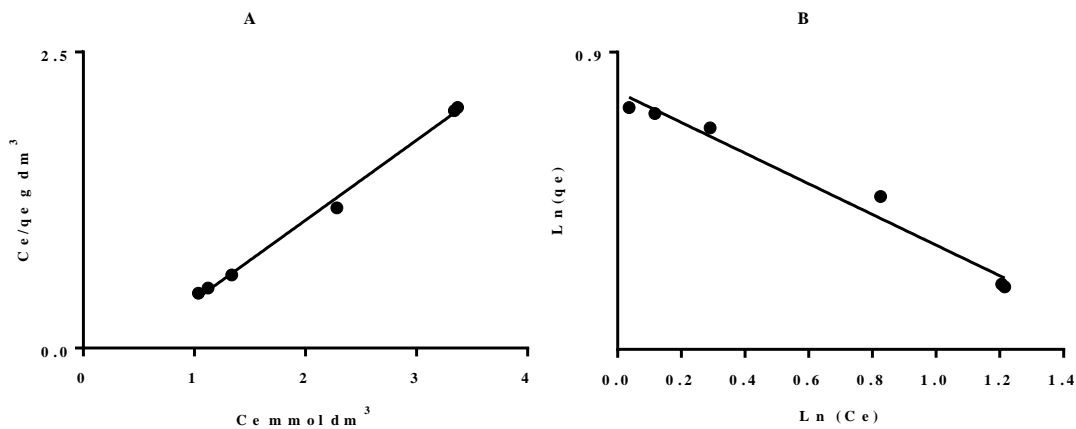
Fig. 3-4 DEMP sorption isotherm model A) Langmuir model B) Freundlich model.

Table 3.1 The profile of two models used to describe DEMP behaviour in soil. The data of DEMP sorption were assessed with both Freundlich and Langmuir models.

Table 3.1 Isotherm constant of two parameter models for DEMP sorption by linear regression.

Isotherm	Transformed		Slop	Intercept
	x-values	y-values		
Langmuir	Ce	Ce/qe	aL/KL	1/KL
Freundlich	Ln (Ce)	Ln (qe)	bF	Ln (aF)

Comparing the values of R^2, DEMP behaviour in soil demonstrated that the Langmuir model was the best fit to our data rather than the Freundlich model (Table 3.2), as long as, the Langmuir adsorption model is used to characterise the equilibrium between the chemical absorbent and adsorbent system. Hence, the Langmuir model, suggests that DEMP adsorbed has occurred on one molecule.

Furthermore, the homogeneity of the surface, which assumed there is no a sideways interaction, could have happened between an adjacent adsorbed of molecule in particular, when only one molecule takes one site on the surface (Liu et al., 2019).

Table 3.2 Data of DEMP isotherm constant of two parameter models for DEMP sorption by linear regression.

Freundlich model		Langmuir isotherm	
Freundlich aF (Freundlich isotherm)	2.301	Langmuir KL L g^{-1}	0.142
Freundlich bF (Freundlich constant)	0.258	Langmuir aL L $mmol^{-1}$	4.401
R^2	0.97	R^2	0.98
		Saturation capacity qm mmol g^{-1}	1.6

In contrast, the chemical compounds in the soil have different approaches of sorption. A first scenario (Shariff, 2011) suggested that the chemical compound is subjected to a quick removal from the solution at the beginning, then adsorbed on soil sites. Secondly, Chaudhary and Prasad (1999) described that a chemical first goes through the sorption sites of clay colloids, organic matter, and soil organic matter colloid complexes. A final scenario is the occurrence of a rapid absorption of the chemical substance in the soil due to the presence of many vacancies' sites.

Once these vacancies are full, this results in a decrease of the chemical, or chemicals that passed through the column.

In the current study, the high saturated soil (hydraulic conductivity) with a small amount of carbon allowed an amount of DEMP to pass via the soil column gradually. However, these stages depended essentially on the soil characterisation, for instance, negatively with the pH, and positively with organic carbon content (Kah and Brown, 2007). In addition, sorption is positively impacted by exchangeable and hydrolytic acidity (Kodešová et al., 2015).

Furthermore, the temperature and the pH of soil played a vital role in adsorption. Predominantly, the sorption decreased by increasing the soil pH and temperature (Liu et al., 2010). Hence, the effect of pH, in particular, had an impact on the soil's particle charge (Kah and Brown, 2006).

3.5 DEMP Hydrolysis in buffered media

The hydrolyses of DEMP in various aqueous buffered solutions pH 6.0, 7.0 and 10.0 were investigated at three different temperatures 25°C, 30°C, and 35°C. These represent acidic, base and neutral conditions. The DEMP hydrolysis reactions were evaluated using the integrated form of PFO under a constant pH of different buffer solutions to calculate the rate of reaction and half-life (DT_{50}).

During the reaction, samples were taken and extracted via SPE and directly analysed by GC-FID. The rate of DEMP reaction was measured via plotting the natural logarithm of DEMP concentrations versus time (day) for different temperatures by applying Eq. (3.12). The slope= -k represents the rate constant of DEMP reaction.

$$ln\frac{[DEMP]t}{[DEMP]o} = -kt \dots\dots\dots\dots\dots\dots\dots\dots\dots\dots\dots\dots\dots\dots\dots \text{(3.12)}.$$

While the half-life of DEMP in various buffer solutions was estimated using Eq. (3.13).

$$\text{Half-life} = \frac{lin\,[0.5]}{-k} \dots\dots\dots\dots\dots\dots\dots\dots\dots\dots\dots\dots\dots \text{(3.13)}.$$

A plot of the natural logarithm DEMP versus time has been given a straight line for each value of the pH 6.0, pH 7.0, and pH 10.0 with the slope representing the rate of DEMP reaction. The observed PFO rate constant for DEMP hydrolysis can be evaluated and expressed for the speed of kinetic reaction.

However, the rate constant hydrolysis reactions of DEMP varied according to the temperatures as well as the pH values. The rate constant of DEMP hydrolysis was 0.01, 0.03 and 0.06 day^{-1} at 25°C in the buffered solution pH 6.0, 7.0 and 10.0 respectively. While it scored 0.06, 0.11 and 0.11 day^{-1} at 30°C, additionally it rose, to 0.1, 0.22 and 0.22 day^{-1} at 35°C for the pH 6.0, pH 7.0 and pH 10.0 respectively (Fig. 3-5).
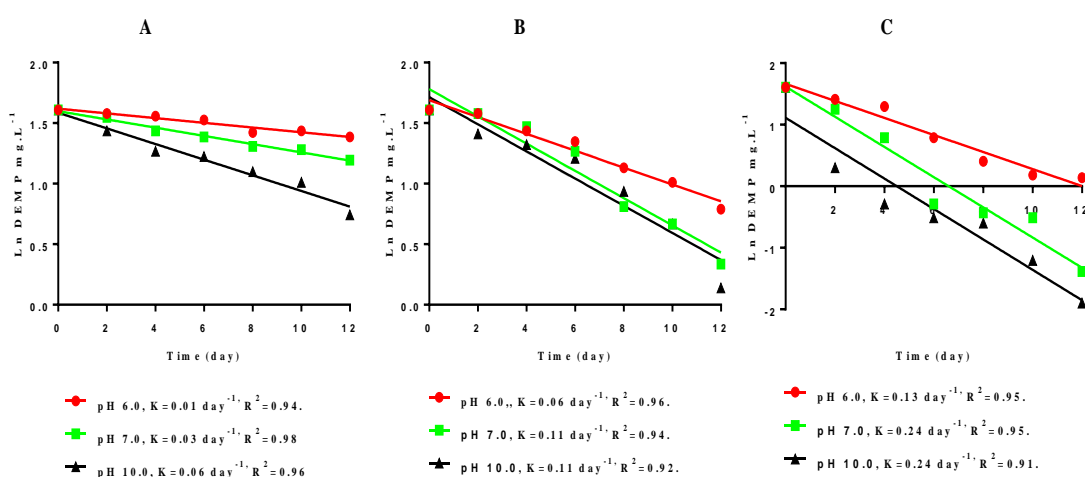
Fig. 3-5 Hydrolysis kinetic of DEMP as a function of pH at: A) 25°C, B) 30°C, and C) 35°C.

Understanding the hydrolysis of DEMP is important for a better realisation of its behaviour in the aquatic environment. This study found that there is hardly any DEMP hydrolysis under acidic environmental conditions. The acid catalysed hydrolysis does not begin to occur, except when pH is extremely low or even negative. Therefore, it is not of significant interest in biological and environmental investigations (Whiteside et al., 2007).

Furthermore, it is interesting to note that the mechanism of DEMP hydrolysis has a high rate of reaction under alkaline circumstances and a high temperature, indicating that the mechanism of DEMP hydrolysis was more influenced by the hydroxide ions catalysed compared to the

acidic and the neutral hydronium ions or water molecules. However, there is a slight difference between the hydrolysis rate constant of DEMP at pH 6.0 and pH 7.0, which suggests there is no significant influence. Whilst there is a significant difference between the rate hydrolysis constant of DEMP in the case of pH 6.0, and pH 7.0, compared to pH 10.0, it can be said that the hydrolysis rate constant reaction indicates that the DEMP is relatively stable in an acidic medium and the neutral medium compared to the alkaline medium.

Stability can be reduced by increasing the pH. This study supports evidence from previous observations (Moon et al., 2015). They concluded that CWA VX suffered rapid hydrolysis of the P-S bond (not P-O bond) at pH 10.0 when using some active catalysts, also resulting in reducing the half-life of the initial concentration to 1.8 minutes.

For DEMP hydrolysis in 0.02M $CaCl_2$ at 30°C, the results reveal that DEMP degradation was fast. The hydrolysis rate constant was 0.259 day^{-1} (Table 3-2) faster than when compared to hydrolysis at different pHs and temperatures. The presence of $CaCl_2$, increased the alkalinity of the medium, and enhanced the hydroxide ion OH^- or water molecule H_2O attack on DEMP. This was confirmed through the low hydrolysis of DEMP under acidic or neutral conditions at 30°C. Otherwise, the DEMP hydrolysis degradation was faster in the case of having a higher pH. This is similar to Khordagui (1995) who found that the presence of divalent metal content (Cu^{+2}, CA^{+2}, and Mg^{+2}) in the Arabian-Persian Gulf (A.P.G.) and high temperatures enables the increase and accelerates the hydrolysis of CWAs.

Another parameter, which indicates chemical persistence in the environment, is half-life (DT_{50}). This is the time required to decrease half of the initial concentration of the reaction. The DT_{50} of DEMP was calculated according to the kinetic PFO (Eq. 3.13). It is noted that DT_{50} varies with pHs and temperature.

The DT_{50} of DEMP was 69.3 days at a pH of 6.0 and decreased to 23.1 days at a pH of 7.0, it then reached 11.5 days at a pH of 10.0 (all at a temperature of 25°C). The values of DT_{50}, at 30°C were 11.55 days, 8.7 days and 8.7 days at the values of pH 6, 7 and 10, respectively.

These values of DT_{50} were decreased to 5.3 days, 2.8 days and 2.8 days at 35°C for the pH values of 6.0, 7.0 and 10.0, respectively. DEMP's half-life in 0.02M $CaCl_2$ at 30°C was 2.6 days as shown (Table 3-3). The effect of the temperature on the rate of DEMP hydrolysis was statistically analysed by measuring the correlations between the temperature and the DEMP

hydrolysis rate at three different pH values. The fit correlations were found to be 0.99, 0.98, and 0.96 in the various pH solution pH 6.0, pH 7.0 and pH 10.0 respectively.

In conclusion, these results indicate that DEMP is relatively stable under acidic and neutral conditions (Table 3-3). Therefore, in this chapter, the DT_{50} of DEMP in the acidic buffered solutions were much longer than in neutral, alkaline, as well as in the 0.02 M $CaCl_2$. These findings differ from those in Hui et al.'s (2010) study; they found the rate of the organic phosphorus pesticide chlorpyrifos hydrolysis slower in the 0.02M $CaCl_2$ solution. However, the findings are broadly consistent in terms of chlorpyrifos hydrolysis in various pHs and temperatures in revealing the rate of hydrolysis as well as the half-times; the persistence of up to 9.9 weeks under acidic and low temperature.

Table 3-3 Kinetic data of DEMP hydrolysis in buffered solutions and 0.02 M $CaCl_2$.

pH-values	At 25°C		At 30°C		At 35°C	
	Rate hydrolysis constant day^{-1}	Half-life (day)	Rate hydrolysis constant day^{-1}	Half-life (day)	Rate hydrolysis constant day^{-1}	Half-life (day)
pH=6.0	0.01	69.3	0.06	11.55	0.13	5.3
pH=7.0	0.03	23.1	0.11	8.7	0.24	2.8
pH=10.0	0.06	11.55	0.11	8.7	0.24	2.8
0.02 M $CaCl_2$	-	-	0.25	2.6	-	-

Furthermore, it is worth noting that the mechanism of hydrolysis of GB is similar to DEMP, where the hydroxyl ion nucleophilic attacks the phosphorus atom of the GB, resulting in influencing the P-F bond and formulation of two acid molecules in particular, under acidic and alkaline conditions (Larson and Weber, 1994).

The effect of OH^- on DEMP hydrolysis was studied by following Eq. (3.14).
pH+pOH=14…………………………………………………………………….... (3.14).
By substituting pH 6.0, 7.0, and 10.0 in Equation (3.14), three different values of OH^- will be generated. Plotting K versus OH^- will give K_B and K_N.

To investigate the role of pH on the hydrolysis of DEMP, a relationship between the logs of the DEMP hydrolysis rate versus different pH levels was plotted. By following Eq. (3.13) and plotting K versus OH⁻, the K_B is 378.8 day⁻¹ and the K_N is 0.02 day⁻¹ at 25°C and K_B is 211.4 day⁻¹ and K_N is 0.09 day⁻¹ at 30°C, while, K_B is 553.5 day⁻¹ and K_N is 0.19 day⁻¹ at 35°C (Fig. 3-6A). The high value of K_B (whether at 25°C, 30°C or 35°C) is due to a small number of pH and temperatures which were examined in this study. However, Fig. 3-6B revealed the relationship between the log of the rate constant as various pH functions at 25°C, 30°C as well as 35°C respectively.
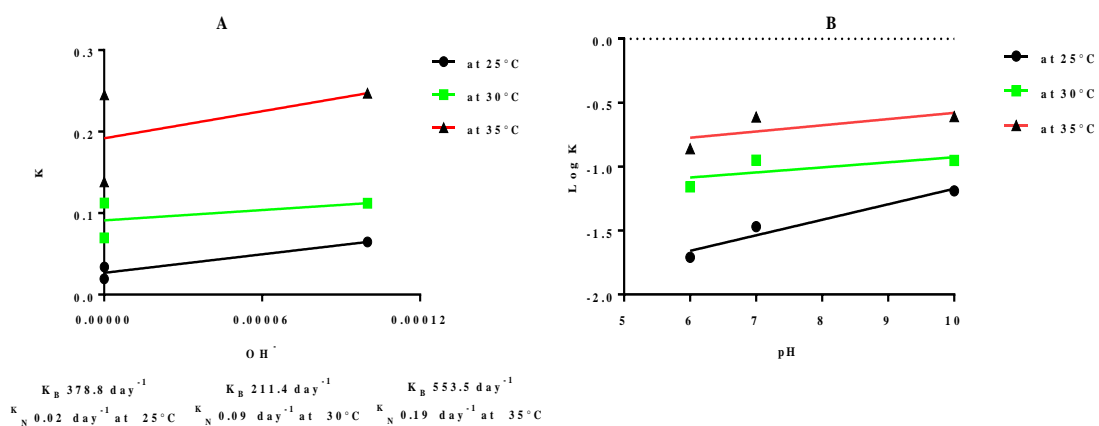
Fig. 3-6 DEMP profile at different pH levels (6.0, 7.0, 10.0) and different temperatures (25°C, 30°C, and 35°C) A) rate constant (K) as a function of OH⁻, B) rate constant (Kh).

Overall, the results of this study indicate that pH and temperatures have a potential impact on the hydrolysis rate of DEMP. These results are similar to those obtained from studies carried out previously. For instance, Zamy et al. (2004) found that the hydrolysis rates of four organophosphorus pesticides (disulfoton, isofenphos, isazofos and profenfos) and two carbamate pesticides (oxamyl and ethiofencarb) were slower in the acid with low temperatures (Hui et al., 2010). As a general conclusion, this present study shows that the degradation rate increased when the pH increased. Consequently, DEMP hydrolysis was faster at the high pH 10.0 and 35°C temperatures than at the low pH and low temperature.

To study the effect of temperature on the DEMP hydrolysis, the Arrhenius equation was calculated according to Eq. (3.15) to extract the Activation energy (Ea).

$$k= Ae^{\frac{-Ea}{RT}}$$ …………………………………………………..…………….……………….…(3.15).

Where: - the k is the rate constant, T is the absolute temperature (in Kelvin), and A is the pre-exponential factor, a constant for each chemical reaction. According to collision theory, A is the frequency of collisions in the correct orientation, Ea is the activation energy for the reaction (in the same units as R*T), R is the universal gas constant (Linert, 2013).

Activation energy (Ea) is the lowest amount of energy required to activate molecules or atoms to start the physical transport or a chemical transformation (Gregersen, 2019). In addition, it can be used as a parameter for DEMP hydrolysis based on the various temperatures. For that reason, the effects of temperatures on DEMP hydrolysis rate constant reaction were determined by the Arrhenius equation application that led to calculating the activation energy of the rate constant of DEMP hydrolysis.

Fig. (3-7) shows the straight lines, representing the activation energy results, which was constructed from the relation between ln k versus 1/t (the inverse of kelvin) to provide the linear plots. These values illustrate a significant difference when the buffered solution used has pH values equal to 6.0 or 7.0, and 10.0. The Ea of DEMP hydrolysis for pH 6.0 was 149.8 KJ mol^{-1}, while it was 150.9 KJ mol^{-1}, and 102.2 KJ mol^{-1} in the buffered solution pH 7.0 and 10.0 respectively, and the R^2 ranges from 0.97 to 0.98.
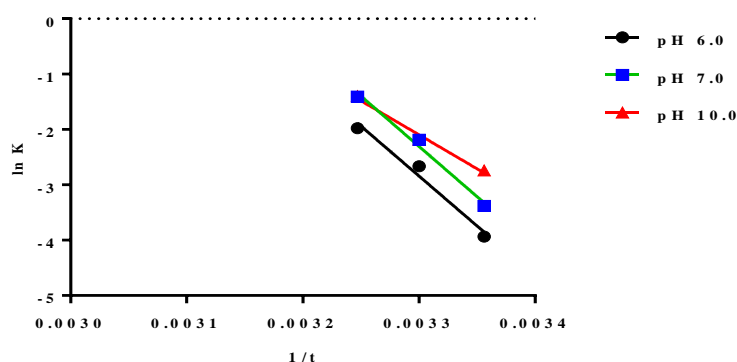
Fig. 3-7 The activation energy of DEMP hydrolysis kinetic at various pH: A) pH6.0, B) pH7.0, and C) pH 10.0.

The DEMP Arrhenius activation energy was lower at a high pH than both acidic and neutral buffered solutions. This might have resulted from the acidic reaction that required high energy to attack the phosphorus atom by the H$^+$. Likewise, Blecker et al. (2002) found that Ea, is independent of the reaction of pH, while, Hyne and Robertson (1955) illustrated that there is

some evidence about the failure of the Arrhenius equation to express the relation between the reaction rate and the temperature.

The Arrhenius equation presumes that there is no connection between temperature and the activation energy. This implies that the increase of temperature is not a unique impact of DEMP hydrolysis, as a higher pH value can increase DEMP hydrolysis with the least Ea. This is likely to indicate that DEMP hydrolysis is not sensibly dependent on only temperature, but also the values of pH. Nevertheless, it is known that a low temperature can lead to the long persistence of chemicals in the environment, particularly under slight pH conditions. This also can be shown by measuring the half-life of chemicals.

This present study suggests that both parameters enhanced the degradation of DEMP. In contrast, Dannenberg and Pehkonen (1998) found that the Ea was high with a high pH. It was 68 and 80 KJ mol^{-1} at pH 5.7 for disulfoton, while it was 98 and 91 KJ mol^{-1} for thiometon at pH 8.5. They attributed to the presence of unknown chemical catalysts or microorganisms that probably minimised their Ea values.

However, this current study showed that pH 6.0, and 7.0 have given the high activation energy of 149.8 KJ mol^{-1} and 150.9 KJ mol^{-1} respectively, compared to pH 10.0, which gave 102.2 KJ mol^{-1}.

The current results confirm that DEMP requires high activation energy to start the hydrolysis, which was roughly at low and neutral pH levels compared to the high pH that recorded 35.7 Kcal mol$^{-1.}$ (149.8 KJ mol^{-1}), 36.0 Kcal mol$^{-1.}$ (150.9 KJ mol^{-1}), and 24.4 Kcal mol^{-1} (102.2 KJ mol^{-1}). These values were not consistent with the range of OPs hydrolysis that ranged between 14 to 22 kcal mol^{-1} (Lartiges and Garrigues, 1995). Their study revealed the effect of pH on Ea was not clear, but it relies on the hydrolysis mechanism as well as the chemical structure of molecules (Huang and Mabury, 2000).

3.6 Conclusions

The present study is the first investigation into the behaviour and breakdown mechanism of the organophosphorus compound DEMP. The kinetic data of DEMP sorption in a soil column fits better to pseudo-second order equations than pseudo-first order. Furthermore, the evaluation of DEMP mobility in soil indicates that the current data were a better fit with the Langmuir model than the Freundlich. DEMP hydrolysis in various media underwent a pseudo-first order reaction. The hydrolysis rate reaction increased with an increase in both temperature and pH. The results of the hydrolysis rate and the half-lives show that DEMP is relatively stable under acidic conditions rather than the neutral and alkaline buffered aqueous media. However, increasing the pH or temperature individually or together decreased this stability. Moreover, the activation energy of DEMP hydrolysis at pH 10.0 was the lowest among the pH 6.0 or pH 7.0. The findings of this research provide insights into DEMP hydrolysis and support the hypothesis that DEMP breaks down due to OH^- and H_2O nucleophilic attack.

3.7 References

Amphlett, J. T.M., Sharrad, C. A., Foster, R. I., Ogden, M. D. (2018) 'Ethylenediamine-funtionalized ion exchange resin for uranium recovery from acidic mixed sulphate-chloride media: Initial column loading studies', *Journal of the Southern African Institute of Mining and Metallurgy*, 118(12), pp. 1251–1257.

Bezzina, J. P., Ogden, M. D., Moon, E. M., Soldenhoff, K. L. (2018) 'REE behavior and sorption on weak acid resins from buffered media', *Journal of Industrial and Engineering Chemistry*. The Korean Society of Industrial and Engineering Chemistry, 59, pp. 440–455.

Blecker, C., Fougnies, C., Van Herck, J.C, Chevalier, J.P., Paquot M., (2002) 'Kinetic study of the acid hydrolysis of various oligofructose samples.', Journal of agricultural and food chemistry, 50 (6), pp. 1602–1607.

Calvet, R. (1972) 'Adsorption of Organic Chemicals in the Soil Environment', Organic Chemicals in the Soil Environmental, vol 1, 83, pp. 49–144.

Chaudhary, K. and Prasad, B. (1999) 'Thermodynamics of Potassium Exchange Reaction in Entisol and Vertisol Using a Kinetic Approach by Miscible Displacement Technique', *Journal of the Indian Society of Soil Science*, 47(2), pp. 221-229.

Dannenberg, A. and Pehkonen, S. O. (1998) 'Investigation of the Heterogeneously Catalyzed Hydrolysis of Organophosphorus Pesticides', Journal of Agriculture and Food chemistry, 46(1), pp. 325–334.

Florian, J. and Warshel, A. (1998) 'Phosphate Ester Hydrolysis in Aqueous Solution: Associative versus Dissociative Mechanisms', Journal of Physical chemistry B, 102 (4), pp. 719–734.

Gregersen, E. (2019) Activation energy, , The Editors of Encyclopaedia Britannica. Available at: https://www.britannica.com/science/activation-energy (Last Accessed: 13 June 2019).

Ho, Y. S., Porter, J. F. and McKay, G. (2002) 'Equilibrium isotherm studies for the sorption of divalent metal ions onto peat: Copper, nickel and lead single component systems', Water, Air, and Soil Pollution, 141(1–4), pp. 1–33.

Hu, S. Zhang Y., Shen G, Zhang H, Yuan Z, Zhang W. (2019) 'Adsorption/desorption behavior and mechanisms of sulfadiazine and sulfamethoxazole in agricultural soil systems', Soil and Tillage Research. Elsevier, 186(November 2018), pp. 233–241.

Huang, J. and Mabury, S. A. (2000) 'Hydrolysis kinetics of fenthion and its metabolites in

buffered aqueous media.', Journal of agricultural and food chemistry, 48(6), pp. 2582–2588.

Hui, T. J., Ariffin, M. M. and Tahir, N. M. (2010) 'Hydrolysis of Chlorpyrifos in Aqueous solutions at different temperatures and pH (Hidrolisis Klorpirifos dalam Larutan Akueus pada Suhu dan pH Berbeza)', The Malaysian Journal of Analytical Sciences, 14(2), pp. 50–55.

Hyne, J. B. and Robertson, R. E. (1955) 'On the Temperature dependence of the Reaction Velocity', Canadian Journal of Chemistry. NRC Research Press, 33(10), pp. 1544–1551.

Jeppu, G. P. and Clement, T. P. (2012) 'A modified Langmuir-Freundlich isotherm model for simulating pH-dependent adsorption effects', Journal of Contaminant Hydrology. Elsevier B.V., 129–130, pp. 46–53.

Kah, M. and Brown, C. D. (2006) 'Adsorption of ionisable pesticides in soils.', Reviews of environmental contamination and toxicology. United States, 188, pp. 149–217.

Kah, M. and Brown, C. D. (2007) 'Prediction of the adsorption of Ionizable pesticides in soils', Journal of Agricultural and Food Chemistry, 55(6), pp. 2312–2322.

Knowles, J. R. (1980) 'Enzyme-Catalyzed Phosphoryl Transfer Reactions', Annual Review of Biochemistry, 49(1), pp. 877–919.

Khordagui, H. K. (1995) 'Fate and control of nerve chemical warfare agents in the desalination industry of the Arabian-Persian Gulf', Environment international. -, 214, pp. 363–379.

Kodešová, R., Grabic, R., Kočárek M., Klement A., Golovko O., Fér M., Nikodem A., Jakšík O. (2015) 'Pharmaceuticals' sorptions relative to properties of thirteen different soils', Science of the Total Environment, 511, pp. 435–443.

Lambert, S. M. (1967) 'Functional Relation between Sorption in Soil and Chemical Structure', Journal of Agricultural and Food Chemistry, 15(4), pp. 572–576.

Larson, R. A. and Weber, E. J. (1994) *Reaction Mechanisms in Environmental Organic Chemistry, Lewis Publishers is an imprint of CRC Press LLC*. PP: 433.

Lartiges, S. B. and Garrigues, P. P. (1995) 'Degradation kinetics of organophosphorus and organonitrogen pesticides in different waters under various environmental conditions.', Environmental science & technology. Easton, Pa.: American Chemical Society, 29(5), PP: 1246- 1254.

Linert, W. (2013) 'Isokinetic relationship', Chem. SOC. Rev.,. Wien: Springer, 18, pp. 477–505.

Liu, Y. Xu Z, Wu X, Gui W, Zhu G. (2010) 'Adsorption and desorption behavior of herbicide diuron on various Chinese cultivated soils', Journal of Hazardous Materials. Elsevier B.V., 178(1–3), pp. 462–468.

Liu, L., Luo, S-L. (2019) 'Application of Nanotechnology in the Removal of Heavy Metal From Water', *Nanomaterials for the Removal of Pollutants and Resource Reutilization*, pp. 83–147.

Moon, S., Wagner, G.W., Mondloch J.E., Peterson, G.W., DeCoste, J. B., Hupp, J.T, Farha, Ok. (2015) 'Effective, Facile, and Selective Hydrolysis of the Chemical Warfare Agent VX Using Zr_6-Based Metal–Organic Frameworks', Inorg. Chem. Inorganic Chemistry, 54(22), pp. 10829–10833.

Nur, T. , Loganathan, P., Nguyen, T.C., Vigneswaran, S., Singh, G., Kandasamy, J. (2014) 'Batch and column adsorption and desorption of fluoride using hydrous ferric oxide: Solution chemistry and modeling', Chemical Engineering Journal. Elsevier B.V., 247, pp. 93–102.

OECD. 2000. Adsorption – desorption using a batch equilibrium method. OECD Guideline for the testing of chemicals 106. Organisation for Economic Cooperation and Development, Paris, France, pp. 1-45.

Rearden, P. and Harrington, P. B. (2005) 'Rapid screening of precursor and degradation products of chemical warfare agents in soil by solid-phase microextraction ion mobility spectrometry (SPME-IMS)', *Analytica Chimica Acta*, 545(1), pp. 13–20.

Shariff, B. R. M. (2012) 'Kinetic & Thermodynamic Study for Adsorption– Desorption of Diazinon with Copper in The Presence of Surfactant', 12(4) pp. 17–31.

Shariff, R. M. (2011) 'Thermodynamic Adsorption-desorption of Metolachlor and 2,4-D on Agricultural Soils', International Journal of Chemistry, 3(4), pp. 134–146.

Tseng, R. L., Wu, F. C. and Juang, R. S. (2010) 'Characteristics and applications of the Lagergren's first-order equation for adsorption kinetics', *Journal of the Taiwan Institute of Chemical Engineers*. Taiwan Institute of Chemical Engineers, 41(6), pp. 661–669.

Torrents, A. and Jayasundera, S. (1997) 'The Sorption of Nonionic Pesticides onto clays and the influence of Natural organic Carbon.', Chemosphere, 35(7), pp. 1549–1565.

Technical report 123. (2019)'Adsorption-desorption Distribution (Kd) and Organic Carbon-water Partition (Koc) Coefficients. Last access 17-04-2020. Website: http://www.ecetoc.org/report/measured-partitioning-property-data/adsorption-desorption-distribution-kd-and-organic-carbon-water-partition-koc-coefficients

Whiteside, T., Carreira, L. and Hilal, S. (2007) 'Estimation of Phosphate Ester Hydrolysis Rate Constants. II. Acid and General Base Catalyzed Hydrolysis', QSAR & Combinatorial Science, 26(5), pp. 587–595.

Yang, S., Doetschman, D. C., Schulte, J. T, Sambur, J. B, Kanyi, C. W, Fox J. D, Kowenje, C. O, Jones, B. R., Sherma, N. D. (2006) 'Sodium X-type faujasite zeolite decomposition of dimethyl methylphosphonate (DMMP) to methylphosphonate: Nucleophilic zeolite reactions I', MICMAT Microporous and Mesoporous Materials, 92 (1–3), pp. 56–60.

Zamy, C., Mazellier, P. and Legube, B. (2004) 'Analytical and kinetic study of the aqueous hydrolysis of four organophosphorus and two carbamate pesticides', International Journal of Environmental & Analytical Chemistry. Taylor & Francis, 84: pp. 14–15.

Chapter IV

Biodegradation Strategies for Organophosphorus Compounds.

Chapter 4 investigates the isolation and adaptation of bacterial consortia to use DEMP as a carbon and phosphorus source. This is achieved through monitoring DEMP concentrations and ethanol production by GC-FID. Two different isolates were tested to degrade DEMP and tested in addition to the degradation of two other organophosphorus compounds, tributyl phosphate and triethyl phosphine-oxide.

4.1 Abstract

Organophosphorus compounds are used as chemical warfare agents and pesticides, and can reside in the environment for a relatively long time, presenting health hazards. Hydrolysis rates of an exemplar OP compound, DEMP, were characterised in aqueous solutions in Chapter 3 and found to be stable under acidic conditions pH 6.0 at 25°C and neutral conditions pH 7.0 at 30°C. Rates could be increased by raising the temperature from 0.01 day^{-1} at 25°C to 0.13 day^{-1} at 35°C at pH 6.0, and at pH 7.0, the rates increased from 0.03 day^{-1} at 25°C to 0.24 day^{-1} at 35°C. Chapter 4 details how a bacterial consortium was successfully enriched from soil regularly exposed to organophosphorus pesticides. Initial DEMP degradation rates were improved from 0.010 h^{-1} to 0.024 h^{-1} following 12-months of adaptive evolution. From this consortium, three bacterial strains were isolated and identified via 16S rDNA barcoding as *Bacillus cereus*, *Micrococcus luteus*, and *Dermacoccus nishinomiyaensis*. Their growth and individual capability to degrade DEMP was evaluated, as well as in synthetic combinations, compared to control *E. coli* cultures and the enriched consortium. The growth rate of *M. luteus* was fastest at 1.52 day^{-1} with a DEMP removal rate of 0.75 mg L^{-1} day^{-1}. Fourier-transform infrared spectroscopy confirmed that the strains' isolates used DEMP during their growth. The strains *B. cereus* and *M. luteus* were also able to break down alterative organophosphorus compounds, namely triethyl phosphine-oxide, and tributyl phosphate. The enzymatic degradation by *B. cereus* was increased to 0.13 and 0.14 day^{-1} for TEPO and TBP respectively. Furthermore, it has increased by using *M. luteus* in 0.12 of TEPO and 0.15 day^{-1} of TBP. In contrast, the hydrolysis rates for TEPO 0.01 day^{-1} and TBP 0.02 day^{-1} after 21 days indicate that the hydrolysis of TEPO and TBP were low and slow.

4.2 Introduction

The results of the DEMP hydrolysis rate constant in Chapter Three indicated that DEMP tends to be more stable under acidic and neutral buffer solutions at temperatures of 25°C and 30°C. Additionally, through a wide review of the degradation of chemicals in the environment by microbes, there are no reports of microorganisms that were isolated to break down DEMP (Fig. 4-1A), because DEMP has never been used in the ecosystem. For that reason, a key issue is the safe disposal of DEMP or to accelerate its degradation using a cost-effective and easily applied method.

One of the greatest challenges was how to obtain a microorganism with a high level of functionality performance. These challenges can be treated by bacterial evolution through the adaptation process. By following this process, bacteria can gain the necessary biophysical and biochemical functions, thereby increasing enzymatic capabilities, optimising the membrane characteristic, and a having regulatory network evolution to the environmental response (Hottes et al., 2013). The reason microorganisms can be used in the biodegradability is because bacteria play a critical role in their adaptive capability and their metabolism (Schmerk et al., 2015). Based on that, an enrichment culture technique (Cycoń' et al, 2013) was used by exposing soil microorganisms to 100 mg L^{-1} DEMP in mineral salts media (MSM) continuously for 12-months, aiming to obtain a bacterial consortium capable of using DEMP as a carbon-phosphorus source or both.

The positive aspect of bacterial adaptation is the capability of microorganisms to degrade not only the adapted compound, but also it might be useful for the bioremediation of other compounds (Singh and Walker, 2006). Accordingly, two bacterial isolates, *B. cereus* and *M. luteus,* were tested after a 12-month adaptation to degrade two other OPs compounds: triethylphosphine-oxide (TEPO) and tributyl phosphate (TBP). The reason for selecting of these substances is because they have a different electrophilicity. The electrophiles are an electron pair where the acceptor positive or neutral attracts an electron and participates in a chemical reaction by accepting an electron to bond with a nucleophile. For that reason, TBP (Fig. 4-1B) and TEPO (Fig. 4-1C) were examined.

TBP is extensively used as a solvent in fuel reprocessing in nuclear energy, hydraulic fluids, plasticizers, industrial additives, as well as CWAs (Berne et al., 2007). This compound is

implicated in causing environmental contamination due to its leakage from the production sites of various industries (Macaskie, 1991; Nakamura et al., 1991). Meanwhile, TEPO has been widely used as a solid acid 31P NMR probe molecule (Quinn et al., 2003; Toihara et al., 2015).

Although the role of bacteria isolated from contaminated soil by pesticides has been examined in their degradation, nevertheless the role of the adaptation process of microorganisms for the compounds has not been yet investigated in the biodegradation of a compound that has never been used. The current chapter will focus on the adaptation of soil microorganisms, leading to the acceleration of enzymatic degradation of DEMP as well as two different OPs compounds, TBP and TEPO.
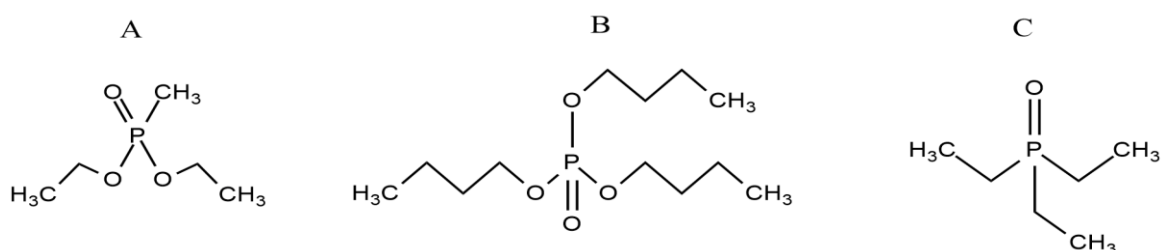
Fig. 4-1 The chemical structure of (A): Diethyl methyl Phosphonate, (B): Tributyl Phosphate (TBP), and (C): Triethyl Phosphine-Oxide (TEPO).

4.3 Aims

The aims of this chapter are to identify, characterise and improve the biodegradation capability of DEMP using environmental microorganisms. This goal has been undertaken via the following strategy:-

1. Isolating a bacterial consortium from soil to adapt it in the laboratory to mineralise DEMP as a carbon and phosphorus nutrient source.
2. Using adaptive laboratory evolution (ALE) to increase growth rates of microbial consortia on DEMP, increasing the rate of DEMP degradation.
3. Investigating the effects of carbon and phosphorus sources that govern DEMP degradation, using growth rate, determination of DEMP quantifications, ethanol production to ascertain which nutrient source provides bacteria with the ideal growth condition, and consequently completes DEMP degradation.

4. Isolating pure cultures of bacteria from the consortia, identified by polymerase chain reaction (PCR), and characterising their growth on DEMP individually and together, as a synthetic consortium, in a community matrix study. This step uncovers which microorganisms exist in the consortium, the capability of individual organisms to grow in the presence of DEMP (as a proxy study of DEMP degradation), and how to potentially improve degradation rates using combinations of bacteria.

5. Understanding whether the bacteria can degrade other OP compounds (TBP) and (TEPO).

4.4   Materials and Methods

To prepare the standard curve of DEMP, 7.9 µL DEMP was dissolved in 100 mg L^{-1} acetone to gain a concentrated stock solution. Flasks were covered with aluminium foil to avoid photolysis degradation. Working standard dilutions were obtained by dilution with acetone in order to be injected by GC-FID.

Ethanol solutions were prepared by dissolving in distilled water. Working dilutions were prepared using distilled water in 5 mL HPLC vials to inject by GC-FID. The stock solutions of both TBP and TEPO were carried out by dissolving 7.39 µL and 6.5 µL in 100 mL acetone. Then the series working solutions were prepared to be ready to inject GC-FID to obtain the standard curves of DEMP, ethanol, TBP, and TEPO respectively (Appendix 1).

For DEMP, TBP, and TEPO degradation studies, after dissolving those substances in acetone using various flasks, N_2 was used for acetone evaporation to use in the growth or degradation experiments. These flasks were covered with aluminium foil to avoid photolysis. MSM and MSM without phosphorus (MSM-P) were prepared to be ready when studying the bacterial consortium growth experiments in the laboratory.

4.4.1 Soil sample collection and its properties

See Chapter 3 Section 3.3.1.

4.4.2 Culture medium

The mineral salts media (MSM) have been used in bacterial adaptation, growth, and DEMP degradation. The compositions are shown in Table 4.1 (Cycoń et al., 2009). All compositions were dissolved in 1 L of distilled water. Then, the pH of the media was adjusted to 7.0 by NaOH 2M before autoclaving. The MSM was autoclaved at 121°C for 15 minutes.

Table 4.1 Compositions of mineral salts media used in this study.

No	mineral salts	Concentrations
1	$(NH_4)_2SO_4$	1 g L^{-1}
2	KH_2PO_4	2 g L^{-1}
3	$NaHPO_4$	1.5 g L^{-1}
4	$MgSO_4. 7H_2O$	1.5 g L^{-1}
5	$CaCl_2.2H_2O$	0.01 g L^{-1}
6	$FeSO_4. 7H_2O$	0.001 g L^{-1}

4.4.3 Enrichment and adaptation technique

To study the bacterial adaptation, the MSM (Table 4.1) with a specific amount of DEMP was prepared by dissolving 100 mg L^{-1} DEMP as a carbon source with acetone in flasks and evaporated by N_2. This enrichment media aimed to feed a bacterial consortium with 100 mg L^{-1} DEMP as a carbon source. The experiment was done by transferring one ml of soil suspension after 10 days of the incubation into fresh MSM +100 mg L^{-1} DEMP. The first consortium was harvested after 1 month, and was repeated at 6 and 12 months by three replications. The incubation conditions were 30ºC and 120 rpm in a Rotary Shaker Incubator.

4.4.4 Effects of carbon and phosphorus sources on DEMP biodegradation and detecting the DEMP metabolite

To investigate the capability of a bacterial consortium in utilising the carbon or phosphorus that was released from 100 mg L^{-1} DEMP in 250 ml flasks, a MSM-P or carbon was prepared (Table 4.1) except for $NaHPO_4$ and KH_2PO_4 which were replaced by 1 g L^{-1} NaCl and 1.04 g L^{-1} K_2SO_4 respectively. 1g L^{-1} of glucose was used as an extra carbon source. The experimental design is presented in Table 4.2.

Table 4.2 Experimental design for studying the effect of carbon and phosphorus sources on the   growth of bacterial consortia in various MSM

No. Of treatment	Source effect	Type of treatment
Treatment 1	carbon	Bacterial consortium + MSM + 100 mg L^{-1} DEMP
Treatment 2		Bacterial consortium + MSM + 1g L^{-1} glucose only
Treatment 3		Bacterial consortium + MSM + 1g L^{-1} glucose + 100 mg L^{-1} DEMP
Treatment 4	control	Bacterial consortium + MSM only
Treatment 5		Bacterial consortium + MSM-P only
Treatment 6	phosphorus	Bacterial consortium + MSM-P + 100 mg L^{-1} DEMP

4.4.5 Preparation of Inocula for degradation studies

A 1 mL of bacterial consortium was inoculated in 5 ml of LB and 10 mM DEMP overnight at 30°C and 120 rpm for 24 hours. Bacteria were centrifuged at 14,000 rpm for 10 minutes. Pellet cells were re-suspended in sterile saline water 0.85% (w/v) NaCl in order to prepare the bacterial suspension (approximately $\approx 10^6$) CFU mL^{-1} to use later in all biodegradation studies.

4.4.6 DEMP extraction and Gas Chromatography analysis

As given in Chapter 3 (3.3.4) and (3.3.5) respectively.

4.4.7 Screening, isolation and purification of DEMP-degrading bacteria

After 12-months of bacterial evaluating adaptation, 1 mL of the last culture adaptation was taken with 9 mL of serial saline water (0.85% NaCl) to make 10-fold serial dilutions (10^{-1}-10^{-10}) onto R2A containing 100 mg L^{-1} DEMP as a carbon and phosphorus source and incubated at 30°C, for 3 days. Bacterial colonies were screened based on the morphological

characterisation. Three different strains were picked up as DEMP-degrading bacteria and sub-cultured with 100 mg L^{-1} DEMP for four times on the R2A plates to obtain a pure culture.

4.4.8 Bacterial strains and their identification

4.4.8.1 DEMP-degrading characterisation and 16s rRNA gene amplification

To identify the bacterial strains, a PCR method was used in conjunction with primers designed to target the gene coding for 16s RNA. The primers used were either: 27F (5'-AGAGTTTGATCMTGGCTCAG-3') or 511R (5'-GCGGCTGCTGGCACRKAGT-3') as described by Liu et al., (2015). Cells from a single colony of the bacteria under investigation were re-suspended in 300 ul of sterile water, and 1 µl used for the subsequent PCR reaction.

PCRs were carried out using the Q5® High-Fidelity PCR kit from New England Bio Labs as per the manufacturer's instructions with the following PCR conditions: a) 1 cycle 98°C 15 minutes, b) 35 cycles Melt 98°C 1 min, Anneal 55°C 1 min, and an Extension 72°C 1 min, c) 1 cycle and 72°C 10 minutes. PCR products were run out on an agarose electrophoresis gel preloaded with ethidium bromide and the fragment of gel containing the 16s RNA gene was cut out with a scalpel.

DNA was recovered from the gel fragment using a QIA Quick Gel Extraction Kit (Qiagen) and following the manufacturer's instructions. An aliquot of the purified DNA was sent to the DNA sequencing Core Genomic Facility at the University of Sheffield, and the resulting DNA sequence was then compared to those in the Blast database online software at the NCBI (National Centre for Biotechnology Information) (https://blast.ncbi.nlm.nih.gov/blast.cgi) for the species identification. Phylogenetic trees were constructed by using http://www.phylogeny.fr.

4.4.9 Biodegradation studies of three bacterial strains

4.4.9.1 Preparing isolate pre-cultures in MSM-P growth medium

A 1 mL of bacterial pellet strains were incubated in the 10 mL of MSM-P in 50 mL falcon tubes (three falcons for each isolate), in addition to three for the consortium and the negative control *Escherichia coli* and the positive control of *Pseudomonas fluorescence* (obtained from Dr. Esther Karunakaran). Falcons were capped well and incubated at 30°C with shaking at 120 rpm for 72 hours.

4.4.9.2 Microplate Reader Method for Measuring Cell Growth

The TECAN microplate reader instrument was used to measure the optical density (OD) using a 96-well. This ran over a 96-hour period. 20 µL of each isolate from the pre-cultures grown were added to 180 µl of MSM-P treated with 100 mg L^{-1} DEMP as carbon and phosphorus sources. The total inoculating volume of each well of a 96-well plate was a 200 µL working volume. *E. coli* (used as negative control) and *P. fluorescence* (as a positive control) were added to the NUNC micro-well 96. The 96-well plate was placed in a Genios Multiwell plate reader from TECAN UK. It was set to take optical density measurements at 595 nm. Measurements were set to be taken every hour over a 98-hour period, with shaking enabled and the incubation temperature at 30°C.

4.4.10 Biodegradation of TBP, and TEPO by *B. cereus* and *M. luteus*

250 mL of flasks was supplemented with 100 mg L^{-1} TBP, and TEPO in acetone. Flasks were incubated in a shaking incubator overnight to evaporate the acetone. All flasks were covered with aluminium foil to avoid the photo degradation effect. Bacterial suspension inocula of *B. cereus*, and *M. leutus* were prepared, as given in (4.4.5). The flasks were supplemented with 190 mL of the MSM plus 10 mL of 10^6 CFU mL^{-1} different bacterial strains. The experiment was performed at 30°C, and 120 rpm. Samples were withdrawn at regular intervals to measure TBP, and TEPO concentration by GC-FID. The experiment was designed as per Table 4.3.

Table 4.3 Experimental designed of biodegradation of TBP and TEPO.

No. Of treatment	Type of treatment
Treatment 1	100 mg L^{-1} TBP only to study hydrolysis of TBP
Treatment 2	100 mg L^{-1} TEPO only to study hydrolysis of TEPO
Treatment 3	*B. cereus* + 100 mg L^{-1} TBP to study enzymatic degradation
Treatment 4	*B. cereus* + 100 mg L^{-1} TEPO to study enzymatic degradation
Treatment 5	*M. luteus* + 100 mg L^{-1} TBP to study enzymatic degradation
Treatment 6	*M. luteus* + 100 mg L^{-1} TEPO to study enzymatic degradation

4.4.11 TBP and TEPO extraction and Gas chromatography analysis

TBP and TEPO were extracted, and analysed by the same method of DEMP extraction detailed in Chapter 3 (3.3.4) and (3.3.5) respectively. The retention time of TBP was 8.1 minutes, while TEPO was 10.4 minutes.

4.4.12 Fourier-transform infrared spectroscopy (FTIR)

The purpose of this experiment is to confirm DEMP degradation by three different strains, using FT-IR spectroscopy. 2 mL of aliquot culture was drawn from each overnight LB culture. Supernatants were removed after centrifugation at 14,000 rpm for 10 minutes. Bacterial cell pellets were washed with saline 0.85% w/v of NaCl and 1 mL of pellet was added into a 50 mL falcon containing 2 mL of MSM-P plus 10 mM DEMP and incubated for 48 hrs. Then, this media was centrifuged at 14,000 rpm for 10 minutes. The supernatant was removed and bacteria left in the shaking incubator at 35°C for half an hour to dry. A small amount of dried bacteria was analysed by FT-IR in triplicate (Gomez et al., 2006). The FT-IR of MSM-P was used as a reference spectrum to determine the changes that occurred in the bacterial strains in the presence of DEMP. The wavenumber ranged between 600-3800 cm^{-1}.

4.4.13 Calculation of DEMP, TBP, and TEPO degradation rate and Statistical analysis

A one-way ANOVA was used to compare the growth of three different consortia plus the control, the comparison of bacterial evolution consortia, and the growth rate of bacterial consortia in various MSM. Furthermore the effect of carbon and phosphorus on consortia growth at $P<0.05$ by using IBM SPSS statistical 25 was examined. A T-test was used to compare between the releases of ethanol from DEMP. All data were calculated as mean ± standard deviation (SD), and the kinetics data were carried out as per Chapter 3 Eq.3.12 and Eq.3.13.

4.5 Results and Discussion

4.5.1 Characterisation of evolved microbial consortia

The objective of this experiment was to compare the evolution of three consortia that adapted to DEMP for three different time periods: 1-month, 6-months, and 12-months. The one-way ANOVA showed the consortium that adapted for 12-months achieved significant difference in the bacterial yield compared to the 1-month adaptation and the control. Therefore, the results (Fig. 4-2A) denote the bacterial yield of a consortium of 12-month's adaptation, which achieved 0.36 ± 0.04, while 6-months and 1-month reached the yield 0.22 ± 0.05 and 0.16 ± 0.02 after 48 hours respectively. In contrast, the control reached 0.09 ± 0.003.

The results obtained show a one-way ANOVA statistical analysis of the bacterial growth rate of three different consortia (Fig. 4-2B). As the figure shows, there was a significant difference at $p<0.05$ in bacterial growth rate for the consortium, which adapted for different periods as follows: 1-month vs 6-months, 1-month vs 12-months, 6-months vs control, and 12-months vs control. However, there was no significant difference in terms of 1-month vs control, and 6-months vs 12-months. The bacterial growth of 12-months and 6-months adaptation was 0.07 h^{-1} compared to the 1-month adaptation 0.02 h^{-1} and the control 0.01 h^{-1}.
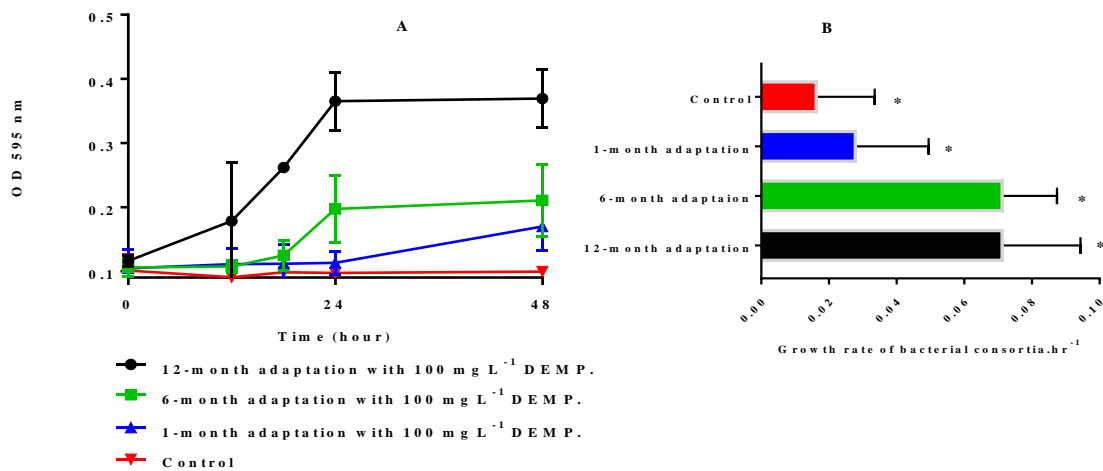
Fig. 4-2 Comparison of evolved microbial consortia A) growth yield of 1-month, 6-months, and 12-months adaptation, B) statistical analysis of three different consortia growth rates. Error bars are standard deviation (n = 5).

Applying selective pressure to bacteria can enable evolution of functional traits to achieve particular objectives, for example, improving bioremediation or biomanufacturing (Cobb et al., 2013). The adaptation process (adaptive laboratory evolution, ALE) drives microorganisms to change their genetic structure (Patel and Rosenthal, 2007). For example, a previous study revealed the role of *Pseudomonas putida* adaptation in degrading p-nitrophenol (PNP) through using the simple salts medium with PNP as a sole carbon source (Nishino and Spain, 1993). It concluded that the adapted bacterial strain over a long period enhanced the bacterial growth, leading to fast growth rate that was much better than the short-term adaptation process, which did not improve the bacterial consortium growth.

4.5.2 Effect of additional carbon and phosphorus sources

4.5.2.1 Growth rate changes

To understand the consortium growth in the media of different compositions, the effect of using an extra source of carbon in the form of 1 g L^{-1} glucose on bacterial growth was studied (Fig.4-3A). A one-way ANOVA showed that using 1 g L^{-1} glucose and 100 mg L^{-1} DEMP achieved a significant increase in consortium growth compared to using DEMP only or the MSM without DEMP at $p<0.05$, whilst there was no significant difference in consortium growth when using glucose or DEMP only. This potentially suggests that using both sources of carbon resulted in an ideal consortium growth. Thus, the data obtained indicates the capability of the consortium to utilise the extra carbon in the medium and the carbon that was released from DEMP to achieve the highest bacterial yield.

The highest yield of the consortium was recorded when using DEMP plus 1g L^{-1} glucose followed 1g L^{-1} glucose only, DEMP only. The lowest was when there was only the consortium in the MSM. The final yields were 1.9 ±0.07, 0.53±0.02, 0.31±0.004 and 0.18±0.001 after 21 days of incubation respectively.

From this data, it is apparent that bacteria have utilised both carbon sources for growth. A previous study by Moneke et al. (2010) found that bacteria have the ability to grow significantly in the mineral salts culture containing glucose as an extra carbon source.

However, Fig. (4-3B) showed the one-way ANOVA for the effect of phosphorus on the consortium growth. It is noted there was no significant growth when using MSM-P plus 100 mg L^{-1} DEMP compared to using MSM-P only, and the only significant growth at $p<0.05$ was achieved when using MSM only versus MSM-P only. This might be due to the absence of phosphorus in the MSM-P, causing a tiny bacterial growth.
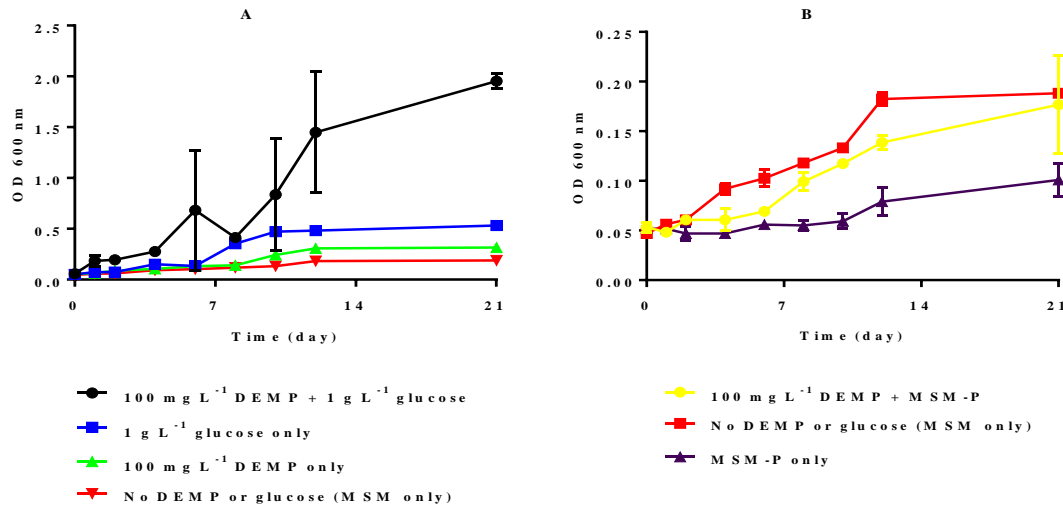
Fig. 4-3 Consortium growth curves based on A) the effect of carbon source, and B) the effect of phosphorus source. Error bars are standard deviation (n = 3).

In terms of the MSM-P, which contains 100 mg L^{-1} DEMP, a bacterial consortium requires time to start degrading DEMP effectively. Consequently, there was also little bacteria growth when using MSM only, but without significant difference from the MSM-P plus 100 mg L^{-1} DEMP. This result suggests that using MSM-P plus 100 mg L^{-1} DEMP did not achieve a significant increase in consortium growth. Therefore, these results illustrate the ability of bacterial consortia to grow in the MSM-P provided with DEMP, but this growth was slow and the bacterial yield reached 0.1761 ± 0.04, while it was 0.101 ± 0.01 in the MSM-P only. In contrast, the growth of bacterial consortia reached 0.188 ± 0.001 in the MSM only after 21 days of incubation.

Accordingly, a one-way ANOVA statistical analysis at $P<0.05$ was carried out (Fig.4-4). The consortium growth was influenced by using different media compositions. The highest growth rate was recorded in the case of using DEMP and 1g L^{-1} glucose together 0.34 day^{-1} or using the glucose only as an extra carbon in the MSM media, which were 0.31 day^{-1} compared to the MSM-P which was 0.14 day^{-1}. Taken together, these results suggest that there is an association

between using an extra carbon source with DEMP and the bacterial growth. Furthermore, there was a difference when using the MSM (in the presence of phosphorus), which was better than using the MSM-P only.
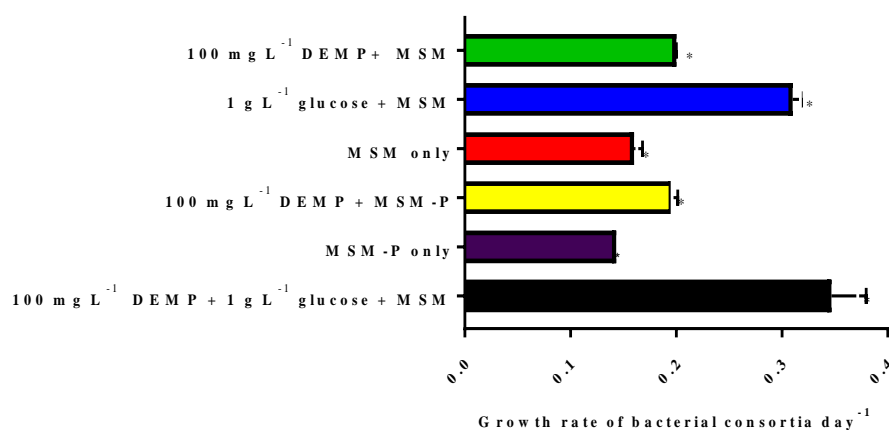
Fig. 4-4 Relative growth rates of bacterial consortia in the different MSM culture media. Data represented shows the means of three independent measurements. *A significant difference in growth rate of consortia at $p < 0.05$. Error bars are standard deviation (n = 3).

4.5.2.2 Quantification of DEMP degradation rates

Biodegradation of OP compounds is a process to break down these substances into eco-friendly substances such as, H_2O and CO_2. The data in Figs. (4-5A and 4-5B) show the bacterial consortia growth, DEMP degradation, and the hydrolysis rate constant of DEMP in the MSM media. It reveals that bacterial consortia can grow and break down 100 mg L^{-1} DEMP in the MSM as a carbon source within 21 days of incubation, faster than that from the MSM-P.

For the bacterial consortia yield in the MSM, the bacterial yield started sharply on day 8 of incubation. It reached 0.31 ±0.004 after 21 days. Meanwhile, the results were confirmed by measuring DEMP concentrations, where concentrations started to decrease from 100 mg L^{-1} on the first day of the incubation to reach 13 mg L^{-1} on the eighth day, then slowly decreased after 21 days to 6.6 mg L^{-1} when the consortia entered the stationary phase. In contrast, the hydrolysis of DEMP was slow, compared to enzymatic degradation.

By comparing the DEMP degradation and the yield of a consortium between the MSM-P and the MSM, we can see that the degradation of DEMP was lower than the MSM. Moreover, the

yield of consortium in the MSM was greater than the MSM-P. The response of bacteria growth in the MSM compared to the MSM-P was likely due to the nutritional requirements (various nutrients) (Table 4-1) where the MSM provides bacteria diverse nutrients, for instance, potassium, sodium and phosphorus, or may raise the pH, driving bacteria for healthy growth (Nottingham et al., 2018). Furthermore, a carbon source is released from DEMP. In contrast, the MSM-P medium lacked potassium, sodium and phosphorus nutrients.

The consortium started to grow after 10 days. The optical density was 0.05 ± 0.005, and reached 0.17 ± 0.04 after 21 days. Meanwhile, DEMP concentrations slowly decreased from 100 mg L^{-1} to 22.6 mg L^{-1} on day 10, and it continued to slowly decrease after 21 days to 14.3 mg L^{-1}.
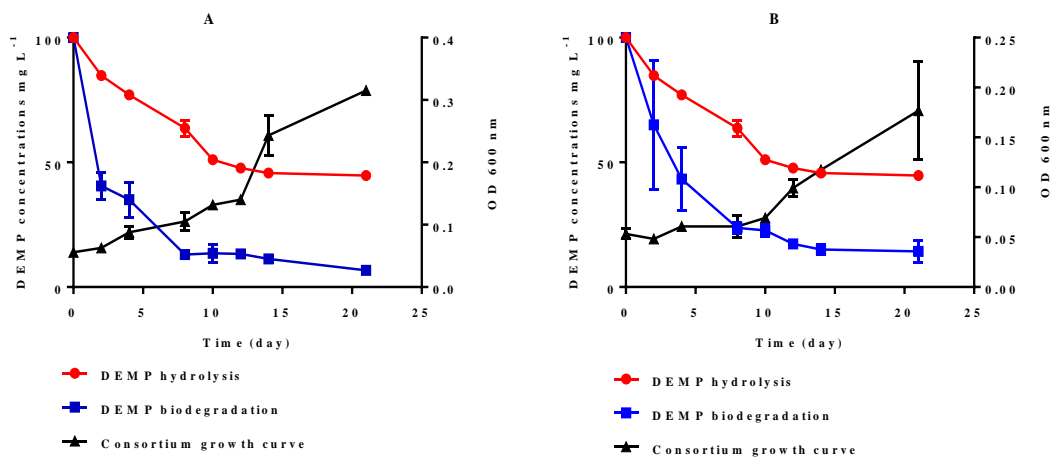
Fig. 4-5 DEMP degradation rate vs. consortium growth A) in the MSM+100 mg L^{-1}DEMP media and B) in the MSM-P+100 mg L^{-1} DEMP. The time course of bacterial growth refers to the change of turbidity (the absorbance) and DEMP degradation in DEMP-contained cultures. Error bars are standard deviation (n = 3).

Strong evidence about the difference between enzymatic degradation, and the hydrolysis rate constant of DEMP was found when further data analyses was performed by kinetic calculations. This difference is highlighted in Table (4-4). It indicates that the rate of DEMP hydrolysis constant was 0.04 days^{-1} compared to the enzymatic degradation rate which was 0.11 days^{-1} in the MSM and 0.09 day^{-1} in the MSM-P. This denotes that consortia were effective in DEMP degradation.

Table 4-4 Kinetic data of DEMP degradation in two types of mineral salt media

Treatments	K (day^{-1})	Regression equation	R^2	DT50 (day)
DEMP+ consortia + MSM	0.117	Ln(C$_t$/C$_0$)= -0.1177X+4.038	0.85	5.8
DEMP+ consortia + MSM-P	0.095	Ln(C$_t$/C$_0$)= -0.0959X+4.2334	0.84	7.2
DEMP+MSM	0.042	Ln(C$_t$/C$_0$)= -0.042X+4.4927	0.86	16.5

The degradation of OPs by microorganisms is usually due to use of phosphorus or a carbon source or both. For example, previous studies have shown the capability of the Rhizobiaceae strains family to utilise the phosphonate glyphosate as a phosphorus source (Liu et al., 1991). In addition, *Flavobacterium* sp. is able to breakdown phosphonate to gain a phosphorus source (Balthazor and Hallas, 1986). Moreover, *Rhodobacter capsulatus* ATCC 23782 is able to degrade 2-aminoethylphosphonate and alkylphosphonates by fission of the C-P bond of phosphonate compounds as a source of phosphorus (Schowanek and Verstraete 1990).

In contrast, other studies have demonstrated that the degradation rate of diazinon OPs by *Serratia marcescens* DI101 was not affected by the absence of a phosphorus or an additional carbon source (glucose or succinate) (Abo-Amer, 2011).

Consequently, it seems possible that these results are due to the importance of carbon and phosphorus in the growth of bacteria, which reflects the significant consumption, and decreasing of DEMP concentrations.

4.5.2.3 Ethanol production measurements

A main characteristic of the biodegradation of DEMP is the formation of ethanol in the culture, as shown in Fig. (4-6). This indicates that the amount of ethanol released into the media is a direct result of DEMP degradation, which can be determined by GC-FID. In contrast, DEMP hydrolysis resulted in a very little ethanol production. The t-test revealed there were statistically significant differences between the release of ethanol from the MSM containing 100 mg L^{-1} DEMP plus consortium versus the control at P<0.05, and the release of ethanol from the MSM-P containing 100 mg L^{-1} DEMP plus consortium, and the control at P<0.05. While, t-test

analysis of ethanol forming in the (MSM and MSM-P) plus 100 mg L^{-1} DEMP had no significant difference.
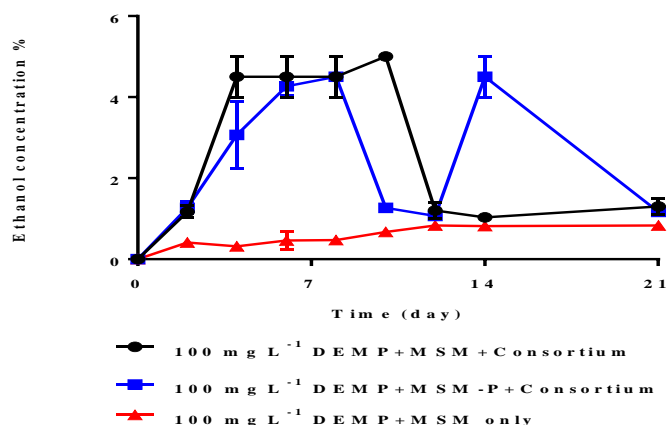
Fig. 4-6 Changes in C_2H_5OH concentrations in the supernatant of the MSM cultures and the MSM without phosphorus media with DEMP. C_2H_5OH levels were monitored during the degradation course of DEMP. Error bars are standard deviation (n = 3).

A positive correlation was found between DEMP biodegradation and ethanol release. It appears that ethanol concentrations were increased at the same time as the growth of consortia and DEMP enzymatic degradation. Meanwhile, it was relatively stable in the case of DEMP hydrolysis.

This is considered another confirmation about the role of consortia using DEMP and realising ethanol as an intermediate substance. The different amount of ethanol released from DEMP biodegradation is due to the consortium activity, where it tries to take advantage of the DEMP as a source of carbon and phosphorus together. There are, however, other possible explanations. The MSM medium (Table 4.1) means potassium, sodium and phosphorus, in addition to carbon are released from DEMP. This kind of media encourages a healthy growth of the consortium. Whereas, the MSM-P does not contain all those minerals, causing a simple growth of bacterial consortia. In consequence, consortia require time to start the DEMP break down compared to the MSM media.

In contrast with the presence of the consortium in the MSM, DEMP hydrolysis resulted in the production of a negligible amount of ethanol in the culture. This observation may support the hypothesis that the degradation of DEMP by bacteria is much more than the hydrolysis. Hence,

this result also confirms that DEMP enzymatic degradation in the MSM and MSM-P is faster than DEMP hydrolysis.

4.6 Isolation and identification of bacterial strains

With the result of the adaptation process of soil microorganisms using an enrichment culture technique containing 100 mg L^{-1} DEMP and plating on R2A media supplemented with 100 mg L^{-1} DEMP four times in the sub-culture, three bacterial strains were selected, based on the characterisation of its morphology. Three different strains in colour were: a white colony, a yellow colony, and a creamy colony.

A PCR with the 16s rRNA primers revealed that these isolates were shown to be a prokaryotic, as indicated by the 16s rRNA gene Fig. (4-7). The 16s rRNA sequence was most closely related to *B. cereus*, *M. lutes* and *D. nishinomiyaensis*, showing high similarity with other strains in the same genera. Bacterial strains were *Bacillus cereus* (white colour colony), *Micrococcus luteus* (yellow colour colony) and *Dermacoccus nishinomiyaensis* (creamy colour colony).

Fig. 4.8 shows the relationship dendrogram between strain *B. cereus, M. luteus* and *Dermacoccus nishinomiyaensis* compared to the other selected bacteria.
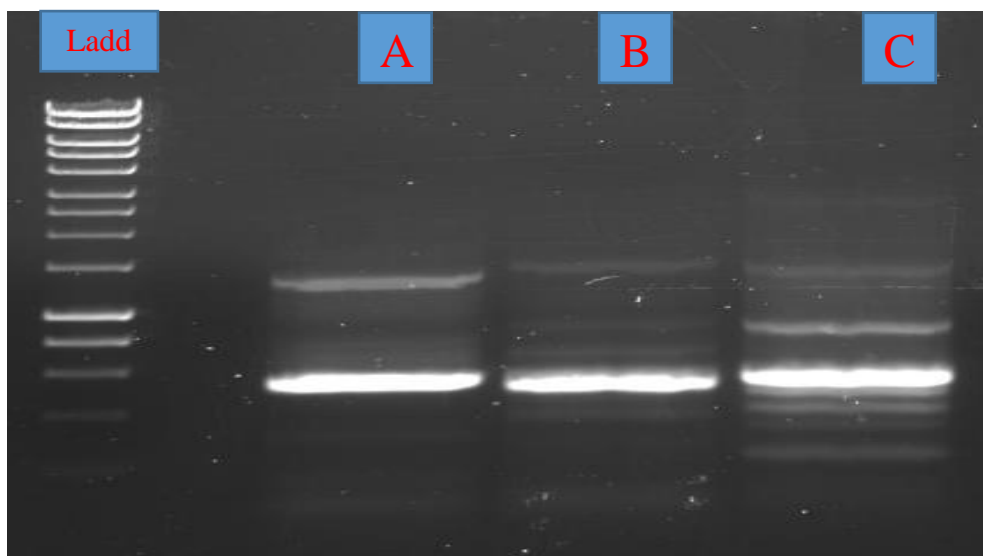

Fig. 4-7 16s ribosomal RNA gene beside molecular marker the right side A) *Bacillus cereus* and B) *Micrococcus luteus* and C) *Dermacoccus nishinomiyaensis*.
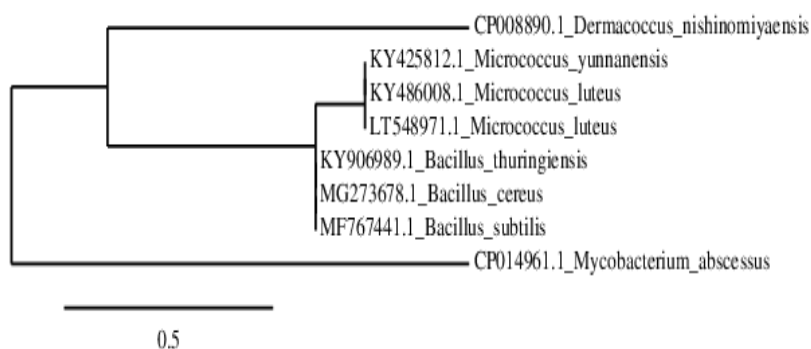
Fig. 4-8 A phylogenetic tree obtained by 16S rRNA gene sequences, showing the position or relationships between strain *Bacillus cereus*, *Micrococcus luteus* and *Dermacoccus nishinomiyaensis* among the phylogenetic neighbours. The scale bar has 0.05 substitutions per nucleotide position. Bootstrap percentages (based on 100 replicates) are shown as nodes: only values greater than 50% are shown. The sequence of *Bacillus subtilis*, *B. thuringiensis*, *Micrococcus thuringiensis, M. yunnanensis* and *Mycobacterium abscessus* were treated as the outgroup.

4.7 Individual growth curve of three-DEMP degrading strains

It is apparent that the growth curves of *B. cereus* and *M. luteus* have perfect growth in the MSM+ 100 mg.L^{-1} DEMP (Fig.4-9). The optical densities reached 1.1±0.01 and 1.05±0.01 on the fourth day. In contrast, no growth of *D. nishinomiyaensis* was recorded. The overall response to the presence of DEMP during the four days was 0.17±0.0004. The ideal indication that can be seen is the growth of individual isolates in the MSM-P because this medium did not contain any carbon and phosphorus source except that released from the DEMP biodegradation. The ability of these isolates to grow ideally, can indicate that DEMP consumed in these media is a source of carbon and phosphorus. In addition, this parameter can be used in assessing the interaction between the isolates. Moreover, it is clearly visible that the log-phase of *Bacillus cereus* and *M. luteus* started after two days, although it was not clear for the bacterium *D. nishinomiyaensis*.
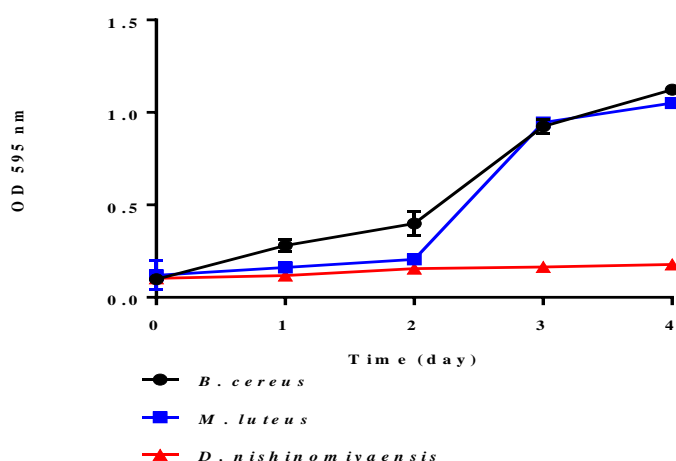
Fig. 4-9 Growth curves for the isolate *B. cereus*, *M. luteus D. nishinomiyaensis* in the MSM-P + 100 mg L^{-1} DEMP. Error bars are standard deviation (n = 3).

As mentioned in the literature review, this is the first report of OPs simulating the CWAs (sarin) isolated by enrichment MSM plus100 mg L^{-1} DEMP after 12-months' adaption. Nevertheless, many articles have reported the capability of *B. cereus* to degrade other OPs pesticides, chlorpyrifos (Vidya et al., 2009), malathion (Singh et al., 2012), and TNT (Mercimek et al., 2013), while another study has shown that *Micrococcus sp.* can degrade OPs pesticides, malathion and chlorpyrifos (Guha et al., 1997; Bhuimbar et al., 2011).

Besides the degradation of OPs, both *B. cereus* and *M. luteus* have the ability to degrade the diuron herbicide. *B. cereus* can degrade 87% of diuron for different metabolites and aniline, but the *M. luteus* can break down diuron directly to aniline (Egea et al., 2017). Furthermore, *M. luteus* and *B. cereus* can degrade petroleum hydrocarbon (Hamza et al, 2012). The reason for the capability of *B. cereus* is that it has the phosphatase enzyme, which enables it to cleave the bond C-P, therefore it can break down phosphates compounds, such as 2-amino methyl phosphonates (Lee et al., 1992).

In contrast, the bacterium *Dermacoccus nishinomiyaensis* has never been used previously in decontamination of soil with xenobiotic compounds, except in the only article by Mirzaie et al., (2014) that reported the high resistance of *D. nishinomiyaensis* to gamma radiation 30 kilo Grays (kGy) and UV light 400 joule per square metre (j m^{-2}), where they suggested potentially using it in bioremediation. Although the bacterium *Dermacoccus nishinomiyaensis*

is isolated from terrestrial habitats, cured meat product and human skin (Cordero and Zumalacárregui, 2000), it could also isolate from the sea sediment and deep-sea mud (Pathom-aree et al., 2006). In our study, the growth of *D. nishinomiyaensis* did not show any significant increase in the presence of DEMP.

This report is considered to be the first in terms of successful adaptation of bacterial consortium in the MSM containing 100 mg.L^{-1} DEMP. Ultimately, both *B. cereus* and *M. luteus* can utilise DEMP as a carbon and phosphorus source. This is attributed to the enzyme that can destroy DEMP to use it as a carbon and phosphorus source in bacterial growth.

4.7.1 Synthetic consortium curves and growth rates-community matrix study

Fig. 4-10 shows the different combinations of bacterial strains for *B. cereus* + *M. luteus*, *M. luteus* +*D. nishinomiyaensis*. All strains clearly have semi-compatibility to grow together, except the combination of *B. cereus* + *D. nishinomiyaensis*, suggesting the potential use of a synthesis consortia after improving them through the ALE in bioremediation. Similarly, for the other growth curves, there was diversity in all exponential phases. In the *B. cereus* + *M. luteus, and M. luteus* +*D. nishinomiyaensis* combinations, the log phase started after 24 hours. This is likely due to all strains having grown in the same media before starting the experiment (see 4.4.9.1). However, for the *M. luteus* +*D. nishinomiyaensis* combination, the bacteria response to growth started after 72 hours. It is believed that the reason for this may be due to the food competition, which caused the delay of bacteria entering the exponential growth stage.

Nevertheless, growth of the combination between *B. cereus* + *D. nishinomiyaensis* was not clear, characterised with the long lag phase. This implies there is no compatibility between them to grow together, or it requires more specific study.

Table 4-5 is considered an essential approach to visualise the growth rate of the three isolates, their combinations in addition to the consortia, positive and negative control using the community matrix, which is the setting of necessary and sufficient conditions to obtain the optimal conditions. The data in this table compares the ability of three isolates' growth, their

combinations, and the positive, negative controls and the natural consortia. It shows that the strain *M. luteus* grew faster by 1.5 day^{-1} than others, followed by the strain *B. cereus* 0.73 day^{-1} then *D. nishinomiyaensis* on 0.57 day^{-1}. While, the mixed consortia were 0.88 day^{-1}. Moreover, when using all isolated strains together, their growth was higher 0.44 day^{-1} compared to all other combinations. However, the only poor performance was registered by *E. coli* which 0.04 day^{-1}, whilst the positive control registered 0.75 day^{-1}.
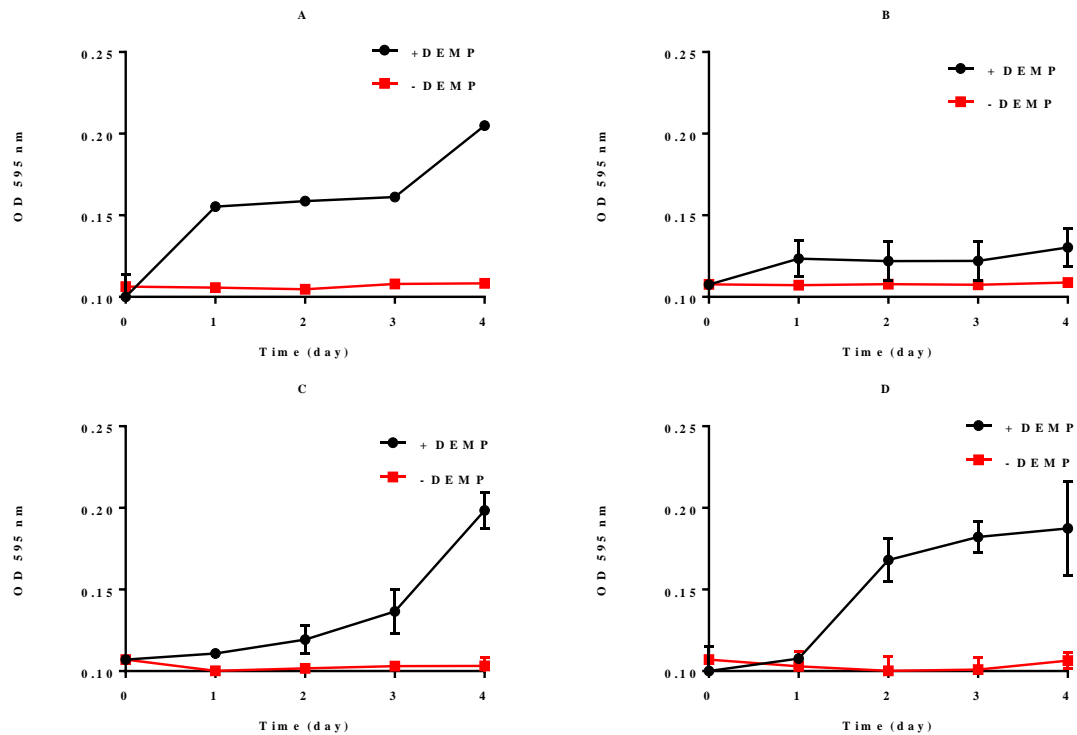
Fig. 4-10 Growth curves for the bacterial combinations A) *B. cereus +M. luteus, B) B. cereus +D. nishinomiyaensisc, C) M. luteus + D. nishinomiyaensis. D) B. cereus + M. luteus +D. nishinomiyaensis in* MSM-P. Error bars are standard deviation (n = 3).

Table 4-5 Community matrix showing all microorganisms (combinations) of bacteria generated (vertical section). The bottom two rows show the growth rate and doubling times of each microorganism.

Isolates	Site (black means isolate present)									
	■						■	■		■
B. cereus	■						■	■		■
M. luteus		■					■		■	■
D. nishinomiyaensis			■					■	■	■
Bacterial consortia				■						
P. flounces					■					
E. coli						■				
Growth rate day^{-1}	0.73	1.52	0.57	0.88	0.75	0.04	0.39	0.15	0.38	0.44
Doubling time day^{-1}	0.89	0.45	1.21	0.78	0.91	15.57	1.77	4.38	1.80	1.56

4.8 Biodegradation of other organophosphorus compounds TEPO & TBP by *B. cereus* and *M. luteus*.

A most surprising aspect of the data was that the strains *B. cereus* and *M. luteus* had the capability of breaking down two other OPs compounds, which were TBP, and TEPO (Fig.4-11), when provided as a source of carbon and phosphorus. These compounds have different chemical bonds (P-O, and P-C). *B. cereus* was able to decrease the concentration of TBP, and TEPO from 100 mg L^{-1} to 5.6, and 6.8 mg L^{-1} during 21 days of incubation. However, *M. luteus* reduced the concentration from 100 mg L^{-1} for both OPs compounds to 7.3, and 4.3 mg L^{-1} TEPO, and TBP, respectively, in the course of 21 days' incubation.
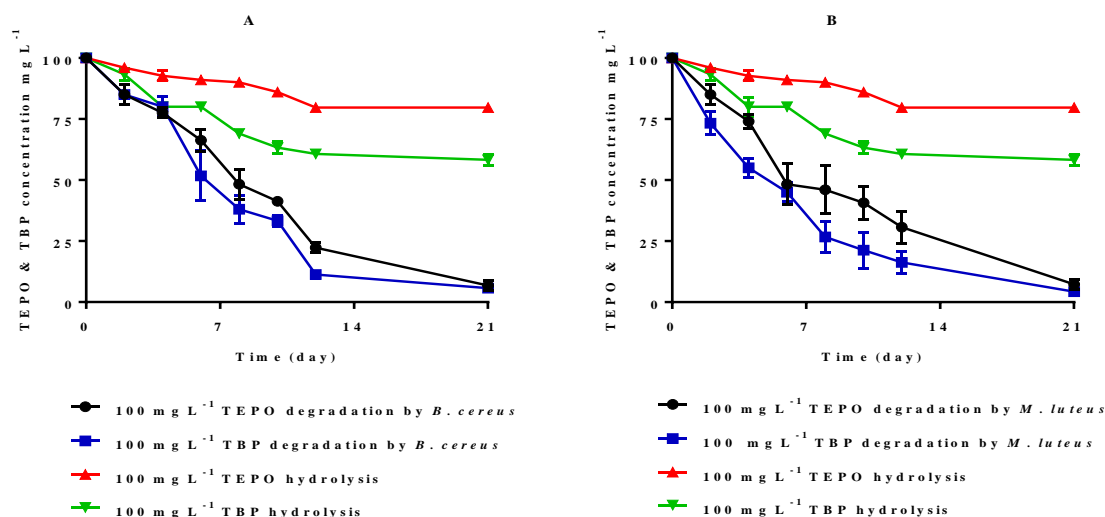
Fig. 4-11 Biodegradation of TBP and TEPO and their hydrolysis over the days in the MSM A): *B. cereus* B): *M. luteus*. Error bars are standard deviation (n = 3).

The biodegradation results of TBP, and TEPO can be confirmed through the kinetic data in Table (4-6). Data in this table can be compared, particularly the rate of enzymatic degradation and hydrolysis. The enzymatic degradation rate for both TBP and TEPO was higher than the hydrolysis rate. This means that the enzymatic degradation contributes to the decreasing of both OPs compounds, which scored 0.13, 0.14, 0.12, and 0.15 day^{-1} for *B. cereus* plus TEPO, *B. cereus* plus TBP, *M. luteus* plus TEPO, and *M. luteus* plus TBP respectively.

In contrast, TEPO, and TBP hydrolysis rates were 0.01 day^{-1} and 0.02 day^{-1}, respectively. According to these results, the DT50 reduced from 60.2, and 25.2 days to 5.2, 4.6, 5.6, 4.6 days for the *B. cereus* plus TEPO, *B. cereus* plus TBP, *M. luteus* plus TEPO, and *M. luteus* plus TBP respectively.

The present study has answered the interesting question about the extent to which the adaptation processes contribute to the breakdown of other OP compounds, such as TBP, and TEPO, which have different chemical bonds. Indeed, both bacterial isolates were capable of utilising two different OPs compounds of TBP, and TEPO effectively.

For the biodegradation of TEPO, despite it having three chemical bonds (P-C), which creates extra stability to the TEPO structure, the enzymatic system has accelerated its breakdown. As

a result, both TEPO and TBP have been degraded by both *B. cereus* and *M. luteus* due to the specific enzymes, e.g. OPH, to break down these bonds.

No current published literature that could be found on TEPO biodegradation by bacteria. Previous studies have shown that selected bacterial isolates, such as *P. putida*, *Comamonas acidovorans,* and *P. vesicularis,* have variable growth capability in liquid culture containing TBP (Thomas and Macaskie, 1996), where TBP transformed into 1-butanol and an inorganic phosphate moiety. For example, the study by Kulkarni et al. (2013) revealed that *Klebsiella pneumoniae* sp. S3 can grow and degrade 1000 mg L^{-1} TBP within 48 hours to biotransform TBP to dibutyl phosphate.

In summary, the results of biodegradation of TEPO were unexpected because it is characterised by slow chemical hydrolysis due to less electrophilicity. Meanwhile, the results of TBP degradation were expected, owing to relatively high electrophilicity. However, the present investigation has clearly revealed that the bacterial enzyme contributed to increasing the degradation rate for both TBP and TEPO by both *B. cereus* and *M. luteus*.

Table 4-6 kinetic data of TEPO and TBP degradation in the MSM media.

Treatments	K(day^{-1})	Regression equation	R^2	DT$_{50}$ (day)
TEPO + *B. cereus*	0.1316	Ln (C1/C0) = -0.1316X+4.8142	0.96	5.27
TBP + *B. cereus*	0.1491	Ln (C1/C0) = -0.1491X+4.7594	0.93	4.64
TEPO + *M. luteus*	0.122	Ln (C1/C0) = -0.122X+4.7334	0.97	5.68
TBP + *M. luteus*	0.1505	Ln (C1/C0) = -0.1505X+4.5998	0.99	4.6
TEPO only	0.0115	Ln (C1/C0) = -0.0115X+4.5802	0.85	60.27
TBP only	0.0274	Ln (C1/C0) = -0.0274X+4.5232	0.82	25.29

4.9 FTIR analysis of three bacterial strains in the presence of DEMP

FT-IR bands of the three bacterial strains (Fig. 4-12- Fig. 4-14) strongly indicate that 10 mM of DEMP was degraded by bacterial strains after 48 hours. Fig. 4-15 shows the FT-IR spectroscopy of DEMP. As revealed in Table (4-7), FT-IR spectra differed in shape and size, and there were characteristic absorbance peaks between 1500-1800 cm^{-1}. This table shows different absorbance peaks for bacteria with and without DEMP.

In general, bands at 1740 cm^{-1} and 1600 cm^{-1} are related to amide groups that were significantly different (Lin et al., 1998). This is because of the dynamics of bacterial growth, which were affected by DEMP presence. Accordingly, the changes in the 1606 cm^{-1} region were evidence that bacterial strains used up DEMP during their growth. Moreover, intensities of amide I (1544 cm^{-1}) and amide II (1655 cm^{-1}) indicated the effect of DEMP on nitrogen metabolism. The observed peaks in amide I (1544 cm^{-1}) and amide II (1655 cm^{-1}), together with the fingerprint of DEMP (900-1300 cm^{-1}) spectra, consolidated the conclusion that only DEMP was used up by the strains as a carbon and phosphorus source during the degradation period.

Moreover, the FT-IR confirmed that there was a correlation between using DEMP by bacteria and an increase in the intensity of bacterium. This might be explained when feeding the bacteria with DEMP compared to the media without supplemental DEMP, as a carbon, and phosphorus source. These results of the FT-IR spectra are in agreement with those obtained by Gumuscu and Tekinay (2013), who found that the intensity of the bacterial spectrum that degrades TNT was higher than bacteria before utilizing TNT. Overall, and according to these data, we can confirm that these microorganisms are a promising tool in bioremediation of DEMP, TBP, as well as TEPO.

Table 4-7 The area of major infrared absorbance peaks at wave numbers between 1500 and 1800 cm^{-1} after 48 hours of growth on 10 mM DEMP.

| Strains	Strain with DEMP			Strain without DEMP		
	Peak I	Peak II	Peak III	Peak I	Peak II	Peak III
B. cereus	1721.0 (s)	1637.64	1543.42	1721.01 (B)	1632.53	1539.37
M. luteus	1726.42 (s)	1633.11	1545.96	1726.33 (B)	1637.97	1541.92
D. nishinomiyaensis	1723.89 (s)	1634.04	1541.22	1723.89 (B)	1639.48	1539.4

*S= Sharp, *B=Broad
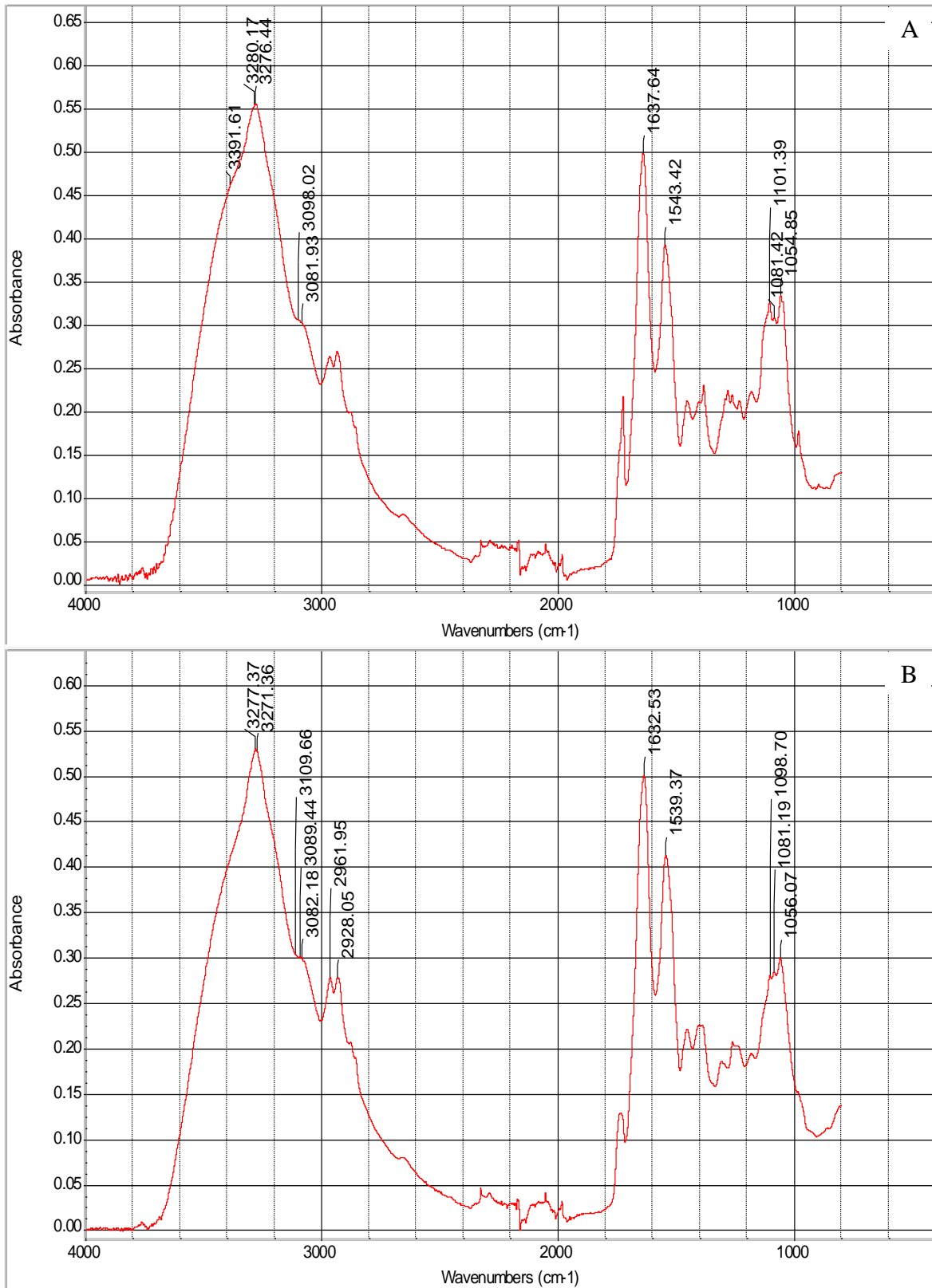
Fig. 4-12 FT-IR spectroscopy of A*) B. cereus* + 10 mM DEMP, B*) B. cereus* – DEM*P*.
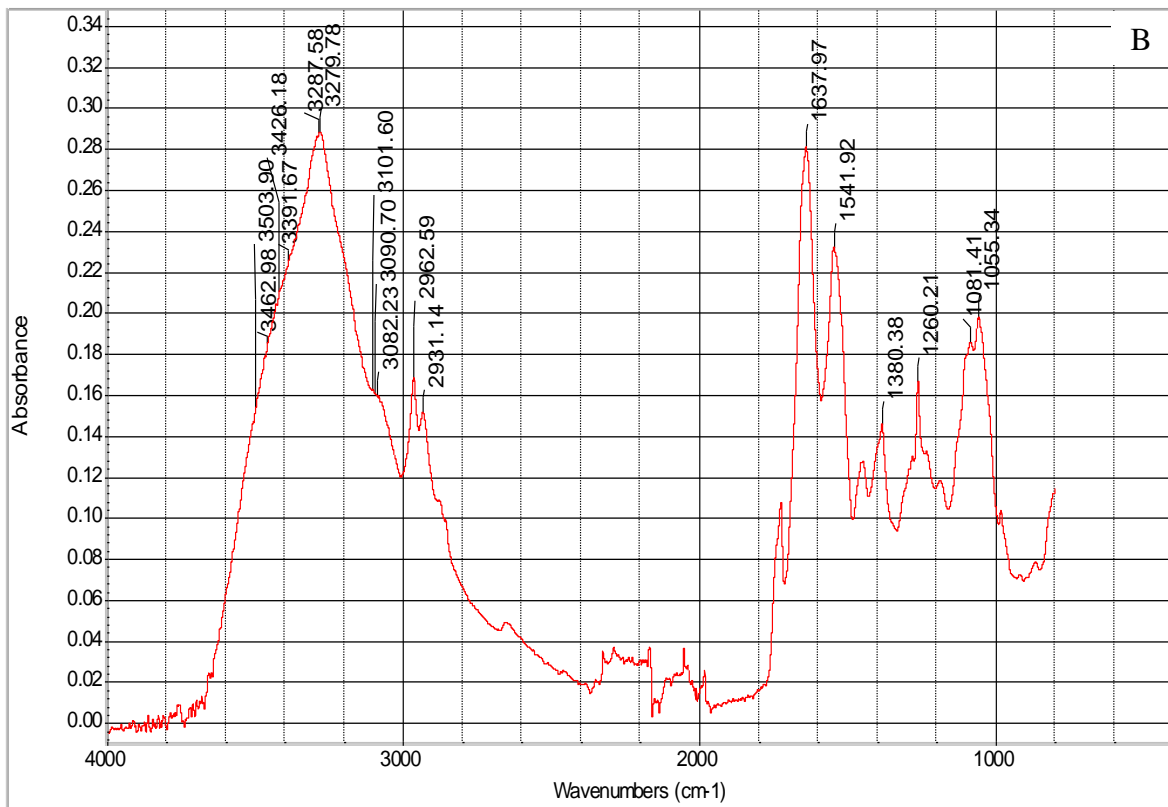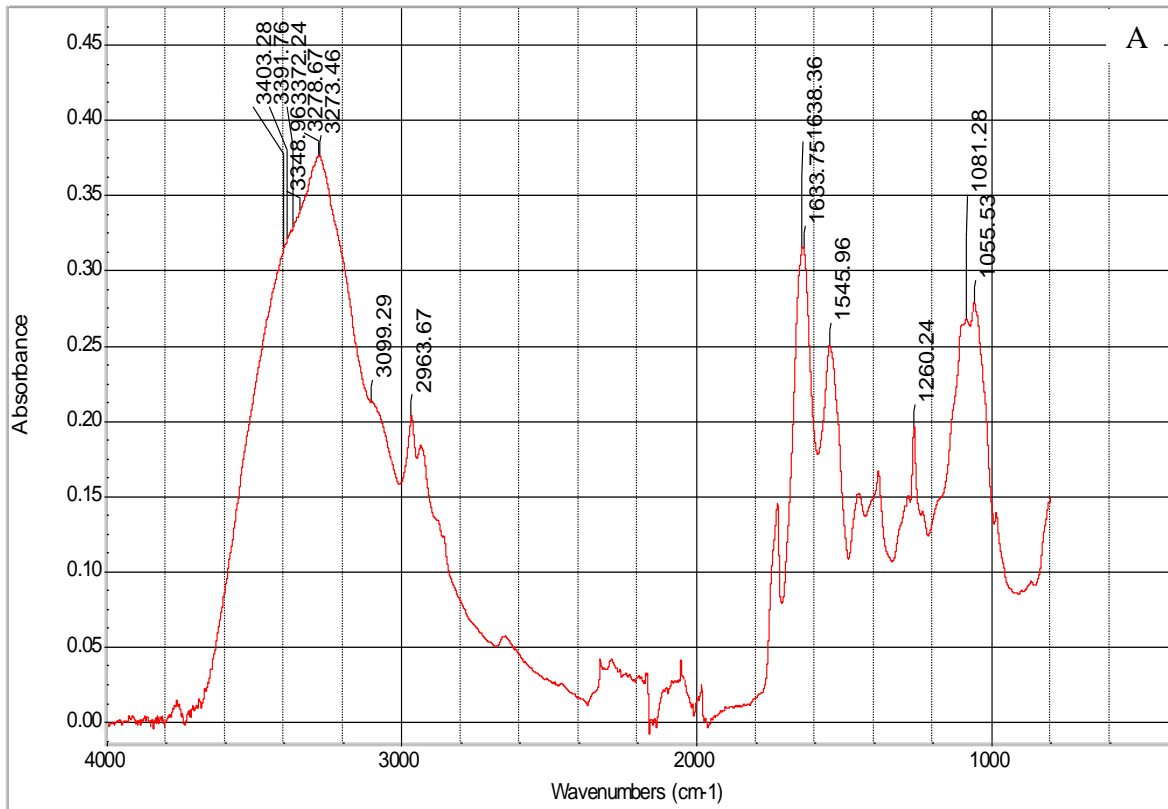
Fig. 4-13 FT-IR spectroscopy of A*) M. luteus* + 10 mM DEMP, B) *M. luteus* – DEMP.
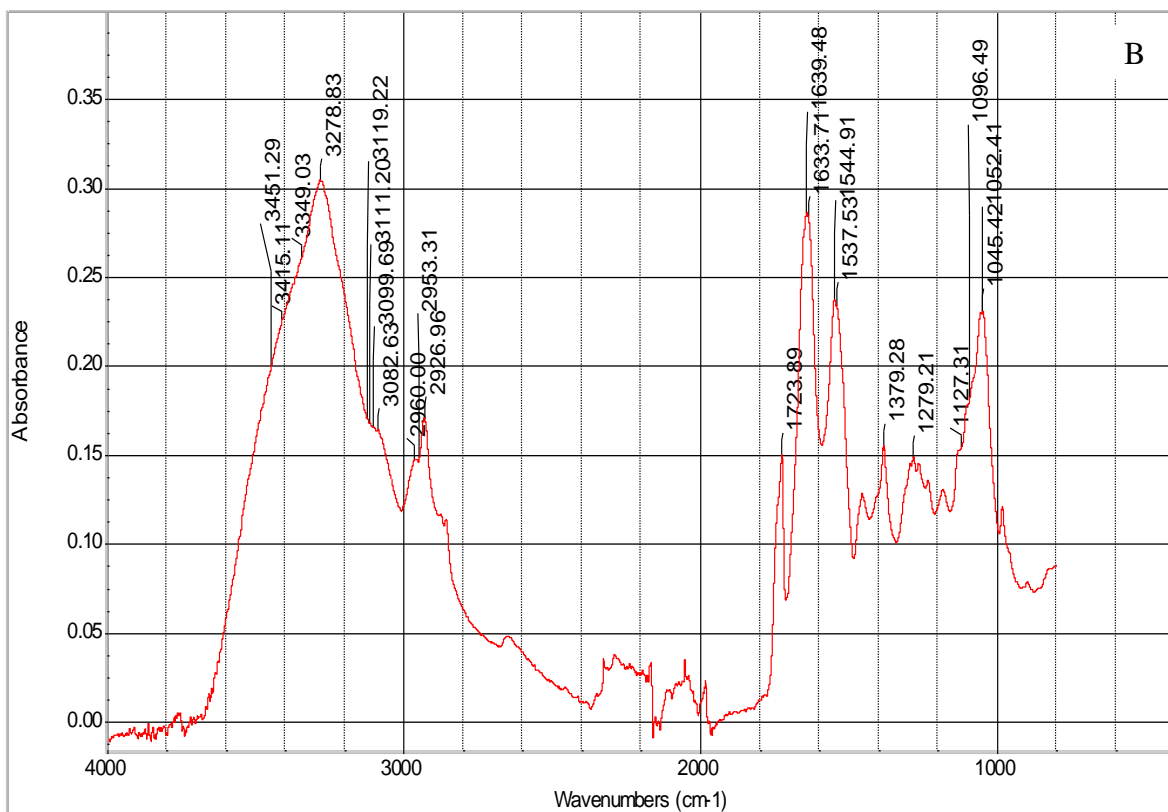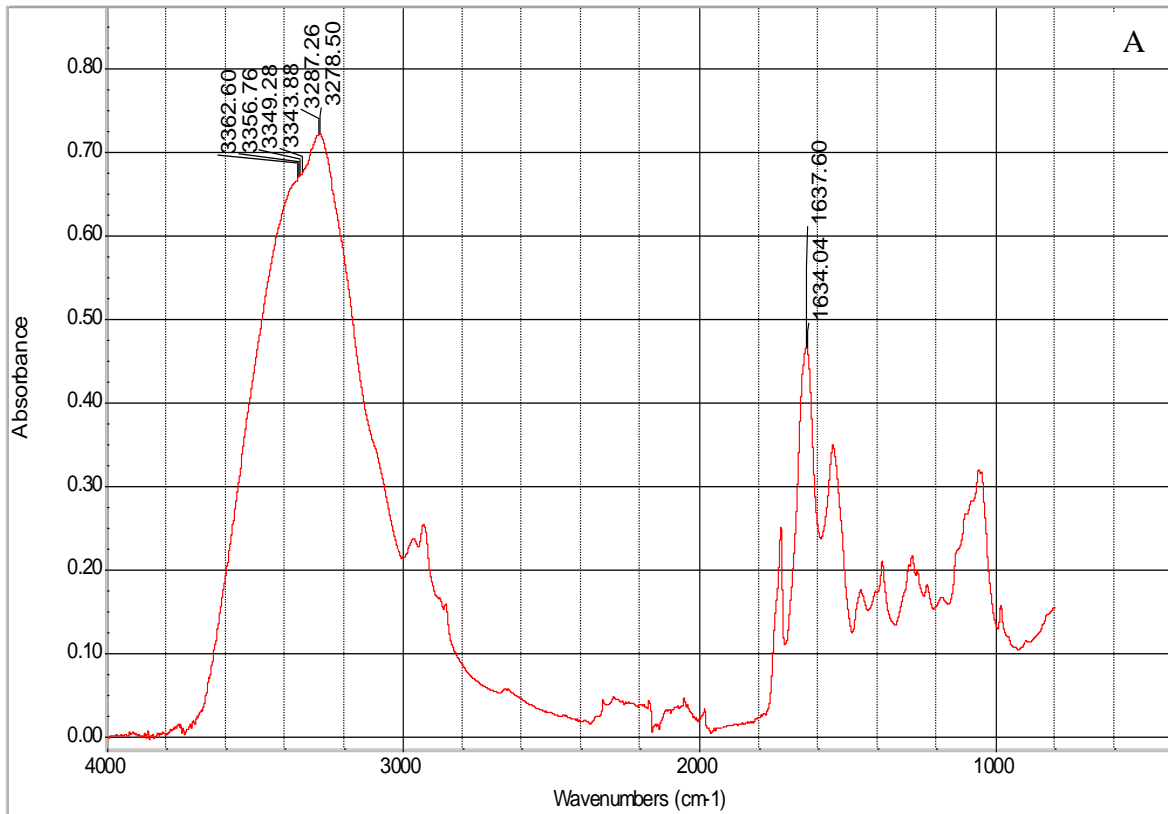
Fig. 4-14 FT-IR spectroscopy of A) *D. nishinomiyaensis* + 10 mM DEMP, B) *D. nishinomiyaensis* – DEMP.
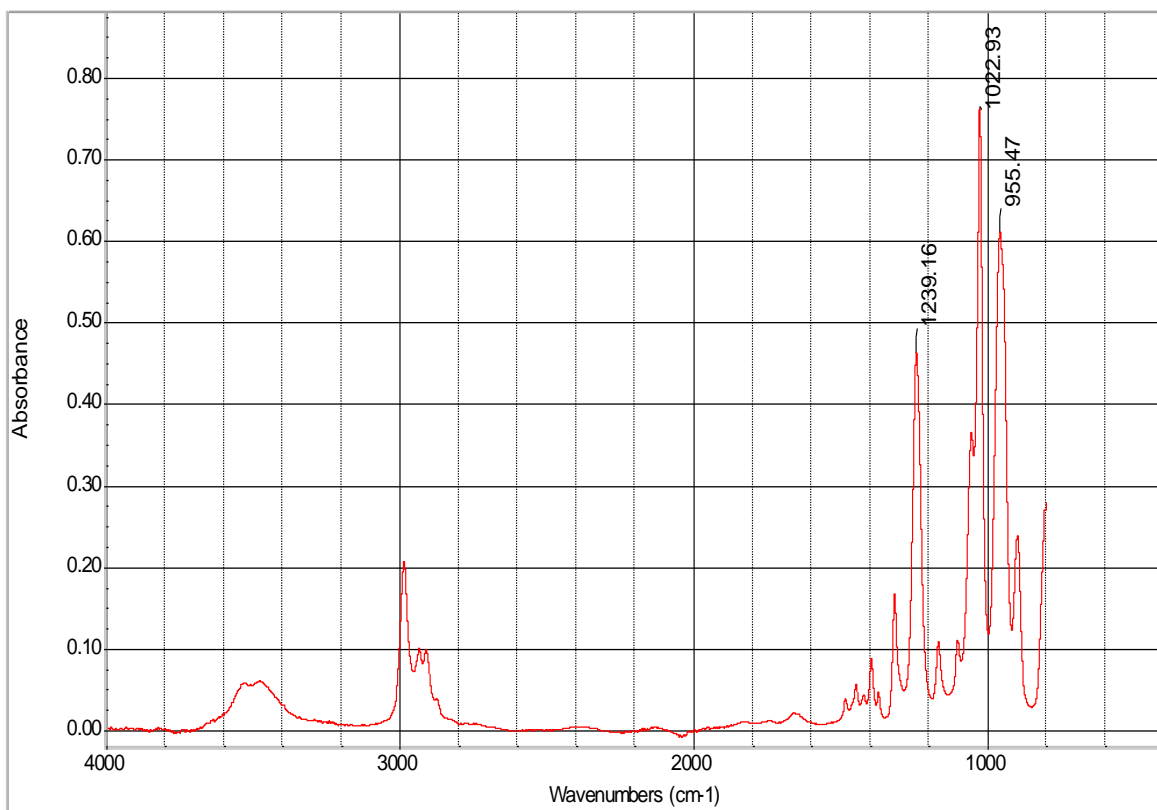
Fig. 4-15 FT-IR spectroscopy of 10 mM DEMP as a background.

4.10 Conclusions

During this investigation, the aim was to adapt a microbial consortium to be better able to use DEMP as a substrate and accelerate its degradation. Additionally, to increase understanding about the use of DEMP, a study into the effect of additional carbon and phosphorus sources on DEMP biodegradation rates was performed. The second goal of this study was to investigate the capability of the microorganisms in the consortia to utilise two different Ops; TEPO, and TBP as a carbon and phosphorus source.

This is the first study of DEMP biodegradation, which mainly relied on the adaptation of the bacterial consortium through the feeding of enrichment media with the target compound of 100 mg L^{-1} DEMP as a carbon and phosphorus source. The outcome showed that following ALE over 12-months, better growth and DEMP degradation rates were achieved. All results were confirmed by quantifying the by-product ethanol and performing FTIR measurements. The highest degradation was obtained by using the consortium in the MSM plus 100 mg L^{-1} DEMP. Three microbial species in the consortium were also isolated and identified using 16s rRNA as *Bacillus cereus, Micrococcus luteus,* and *Dermacoccus nishinomiyaensis*.

The research has also shown that the individual isolates of *B. cereus* and *M. luteus* can grow faster than *D. nishinomiyaensis*, and their combinations. Moreover, *B. cereus* and *M. luteus* can break down different OP compounds, TEPO and TBP, although they differ in chemical structure. In conclusion, we have demonstrated a multi-stage methodology that enables initial enrichment and adaptation of a bacterial consortium to degrade an unknown OP compound, followed by isolation and identification of individual active strains.

4.11 References

Abo-Amer, A. E. (2011) 'Biodegradation of diazinon by Serratia marcescens DI101 and its use in bioremediation of contaminated environment', Journal of Microbiology and Biotechnology, 21(1), pp. 71–80.

Balthazor, T. M. and Hallas, L. E. (1986) 'Glyphosate-degrading microorganisms from industrial activated sludge', Applied and Environmental Microbiology, 51(2), pp. 432–434.

Bassalo, M. C., Liu, R. and Gill, R. T. (2016) 'Directed evolution and synthetic biology applications to microbial systems', Current Opinion in Biotechnology. Elsevier Ltd, 39, pp. 126–133.

Berne, C., Pignol, D., Lavergne, J., Garcia, D. (2007). 'CYP201A2, a cytochrome P450 from Rhodopseudomonas palustris, plays a key role in the biodegradation of tributyl phosphate', Applied Microbiology and Biotechnology, 77(1), pp. 135–144.

Bhuimbar, M. V, Kulkarni, A. N. and Ghosh, J. S. (2011) 'Detoxification of Chlorpyriphos by Micrococcus luteus NCIM 2103 , Bacillus subtilis NCIM 2010 and Pseudomonas aeruginosa NCIM 2036', 3(August 2010), pp. 614–619.

Cobb, R. E., Sun, N. and Zhao, H. (2013) 'Directed evolution as a powerful synthetic biology tool', *Methods*. Elsevier Inc., 60(1), pp. 81–90.

Cordero, M. R. and Zumalacárregui, J. M. (2000) 'Characterization of Micrococcaceae isolated from salt used for Spanish dry-cured ham', Letters in Applied Microbiology, 31(4), pp. 303–306.

Cycoń, M., Wójcik, M. and Piotrowska-Seget, Z. (2009) 'Biodegradation of the organophosphorus insecticide diazinon by Serratia sp. and Pseudomonas sp. and their use in bioremediation of contaminated soil', Chemosphere, 76(4), pp. 494–501.

Cycoń', M., Zmijowska, A., Wo'jcik, M., Piotrowska-Seget, Z. (2013)'Biodegradation and bioremediation potential of diazinon-degrading Serratia marcescens to remove other organophosphorus pesticides. Journal of Environmental Management 117, 7-16.

Egea, T, C., Da Silva, R., Boscolo, M., Rigonato, J., Monteiro, D. A., Grünig, D., Da Silva, H., Van der Wielen, F., Helmus, R., Parsons, J. R., Gomes, E. (2017) 'Diuron degradation by bacteria from soil of sugarcane crops', *Heliyon*. Elsevier Ltd., 3(12), pp. 1-24.

Gomez, L. M., Osorio, C., Amman, E., Hernandez, S. P., Castro, M. E. (2006) 'The spectroscopic fingerprint of TNT between 395 and 495 nm determined from transmission near field optical microscopy measurements', Chemical Physics Letters, 422(4–6), pp. 313–316.

Guha, A., Kumari, B., Bora, T. C., Roy, M. K. (1997) 'Possible involvement of plasmids in degradation of malathion and chlorpyriphos by Micrococcus sp.', Folia microbiologica, 42(6), pp. 574–576.

Gumuscu, B. and Tekinay, T. (2013) 'Effective biodegradation of 2,4,6-trinitrotoluene using a novel bacterial strain isolated from TNT-contaminated soil', International Biodeterioration and Biodegradation. Elsevier Ltd, 85, pp. 35–41.

Hamza, U. D., Mohammed, I. A. and Sale, A. (2012) 'Potentials of Bacterial Isolates in Bioremediation of Petroleum Refinery Wastewater', Journal of Applied Phytotechnology in Environmental Sanitation, 1(3), pp. 131–138.

Hottes, A. K., Freddolino, P. L., Khare, A., Donnell, Z. N., Liu, J. C., Tavazoie, S. (2013) 'Bacterial Adaptation through Loss of Function', PLoS Genetics, 9(7):1-13.

Kulkarni, S. V., Markad, V. L., Melo, J. S., D'Souza, S. F., Kodam, K. M., (2013) 'Biodegradation of tributyl phosphate using Klebsiella pneumoniae sp. S3', Applied Microbiology and Biotechnology, 98(2), pp. 919–929.

Lee, K. S., Metcalf, W. W. and Wanner, B. L. (1992) 'Evidence for 2 Phosphonate Degradative Pathways in Enterobacter-Aerogenes', Journal of Bacteriology, 174(8), pp. 2501–2510.

Lin, S. F., Schraft, H. and Griffiths, M. W. (1998) 'Identification of Bacillus cereus by fourier transform infrared spectroscopy (FTIR)', *Journal of Food Protection*, 61(7), pp. 921–923.

Liu, A. Ch., Chou, Ch.Y., Chen, L. L., Kuo, Ch.H. (2015) 'Bacterial community dynamics in a swine wastewater anaerobic reactor revealed by 16S rDNA sequence analysis', Journal of Biotechnology. Elsevier B.V., 194, pp. 124–131.

Liu, C. M., McLean, P. A., Sookdeo, C. C., Cannon, F. C. (1991) 'Degradation of the herbicide glyphosate by members of the family Rhizobiaceae', Applied and Environmental Microbiology, 57(6), pp. 1799–1804.

Macaskie, L. E. (1991) 'The application of biotechnology to the treatment of wastes produced from the nuclear fuel cycle: Biodegradation and bioaccumulation as a means of treating radionuclide-containing streams', Critical Reviews in Biotechnology, 11(1), pp. 41–112.

Mercimek, H. A., Dincer, S., Guzeldag, G., Ozsavli, A., Matyar, F. (2013) 'Aerobic Biodegradation of 2,4,6-Trinitrotoluene (TNT) by Bacillus cereus ??solated from Contaminated Soil', Microbial Ecology, 66(3), pp. 512–521.

Mirzaie A., Mehrabadi J. F, Mozaffari N. A., and Nejadsatari T. (2014). "Unique biodiversity of radiation resistant bacteria isolated from Iranian radioactivity site and analysis of their pigments". Iranian J Publ Health, Vol 43 (2). Abs. Proceeding of 15', Iranian J Publ Health, 43(2):pp 1-150.

Moneke, A. N., Okpala, G. N. and Anyanwu, C. U. (2010) 'Biodegradation of glyphosate herbicide in vitro using bacterial isolates from four rice fields', African Journal of Biotechnology, 9(26), pp. 4067–4074.

Nakamura, A. (1991) 'Tri-n-butyl phosphate'. Geneva: World Health Organization. Programme., United Nations Environment, Organisation., International LabourOrganization., World Health, Safety., International Program on Chemical. P:78. Available at: http://catalog.hathitrust.org/api/volumes/oclc/23055463.html.

Nishino, S. F. and Spain, J. C. (1993) 'Cell Density-Dependent Adaptation of Pseudomonas putida to Biodegradation of p-Nitrophenol', Environmental Science and Technology, 27(3), pp. 489–494.

Nottingham, A. T., Hicks, L. C., Ccahuana , A. J. Q., Salinas, N., Bååth, E., and Meir, P.(2018) 'Nutrient limitations to bacterial and fungal growth during cellulose decomposition in tropical forest soils', *Biology and Fertility of Soils*. Biology and Fertility of Soils, 54(2), pp. 219–228.

Patel, S. S. and Rosenthal, K. S. (2007) 'Microbial adaptation: Putting the best team on the field', *Infectious Diseases in Clinical Practice*, 15(5), pp. 330–334.

Pathom-aree, W., Nogi, Y., Ward, A. C., Horikoshi, K., Bull, A. T., Goodfellow, M. (2006) 'Dermacoccus barathri sp. nov. and Dermacoccus profundi sp. nov., novel actinomycetes isolated from deep-sea mud of the Mariana Trench', International Journal of Systematic and Evolutionary Microbiology, 56(10), pp. 2303–2307.

Quinn, C. R., Clark, J. H., Tavener, S. J., Wilson, K. (2003) 'Promoter effects in the polymerisation of a mixed hydrocarbon feed with silica-supported BF3', Green Chemistry, 5(5), pp. 602–605.

Schmerk, C. L., Welander, P. V., Hamad, M. A., Bain, K. L., Bernards, M. A., Summons, R. E., Valvano, M. A. (2015) 'Elucidation of the Burkholderia cenocepacia hopanoid biosynthesis pathway uncovers functions for conserved proteins in hopanoid-producing bacteria', Environmental Microbiology, 17(3), pp. 735–750.

Schowanek, D. and Verstraete, W. (1990) 'Phosphonate utilization by bacterial cultures and enrichments from environmental samples', Applied and Environmental Microbiology, 56(4), pp. 895–903.

Singh, B. K. and Walker, A. (2006) 'Microbial degradation of organophosphorus compounds', *FEMS Microbiology Reviews*, 30(3), pp. 428–471.

Singh, B., Kaur, J. and Singh, K. (2012) 'Biodegradation of malathion by Brevibacillus sp. strain KB2 and Bacillus cereus strain PU', World Journal of Microbiology and Biotechnology, 28(3), pp. 1133–1141.

Thomas, R. A. P. and Macaskie, L. E. (1996) 'Biodegradation of tributyl phosphate by naturally occurring microbial isolates and coupling to the removal of uranium from aqueous solution', *Environmental Science and Technology*, 30(7), pp. 2371–2375.

Toihara, N., Yoneyama, Y., Shimada, A., Tahara, S. & Sugahara, Y. (2015) 'Intercalation of triethylphosphine oxide bearing a phosphoryl group into Dion-Jacobson-type ion-exchangeable layered perovskites', Dalton Transactions. Royal Society of Chemistry, 44(7), pp. 3002–3008.

Vidya Lakshmi, C., Kumar, M. and Khanna, S. (2009) 'Biodegradation of chlorpyrifos in soil by enriched cultures', Current Microbiology, 58(1), pp. 35–38.

Chapter V

Generating a New *Bacillus cereus* Strain for Improved Biodegradation of DEMP

In this chapter, the overall aim is to apply random mutagenesis and DEMP substrate selection to isolate Bacillus cereus strains with enhanced DEMP degradation rates.

5.1 Abstract

The current chapter aims to improve the capability of the wild-type (WT) strain of *Bacillus cereus* to achieve a fast-complete of DEMP degradation, employing ultraviolet radiation (UVR) and ethidium bromide (EthBr). 10 mutants were screened, based on rapid growth rates and bacterial yield compared to the WT. The best mutant that achieved the highest growth rate and bacterial yield was selected for *In-Situ* bioremediation. The results demonstrated that the WT responded to both mutagens. UVR reduced the mutant number from 100% to 45.6% after 5 minutes of exposure, while, mutants were reduced from 100% to 2.4% using EthBr after 30 minutes of exposure. Bacterial mutants that were exposed to EthBr for 12 minutes (BM12) had the highest growth rate value of 0.38 day^{-1} compared to the WT of 0.32 day^{-1} in the medium provided with 200 mg L^{-1} DEMP only. BM12 produced the highest bacterial biomass (O.D.$_{600nm}$ = 0.53) compared to the WT (O.D.$_{600nm}$ = 0.30). Both BM12 and the WT contributed to degradation of DEMP by 95.1% and 91.6%, respectively, compared to 22.9% of DEMP hydrolysis in soil. This suggests that the random mutagenesis and selection strategy developed in this chapter has been able to produce an improved DEMP degradation strain.

5.2 Introduction

B. cereus was isolated from the enriched and adapted bacterial consortia in Chapter 4, originally collected from the Spen Farm, Tadcaster, England. There are multiple strategies for improving desirable bacterial function, but due to the underlying genetic complexity of cells, the most attractive option is by increasing genetic diversity using random mutagenesis and selecting for specific functions.

Two different types of mutation can be achieved. Induced mutation, which can be performed by using chemical or physical mutagens, and the spontaneous mutations that occur in nature without intervention (Snyder et al., 2013). Ultraviolet radiation (UVR) and chemical mutagenesis are the most widely used tools to cause mutation, due to their ability to bring about a change in a single nucleotide and /or deletions only (Bose, 2016). For instance, UVR can cause a mutation by exciting the electrons in DNA, after the absorption by pyrimidine bases double bonds, like cytosine and thymine. In DNA, this results in the forming of extra bonds between adjacent pyrimidine bases, and forming a four-membered tight ring (Goodsell, 2001).

Meanwhile, the chemical mutagen by ethidium bromide (EthBr) acts through intercalating a single base between adjacent bases, leading to new DNA sequences and that raises the mutation during the bacterial replication (Dale and Park, 2014).

Several cross-sectional studies suggest an association between using physical and chemical mutagens and increasing enzyme production. In this field, Venkata and Divakar (2013) applied the random mutagenesis using UVR and ethidium bromide (EthBr), ethyl methane sulfonate (EMS) to improve the production of fibrinolytic protease enzyme of *B. cereus*. Idise et al. (2010) improved both *B. cereus* and *P. aeruginosa* using UV and nitrous acid. They increased petroleum product degradation from 98.9% to 99.7% by *B. cereus*, and from 91.3% to 98.0% by *P. aeruginosa.* Additionally, Dai and Copley (2004) used genome shuffling that led to *Sphingobium chlorophenolicum* achieving faster degradation of pentachlorophenol (PCP) compared to the WT. Furthermore, they reported that the mutant strain increased their ability to tolerate the highest concentration of PCP between 6-8 mM compared to the WT that cannot tolerate more than 0.6 mM PCP.

Similarly, Panchamoorthy et al. (2009) demonstrated the effectiveness of random mutagenesis by using UVR and EthBr with *Bacillus* sp. through increasing the degradation of Congo red up to 3000 mg L^{-1}, while it was 100-1000 mg L^{-1} by the WT. In addition, the mutant reduced the time required to complete degradation by 12-30% compared to the WT.

A study by Alsulami et al. (2014) established that using a biological mutation (Maillard reactions) enhanced *Bacillus subtilis*, *Aeromonas hydrophila*, *Pseudomonas fluorescens*, and *Pseudomonas aeruginosa* to degrade isoprenoids (pristine, python) and n-alkanes in oil. This mutation contributed by increasing the percentage of degradation from 60.6 to 92.5% by *B. subtilis*, and the other species ranged from 37 to 72.3%. Meanwhile, the biodegradation increased from 78 to 87.5% by using the bacterial consortium.

Enhancing the capability of microbes to break down contaminants could be performed by either the modification of the environment or by microorganisms. This modification of microbes can occur via the mutagenesis (Idise et al., 2010). From the data in Chapter Four that have proven the capability of *B. cereus* to break down 100 mg L^{-1} DEMP efficaciously, this chapter attempts to show how the physical-chemical mutagens can increase the capability of *B. cereus* to mineralise 200 mg L^{-1} DEMP.

5.3 Methodology

5.3.1 Mutagenesis induced of bacterial strain

To create bacterial mutants by UVR, *B. cereus* was grown by inoculating 1:19 bacteria: LB (20 mL final volume) for 24 hours at 30°C and 120 rpm. 10 mL of bacterial broth was then taken in an open petri dish and placed under the germicidal lamp. The UV lamp (Plexiform, Poker 1X 15 W, cod: PK524, made in Italy) 220-240v 50/60 Hz g13 was adjusted horizontally. The distance between the lamp and the petri dish was less than 5 cm. 2 mL of a bacterial broth was withdrawn after 1 minute, 2 minutes, 3 minutes, 4 minutes, and 5 minutes by sterile tips into an Eppendorf. This was done by using a digital timer and by manually adjusting the power switch of the UV lamp. Each Eppendorf was covered with aluminium foil and stored in a 30°C shaking incubator overnight (under dark conditions to avoid the photolysis reaction) for later use in scoring the number of colonies.

The chemical mutagenesis was applied on a new bacterial broth. 20 mL of bacterial growth was centrifuged at 14,000 rpm for 10 minutes. The cell pellet was resuspended in 20 mL of 0.85% saline solution containing 20 µg mL^{-1} ethidium bromide (EthBr) solution and it was shaken well for 30 minutes in an orbital shaker. Samples were taken every 6 minutes and serially diluted between (10^{-1} to 10^{-5}) for viable cell counting and screening was done. The viability cell count was carried out by the spread plate technique and % survival was calculated using the equation:

$$S\% = \frac{Ni - Nd}{Ni} \times 100.$$

Where: S is the % survival, Ni is the initial viable cell count, and Nd is the viable cell count after mutation. For counting mutated bacterial, the software image J 1.52 g Wayne Rasb and the National Institute of Health, USA, was used to manage the bacterial pictures. The analysed particles were calculated according to size and the adjustment of the perfect number of the circularity. The circularity was between 0.3-1.00.The scale of the pictures was 244 pixels wide, and the height was 252 pixels.

5.3.2 Experimental setup of bacterial growth curves

The first bacterial colony to appear in the plate containing 200 mg L^{-1} DEMP was picked by using a sterile loop. The selected colony was inoculated into 5 mL of LB broth supplemented with 10 mM DEMP. The samples were incubated overnight. After 24 hours, 1 mL of each sample was transferred to the 1 mL of a sterile Eppendorf.

A bacterium pellet was harvested by using the centrifuge at 14,000 rpm for 10 minutes. The bacterial cell was resuspended in 1 mL of 0.85% saline solution. Then, the serial (10^{-1} to 10^{-5}) dilutions were prepared. 100 μL was spread on R2A media containing 10 mM DEMP and incubated at 30°C for 24 hours. Then, an early colony was selected and placed in 50 mL LB containing 10 mM DEMP in a shaker incubator at 120 rpm and 30°C overnight.

A pellet was centrifuged at 14,000 rpm and it was resuspended with a saline solution of 0.85%. 10 mL of strain culture was placed into 90 mL of MSM containing 200 mg L^{-1} DEMP ± 5 g L^{-1} glucose in a 250 mL conical flask, then stored in the rotary incubation under 30°C and 120 rpm. The experiment was designed as shown in Table 5-1 for the monitoring of a bacterial growth curve. The growth of bacterial culture was carried out using a Spectrophotometer at 600 nm each for three days.

Table 5-1 Experiment design for the mutants and the WT- bacterial strains growth.

No.	Type of bacteria	Treatment (factor)
1	Bacteria exposed to 1 minute of UV-irradiation light (which is coded BM1)	DEMP ± glucose
2	Bacteria exposed to 2 minutes UV-irradiation light (which is coded BM2)	DEMP ± glucose
3	Bacteria exposed to 3 minutes UV-irradiation light (which is coded BM3)	DEMP ± glucose
4	Bacteria exposed to 4 minutes UV-irradiation light (which is coded BM4)	DEMP ± glucose
5	Bacteria exposed to 5 minutes UV-irradiation light (which is coded BM5)	DEMP ± glucose
6	Bacteria exposed to minutes 6 minutes of the EthBr (which is coded BM6)	DEMP ± glucose
7	Bacteria exposed to 12 minutes of the EthBr (which is coded BM12)	DEMP ± glucose
8	Bacteria exposed to 18 minutes of the EthBr (which is coded BM18)	DEMP ± glucose
9	Bacteria exposed to 24 minutes of the EthBr (which is coded BM24)	DEMP ± glucose
10	Bacteria exposed to 30 minutes of the EthBr (which is coded BM30)	DEMP ± glucose
11	Bacteria non-exposed to UV- light or EthBr (which is coded WT)	DEMP ± glucose

5.4 *In-situ* bioremediation

5.4.1 Biodegradation of DEMP in soils

To examine the capability of WT and BM12 to degrade DEMP in soil, both strains were used. Nine flasks were prepared, and each flask was filled with 100 g of soil after twice autoclaving at 121°C for 15 minutes. 100 g of soil was mixed with 20 mL acetone containing 200 mg L^{-1} DEMP. After solvent evaporation, each soil sample was thoroughly treated with 10 mL of 10^6 in distilled water for both bacterial suspensions under sterile conditions. While the control treatment was applied using 20 mL of 200 mg L^{-1} DEMP dissolved in acetone, after evaporation, the soil was treated with distilled water only to monitor the rate of DEMP hydrolysis in the soil. All flasks were then covered with aluminium foil to avoid photolysis and incubated in the rotary shaker incubator at 30°C at 120 rpm. 5 g of each sample was taken at regular intervals to monitor DEMP concentrations. The experiment was carried out according to the procedure given in Table 5-2. DEMP extraction was done as per Chapter 3 (3.3.4). The

extraction of ethanol was carried out by centrifuging the sample and 1 mL of aliquot was taken directly into the GC - FID.

Table 5-2 Experiment design for biodegradation of DEMP in the soils.

No. of condition	Type of treatment
Treatment 1	Three flasks contain 100 g sterile soils + 20 mL of DEMP 200 mg L^{-1} + 10 mL of the WT 10^6 CFU mL^{-1}.
Treatment 2	Three flasks contain 100 g sterile soils + 20 mL of DEMP 200 mg L^{-1} + 10 mL of the BM12 10^6 CFU mL^{-1}.
Treatment 3	Three flasks contain 100 g sterile soils + 20 mL of DEMP 100 mg L^{-1} only + 10 mL of distilled water only.

5.4.2 Bacterial colonies' counts

Bacteria are grown in a solid medium in petri dishes for identification, and the number of colonies. In this experiment, bacterial colonies were counted using a 1g of soil sample that was treated with 1 mL of distilled water and mixed using the vertex. 100 µL of soil solution was transferred into 1 mL LB media and three different dilutions were then performed. 10 µL was spread on the LB plates. All plates were kept in a shaking incubator at 30°C for overnight incubation. The following day, bacterial colonies were calculated.

5.5   Statistical analysis of data

The results given in (5.6.3) and (5.6.4) represent the comparison of different growth rates of the mutants and WT. They were analysed using an independent t-test with two-tailed significance. Based on the results of Levene's test, equal or unequal variances were assumed. The ethanol concentration % released in soil was analysed by a t-test (two-sample) assuming equal variances. Meanwhile, *in*-situ bioremediation of DEMP (5.6.5), and bacterial colony counts were performed by a SPSS one-way ANOVA using IPM Statistical version 25 and the significance level applied was 0.05. Kinetic data of DEMP degradation was calculated based on the pseudo-first order. The percentage degradation of DEMP was calculated by applying the equation:- $DEMP\% = \frac{initial\ DEMP\ concentration - final\ DEMP\ concentration}{initial\ DEMP\ concentration} \times 100$ (Debasmita and Rajasimman 2013).

5.6 Results and Discussion

5.6.1 Mutant dose-response analysis

To assess the mutation effect and the capacity of bacterial colonies' survival %, a dose–response analysis was accomplished. Table 5-3 illustrates the correlation between the exposure period and the dose-response of UVR and EthBr mutagens. Dosages ranged between 1-5 minutes during UV exposure, and 6 - 30 minutes during the exposure to the EthBr. The table shows that the survival of bacterial capacity diminished dramatically throughout the increase of dosage. The decline in bacterial mutants is due to the influence penetration of the UVR and EthBr into the bacterial cell, thereby destroying the intracellular organelles or reacting with DNA, causing potential damage in the structure of proteins (Panchamoorthy et al., 2009). Furthermore, the effect of UVR can occur by impacts on the DNA lesion cytoplasmic, leading to a break in the DNA strand (Rastogi et al., 2010). It is noted that this impact was increased by increasing exposure time.

Table 5-3 Dose-response values for UV and chemical mutagenesis.

|	UV mutagenesis		Chemical mutagenesis	
No. of strain	dose, time of exposure (min)	Response % survival	dose, time of exposure (min)	Response % survival
1	0	100	0	100
2	1	88.8	6	40.7
3	2	86.4	12	37.04
4	3	66.6	18	35.8
5	4	59.2	24	29.6
6	5	45.6	30	2.4

5.6.2 Kinetic growth curves

There is a clear trend of the bacterial strains' growth curves for both the WT, and the mutant strains in the MSM containing 200 mg L^{-1} DEMP (Fig. 5-1). From the chart, it can be seen that the BM12 strain has supremacy in achieving a bacterial yield that reached 0.59±0.07 compared

to the rest of the mutants and the WT. In addition, Fig. 5-2 shows the results obtained from the bacterial growth with 200 mg L^{-1} DEMP and an extra carbon source of 5 g L^{-1} glucose. The majority of mutant strains proved their capability by achieving the ideal growth in comparison to the WT. BM5 achieved the highest yield 2.2 ± 0.005, while the WT reached 1.35 ± 0.06.

In the current results, the function of all bacterial mutants has increased with the growth compared to the WT, due to the selection procedure applied, in particular when two sources of carbon used 200 mg L^{-1} DEMP and 5 g L^{-1}. In this field, a study by Dwivedi et al. (2017) demonstrated that *Alcaligenes* sp. M2 and *Corynebacterium* sp. M1, which were placed under a UVR lamp (15W) resulted in a high petroleum hydrocarbon degradation compared to their parent strains. Furthermore, that study suggested that using the mutant strain in petroleum hydrocarbon bioremediation in water and soil, can be effective. Conclusively, the BM12 underwent fast growth compared to the WT when using one source of carbon, suggesting it can be used later in the *in*-situ bioremediation of DEMP.
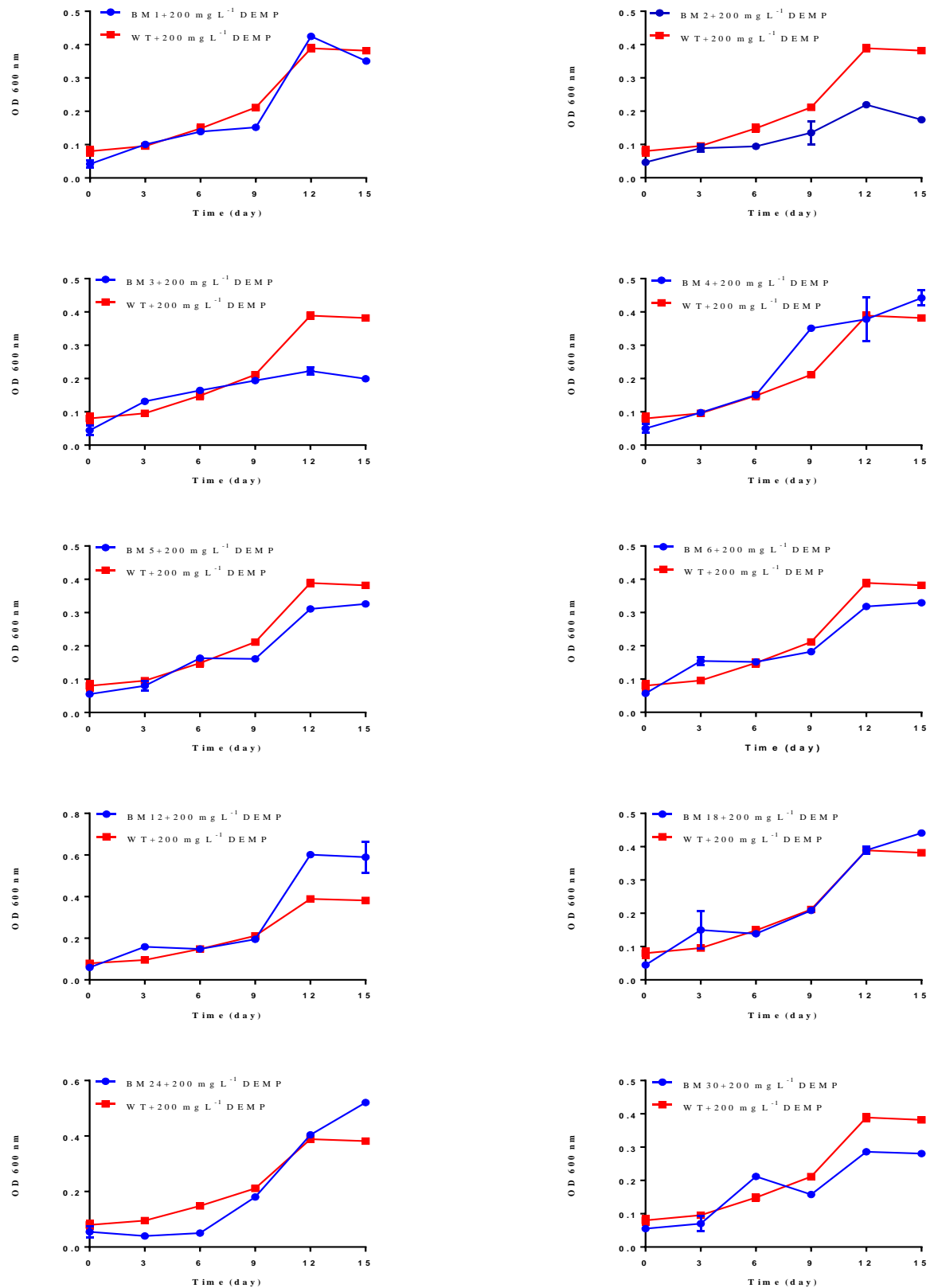
Fig. 5-1 Growth curves of different mutants of *B. cereus* with 200 mg L^{-1} DEMP only. Squares indicate the WT strain and circles indicate the mutants. Error bars are standard deviation (n = 3).
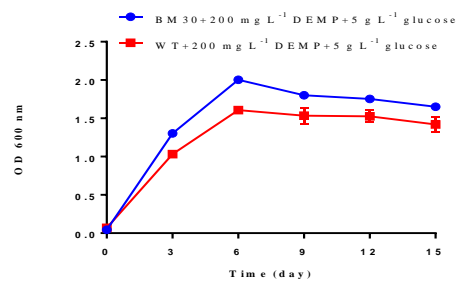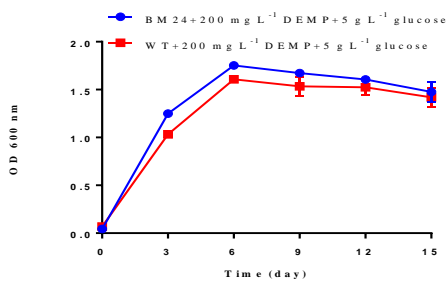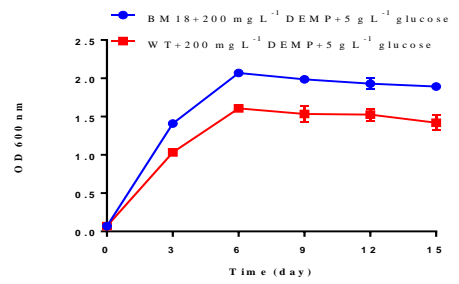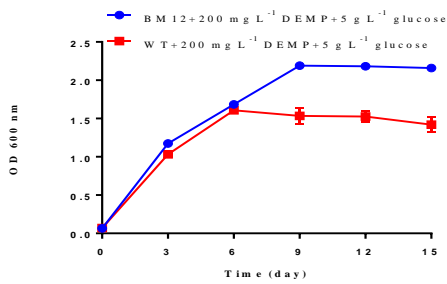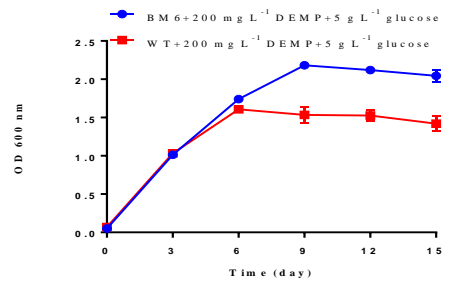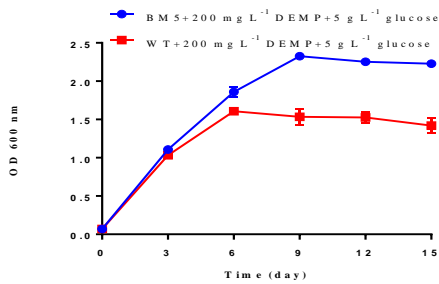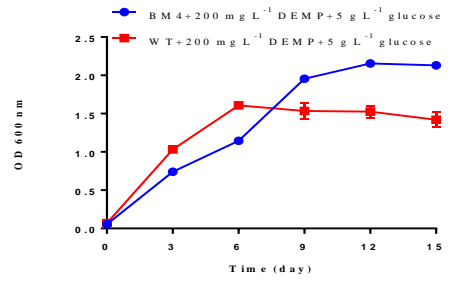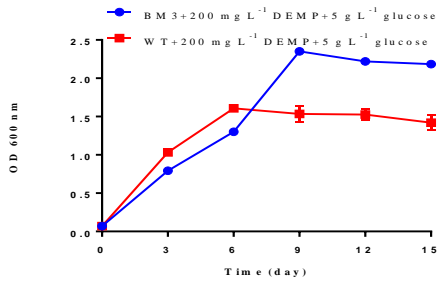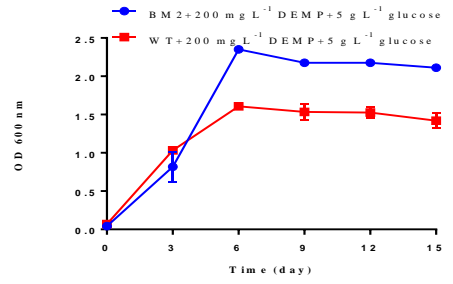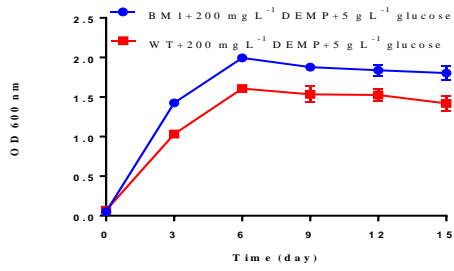
Fig. 5-2 Growth curves of different mutants of *B. cereus* with 200 mg L^{-1} DEMP and 5 g L^{-1} glucose. Squares indicate the WT strain and circles indicate the mutants. Error bars are standard deviation (n = 3).

5.6.3 Growth rate of bacterial strains

Fig. 5-3A shows growth rates of bacterial strains and the WT in the presence of DEMP only. The BM12 scored the highest growth rate 0.38±0.01 in comparison to the WT 0.32±0.02. While the lowest growth rate was recorded for the BM3 0.05±0.014. Fig. 5-3B shows the highest growth rate was achieved by BM2 0.67+0.04 and the lowest were BM3 0.39±0 and BM5 0.39±0.028 in the MSM providing 200 mg L^{-1} DEMP and 5 g L^{-1} glucose together.
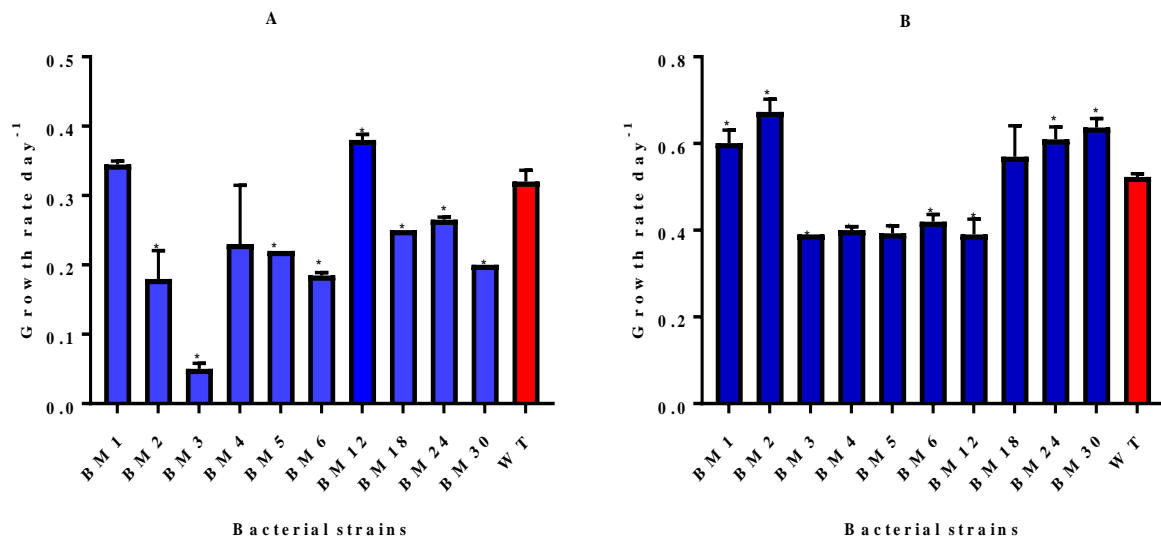
Fig. 5-3 Shows the growth rates of A) The mutants and the WT strain with a 200 mg L^{-1} DEMP in the MSM media without glucose, B) The mutants and the WT strain in the MSM media containing 200 mg L^{-1} DEMP and 5 g L^{-1} glucose. * Significant difference to the WT strain ($p < 0.05$). Error bars are standard deviation (n = 3).

In this study, the growth rates of mutants BM2, BM3, BM4, BM5, BM6, BM18, BM24, and BM30 in the MSM containing 200 mg L^{-1} DEMP were lower than the WT, except for BM1. However, when using two sources of carbon (200 mg L^{-1} DEMP and 5 g L^{-1} glucose), the mutants BM1, BM2, BM18, BM24, and BM30 achieved the highest growth rates compared to the WT except for BM3, BM4, BM5, BM6 and BM12.

This difference in the bacterial mutant strains likely resulted from increasing or decreasing the secretion of enzymes or even formulation of a new enzyme or physiological occurrence changes in the bacterial cells. One study has confirmed the use of UVR in *B. mojavensis* PTCC 1723 to increase a xylanase enzyme production (Ghazi et al. 2014). In addition, the study by

Javed et al. (2011) found that using UVR and EthBr improved thermophilic fungi to produce a cellulose compared to the WT strain. Consequently, the interpretation of this effect is quite difficult, and might need more study to explain the impact of a random mutation mechanism.

5.6.4 Growth yield of bacterial strains

Fig. 5-4A shows the bacterial yield with 200 mg L^{-1} DEMP only. Thereby, Fig. 5-4B illustrates the bacterial yield with an additional carbon source (200 mg L^{-1} DEMP + 5 g L^{-1} glucose). There was a relationship between the bacterial yield when using 200 mg L^{-1} DEMP only, and using 200 mg L^{-1} DEMP plus 5g L^{-1} glucose as a carbon source.

The outcomes confirmed there was a significant difference between these two groups. The highest yield was obtained when using two carbon sources, while it was comparatively low when one source had been used. The positive dynamic of bacterial growth in the presence of two carbon sources is better than one source of carbon. For that reason, bacteria can grow ideally due to an abundance of nutrient food.

In this scope, Ravinder et al, (2003) proved the exposure of *Aspergillus oryzae* (MTCC 1846) to EMS for one hour resulted in three strain mutants Shan 1, Shan 2, and Shan 3. These strains grew profusely and produced a high percentage of protein on de-oiled rice bran. Furthermore, the mutant strain Shan2 achieved the highest growth rate in the presence of cellulose, glucose, and maltose.
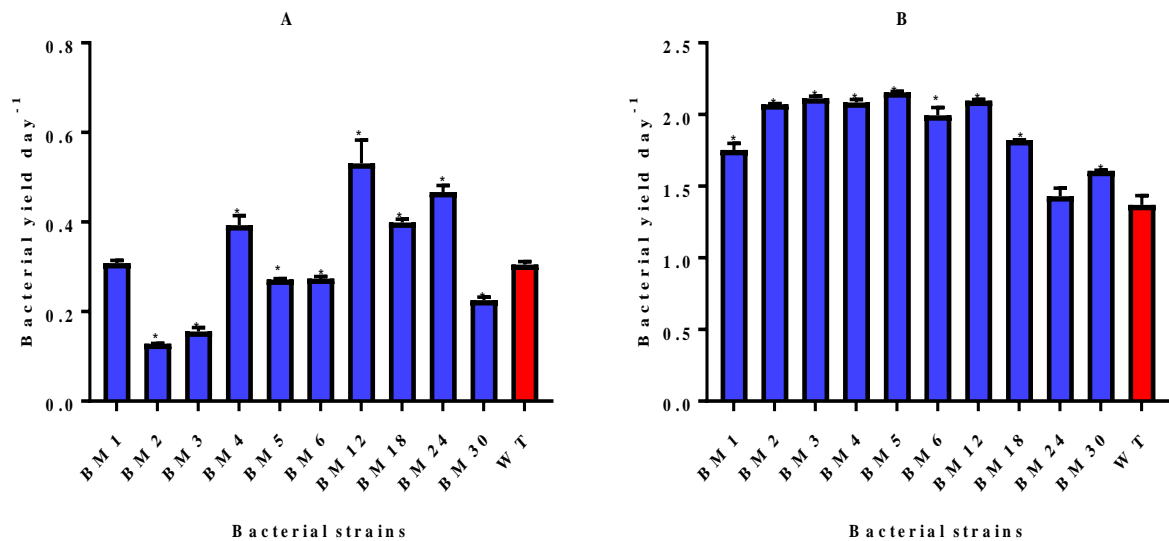
Fig. 5-4 Shows the bacterial yield of A) The mutants and the WT strain in the MSM media containing 200 mg L^{-1}DEMP, B) The mutants and the WT strain in the MSM media containing 200 mg L^{-1} DEMP and 5g L^{-1} glucose. * Significant difference to the WT strain (p < 0.05). Error bars are standard deviation (n = 3).

5.6.5 *In-situ* bioremediation of DEMP in soil

Fig. 5-5A shows the DEMP degrading by the WT and the BM12, in addition to DEMP hydrolysis in soil. A one-way ANOVA test was used to analyse the findings of the significant differences among them. The results illustrate that DEMP concentrations decreased significantly after two days from the treatment. After 12 days, there was a significant difference in the decrease of DEMP concentrations at P<0.05 between DEMP hydrolysis and using the WT, and the BM12, but there was no significant difference between the WT and the BM12.

During a period of 12 days, DEMP concentrations were monitored. Both the WT and the BM12 achieved a sharp degradation for DEMP after 2 days of application. The WT decreased DEMP concentrations from 200 mg L^{-1} to 66.5 mg L^{-1} after 2 days, while it reached 66.4 mg L^{-1} by the BM12. In addition, the soil that was not treated with bacterial strains was almost stable, and DEMP concentrations were 184 mg L^{-1} on the second day. This continued deterioration of the DEMP by the WT reached 16.7 mg L^{-1} and up to 9.6 mg L^{-1} by the BM12. The DEMP concentration was 154.2 mg L^{-1} in the control treatment.

The results shown in Fig. 5-5B compare DEMP degradation %. The degradation % of the inoculated soil with the BM12 was 95.1% more than the WT, which was 91.6%, compared with non-inoculated soil that was 22.9%.
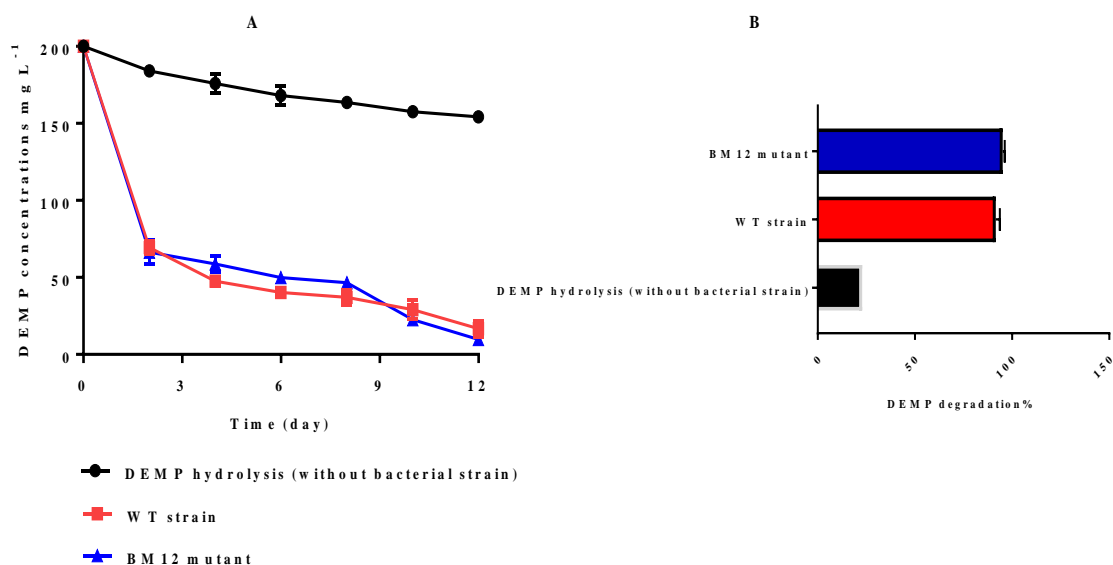
Fig. 5-5 A) Concentration of DEMP in the various treated soils. A significant difference in reduction of DEMP concentration between using the BM12 and soil not treated by bacterial strain. A significant difference was found between the WT and soil not treated by a bacterial strain in reduction of DEMP concentrations. No significant difference between using the BM12 and the WT in degradation of DEMP concentration. Error bars are standard deviation (n = 3), and B) Degradation rate percentage of DEMP in clay soil. Error bars are standard deviation (n = 3).

A pseudo-first order kinetic model was designed to compare the enzymatic degradation rate of DEMP and the hydrolysis rate constant. Thus, Table 5-4 shows that the enzymatic rate constant of DEMP for both bacterial strains was between 0.16 day^{-1} and 0.20 day^{-1} for the WT and the BM12, respectively.

In contrast, it was 0.02 day^{-1} in non-treated soil with bacterial strains. Consequently, the time required to dissipate 50% of the initial concentration of DEMP varied. This parameter is called 'half-life'. Table 5-4 shows three different parameters that were applied to compare between the roles of two bacterial strains versus the hydrolysis rate of DEMP in the environment.

Table 5-4 Kinetic data of DEMP degradation in the soils.

Type of soil	Parameters			
	Degradation rate Constant K day^{-1}	Regression equation	R^2	DT$_{50}$ (day)
DEMP hydrolysis	0.02	Ln (C1/C0) = - 0.0208×+5.2679	0.95	33
WT	0.16	Ln (C1/C0) = - 0.1685×+ 4.8828	0.87	4.1
BM12	0.20	Ln (C1/C0) = - 0.2049×+ 5.0444	0.88	3.3

Many reasons can cause the degradation of organic pollutants in soil. An important one is the chemical hydrolysis in sterile organic soil and sterile sandy soil (Miles et al., 1979). This hydrolysis occurs once the chemical compound reacts with water, but based on the present experimental results and the results in Chapter 3, the hydrolysis of DEMP was slow, hence the fast degradation of DEMP occurred using the WT and the BM12.

In comparison, between the growth of the BM12 and the WT in media and soil, there was a significant difference in the growth in the media, but not in the soil. This is probably because bacterial growth in the defined media was under ideal conditions, such as pH and nutrients. In contrast, the soil system had uncontrolled circumstances, for instance, nutrients and pH are changeable, leading to encouraging or discouraging strains' growth, and resulting in various activity reactions of the strains; typically, these reactions are positive. Hence, we have seen different behaviours of strains in the media and soil. Besides the chemical degradation of pollutants in soil, microbial activity also accelerates the degradation of contaminants.

Previous studies have shown that *B. cereus* has the potential capability to break down an organic pollutant to gain a carbon source. This capability resulted from the production of the organophosphorus hydrolase (*oph*) enzyme (Duraisamy et al., 2018). Additionally, Maya et al. (2011) reported that *Bacillus sp*. has the possibility to degrade 25-200 mg L^{-1} chlorpyrifos CP and its hydrolysing metabolite trichloropyridinol TCP 25-100 mg L^{-1}.

Another study has shown that the ability of *B. cereus* and *Klebsilla pneumonia* in degradation of OPs Profenofos pesticide effectiveness with a maximum growth rate having been recorded for the *B. cereus* and reaching 0.518 and *K. pneumonia* 0.398 on the fifth day (Jayasri and Naidu, 2014).

Whereas, Ishag et al. (2016) proved that *B. cereus* strain ATCC14579T was superior to the *B. subtilis* and *B. safensis* in breaking down the OPs dimethoate and malathion in MSM. However, Shukor et al. (2009) revealed that the *B. cereus* strain (DRY135) can grow on acrylamide and use nitrogen and carbon sources. Additionally, they reported that *B. cereus* degradation was at 90% of 1000 mg L^{-1} within 10 days of incubation with concomitant cell growth.

The obvious evidence of DEMP break downs is the formation of ethanol in the medium. This is because the degradation of DEMP resulted in the release of alcohol (ethanol) as the final product. Therefore, the detection of ethanol in the media can be potential evidence about the biodegradation of DEMP (see Scheme 2-1, Scheme 2-2, and Scheme 2-3 in Chapter 2). No ethanol concentrations were detected in the soil treated with DEMP only due to the low rate of DEMP hydrolysis. Fig. 5-6A shows the amount of ethanol formation. There was no significant difference between the soil treated with WT and BM12.

The degradation of DEMP can increase the number of bacterial cells and thus facilitate the process of DEMP degradation by those strains. Accordingly, the statistical analysis of a one-way ANOVA, showed a significant difference between the WT, and the BM12 with the control group in the bacterial colony counts at ($p<0.05$). It appears that soil treated with both the WT and the BM12 achieved a significant increase in the bacterial colonies after 12 days of incubation. The maximum colonies' number achieved by the BM12 on the twelfth day $1.10E \times 10^5$, was more than the WT $4.40E \times 10^4$, and the control $8.00E \times 10^3$ (Fig. 5-6B).

However, the increase in bacterial colony numbers in the soil had a positive impact on DEMP degradation. It appears that both strains utilise DEMP as a carbon and phosphorus source, and this results in the increase in bacterial colonies in the cultural media or site of application, as confirmed in Chapter 4. This study suggests using the BM12 and the WT strains DEMP *In*-situ bioremediation due to the strains' capabilities of utilising DEMP.
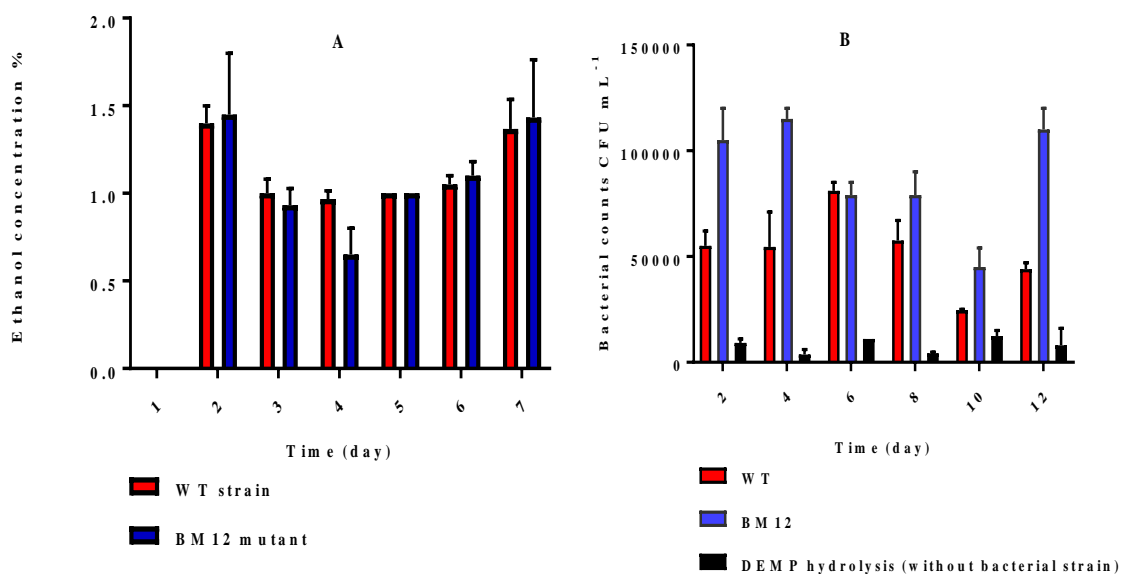
Fig. 5-6 A) Ethanol released after DEMP biodegradation by WT strain and, BM12-mutant strain in soil. No significant difference between these strains in concentration of ethanol. Error bars are standard deviation (n = 3), and B) Bacterial colonies in soil. A significant difference in bacterial counts among the WT, the BM12 and soil not treated by any bacterial strains. Error bars are standard deviation (n = 3).

5.7 Conclusions

This study aimed to improve DEMP degradation by *B. cereus* using a combined physical-chemical mutagenesis approach. The selection procedure required isolation of the earliest bacterial colony that appeared on a plate treated with 200 mg L^{-1} DEMP. Mutant characterisation was performed by comparing the growth rate and bacterial biomass of the WT strain against the mutant strains in the MSM containing 200 mg L^{-1} DEMP in flasks. Based on the growth rate and bacterial biomass production, the best strain mutant was evaluated for *in-situ* bioremediation in soils. This mutant BM12 strain significantly reduced DEMP concentrations in comparison to DEMP hydrolysis in soil. The degradation of DEMP resulted in ethanol release, whilst DEMP hydrolysis did not form ethanol due to slow DEMP hydrolysis. Ultimately, both BM12 and WT strains are promising tools in the decontamination of soil and water with exemplar OP, DEMP.

5.8 References

Alsulami, A. A., Altaee, A. M. R. and Al-kanany, F. N. A. (2014) 'Improving oil biodegradability of aliphatic crude oil fraction by bacteria from oil polluted water', *African Journal of Biotechnology*, 13(11), pp. 1243–1249.

Bose, J. L. (2016) 'The genetic manipulation of staphylococci': methods and protocols. Methods in Molecular Biology 1373, Springer protocols. Humana Press. Series Editor John M. Walker, School of Life and Medical Sciences University of Hertfordshire, Hatfield, Hertfordshire, AL10 9AB, UK. PP: 186.

Dai, M. and Copley, S. D. (2004) 'Genome Shuffling Improves Degradation of the Anthropogenic Pesticide Pentachlorophenol by Sphingobium chlorophenolicum ATCC 39723', 70(4), pp. 2391–2397.

Dale, W. J. and Park, F. S. (2014) *Molecular Genetics of Bacteria 5th edition. University of Surrey, UK.* John Wiley & Sons, Ltd. PP 388.

Debasmita, N. and Rajasimman, M. (2013) 'Optimization and kinetics studies on biodegradation of atrazine using mixed microorganisms', *Alexandria Engineering Journal*. Faculty of Engineering, Alexandria University, 52(3), pp. 499–505.

Duraisamy, K., Muthusamy, S. and Balakrishnan, S. (2018). An eco-friendly detoxification of chlorpyrifos by Bacillus cereus MCAS02 native isolate from agricultural soil, Namakkal, Tamil Nadu, India. Biocatalysis and Agricultural Biotechnology 13: 283–290.

Dwivedi A., Kumar, A. and Bhat, J.L. (2017) 'Effect of Uv Radiation on the Growth and Petroleum', *Octa Journal of Environmental Research*, 5(1), pp. 32–40.

Ghazi, S., Sepahy, A. A., Azin, M., Khaje, K. (2014) 'UV mutagenesis for the overproduction of xylanase from Bacillus mojavensis PTCC 1723 and optimization of the production condition', *Iran J Basic Med Sci, Vol.*, 17(11), pp. 844–853.

Goodsell S. David (2001) 'The Molecular Perspective: Ultraviolet Light and Pyrimidine Dimers', *The Oncologist*, 6, pp. 298–299.

Idise, O. E., Ameh, J. B., Yakubu, S. E. and Okuofu, C. A. (2010) 'Modification of bacillus cereus and pseudomonas aeruginosa isolated from a petroleum refining effluent for increased petroleum product degradation', *African Journal of Biotechnology*, 9(22), pp. 3303–3307.

Ishag, A. E. S. A., Abdelbagi, A. O., Hammad, A. M. A., Elsheikh, E. A. E., Elsaid, O. E., Hur, J., Laing, M. D. (2016) 'Biodegradation of Chlorpyrifos, Malathion, and Dimethoate

by Three Strains of Bacteria Isolated from Pesticide-Polluted Soils in Sudan', *J. Agric. Food Chem. 2016,* 64, pp. 8491–8498.

Javed, M. M., Ul-Haq, I. and Mariyam, A. I. (2011) 'Multistep mutagenesis for the over-expression of cellulase in humicola insolens', *Pak. J. Bot.,* 43(1), pp. 669–677.

Jayasri, Y. and Naidu, M. D. (2014) 'Biodegradation of Profenofos Pesticide by Efficient Bacillus Cereus and Klebsilla Pneumonia Bacteria', *IJSRD - International Journal for Scientific Research & Development*, 2(07), pp. 604–606.

Maya, K., Singh, R. S., Upadhyay, S. N., Dubey, Suresh K. (2011) 'Kinetic analysis reveals bacterial efficacy for biodegradation of chlorpyrifos and its hydrolyzing metabolite TCP', *Process Biochemistry*. Elsevier Ltd, 46(11), pp. 2130–2136.

Miles, J. R. W., Tu, M. and Harris, C. R. (1979) 'Persistence of Eight Organophosporus Insecticides in Sterile and Non-Sterile Minerai and Organic Soils', *Bull. Environm. Contam. Toxicol*, 318(718), pp. 312–318.

Panchamoorthy, K., Murugesan, S., Abraham, J., Muthukumar, K. (2009) 'Bioresource Technology Bacillus sp . mutant for improved biodegradation of Congo red : Random mutagenesis approach', *Bioresource Technology*. Elsevier Ltd, 100(24), pp. 6295–6300.

Rastogi, R. P., Kumar, A., Tyagi, M. B., Sinha, R. P. (2010) 'Molecular Mechanisms of Ultraviolet Radiation-Induced DNA Damage and Repair', Journal of Nucleic Acids, PP: 1-32.

Ravinder, R., Rao, L. V. and Ravindra, P. (2003) 'Studies on Aspergillus oryzae Mutants for the Production of Single Cell Proteins from Deoiled Rice Bran', 41(3), pp. 243–246.

Shukor, M. Y., Gusmanizar, N., Azmi, N. A., Hamid, M., Ramli, J., Shamaan, N. A., Syed, M. A. (2009) 'Isolation and characterization of an acrylamide-degrading Bacillus cereus', *J. Environ. Biol.*, 30(1), pp. 57–64.

Snyder, L., Peters, J. E., Henkin, T. M., Champness, W., Silhavy, T. J. (2013) Molecular Genetics of Bacteria 4th edition Molecular Genetics of Bacteria The single most comprehensive and authoritative textbook on bacterial molecular genetics. PP:711.

Venkata, N. R. E. and Divakar, G. (2013) 'Bacillus Cereus GD 55 Strain Improvement by Physical and Chemical Mutagenesis for Enhanced Production of Fibrinolytic Protease', *International Journal of Pharma Sciences and Research*, 4(5), pp. 81–93.

Chapter VI

Designing an automated fluidic system device for monitoring bacterial evolution

Chapter six provides a protocol for constructing an automated device with various functionalities, in a particular bacterial adaptation for utilising DEMP.

6.1 Abstract

This chapter's aim is to design and build an automated continuous bioreactor device to support bacterial adaptation to DEMP. The objective was to allow cells to better utilise DEMP through controlled dosing with this OP compound over a longer-term period, and thereby increase the rate of evolution to enhance bioremediation. This device required design through two stages. The first involved constructing a glass bioreactor connected to a LUX sensor and LED light via CoolTerm software to monitor light transmittance as a proxy for bacterial growth. To confirm the bioreactor's performance, four different experiments were carried out for various periods using different inoculum levels of *B. cereus*, 200 mg L^{-1} DEMP, and 5 g L^{-1} glucose. The first tests were undertaken to confirm that reduced flux corresponded to the growth of *B. cereus* cells. A decrease in light transmission was recorded from 467 LUX to 454 LUX after 0.8 days, followed by a reduction from 309 LUX to 297 LUX after 3 days in the second experiment. In the third, the LUX decreased from 192 LUX into 96 LUX after 4.9 days. While the value of LUX reduced from 91 LUX to18 LUX after 2.5 days in the fourth experiment. These results indicated that the bioreactor is suitable to use. Another experiment was performed to compare the bacterial yield data that was recorded by CoolTerm software versus the spectrophotometry simultaneously. It was noted that while the LUX values of the bioreactor decrease from 90 LUX to 13 LUX, the spectrum values increase from 0.02 to 1.71 in the flasks after 7 days, simultaneously. This result indicates the efficiency and accuracy of the bioreactor and the software used to follow increased bacterial population. The second stage led to the development of this bioreactor including an automated continuous fluidic system using electronic boards, software, and pumps. However, due to time constraints, the reactor was tested with ALE for DEMP utilisation.

6.2 Introduction

Following the successful adaptation process in Chapter 4, improving the bacterial consortia capability to use DEMP as a carbon and phosphorus source, together with further improvement of the isolated strain *B. cereus*, this chapter focuses on creating an automated device that can rapidly increase the rate of physiological evolution, recording the bacterial changes automatically using CoolTerm software in real time (see Appendix 6).

The aim of establishing this device was to overcome the relatively long time it took to adapt the microbial consortium in Chapter 4 to a more efficient use of DEMP as substrate. A 12-month period was required and the disadvantages of using sub-culturing during batch growth for ALE has been well described. Hence, the purpose of the current study was to construct a continuous device that could be used to adapt bacterium under various conditions. Similar devices have been demonstrated for increasing the resistance of bacteria to antibiotics [1].

Although the experiment within this chapter was not completed, the engineering processes and methodologies developed were undertaken over several years of the project. It therefore provides a 'blueprint' for further studies where ALE can be applied in an automated, continuous system, for bioremediation purposes.

6.3   The first version design

6.3.1 Overview of the procedure

6.3.1.1   Construction of Arduino nano 3.0 V

This is the smallest electronic breadboard-friendly that depends on the ATmega 328. The function of the Arduino nano 3.0 V is similar to the Arduino Duemilanove, but the package is different. There are 14 digital pins that could be used for analogue input and an analogue reference 5V (AREF) jumper. These pins are designed to work with Transmit (TX), Receive (RX), Ground (GND), and Attention (program cable only ATN). This microcontroller displays more data memory space and programming [2].

6.3.1.2 Construction of the LCD 110 Modules

This is an electronic digital liquid crystal display. It allows light to be linked to the backlight and the GND. Part of the screen becomes black when tested with the data interface level 2.7-5V [3].

6.3.1.3 Construction of light intensity sensor

This is the BH1750FVI Digital Light Intensity Sensor Module for the AVR Arduino 3V-5V power AM. In this design, it can be used to detect changes in the turbidity solution [4].

6.3.1.4 Construction of the power supply

This is a DC-DC 2-24V to 2-28V adjustable, power module 2A SX1308, containing a boost converter [5].

6.3.1.5   Using a LED Diode Kit

This is a 3mm light-emitting diode (LED). A 5mm LED can provide a range of clear light emitting diodes in different colours [6].

6.3.1.6 Assembling of the components

The final step of this procedure started by assembling all the components (Fig. 6.1). The bioreactor was connected with the optical LED on the opposite side of the light sensor. The wavelength of LED is 595 nm because it is characterised with a narrow angle of light emitted. Both the LED and the sensor connect directly to the computer. The function of an optical system is the detection, monitoring and recording of any changes in bacterial growth inside the bioreactor. Data of bacterial populations are registered automatically through estimating the turbidity at 600 nm in the bioreactor. The output data, as a digital direct recording can be obtained every 10 minutes using CoolTerm software. Furthermore, the bioreactor vial contains a magnetic stirrer to mix bacteria with a medium. However, the bioreactor can be refreshed with bacterial suspension, chemical substrate and MSM manually.
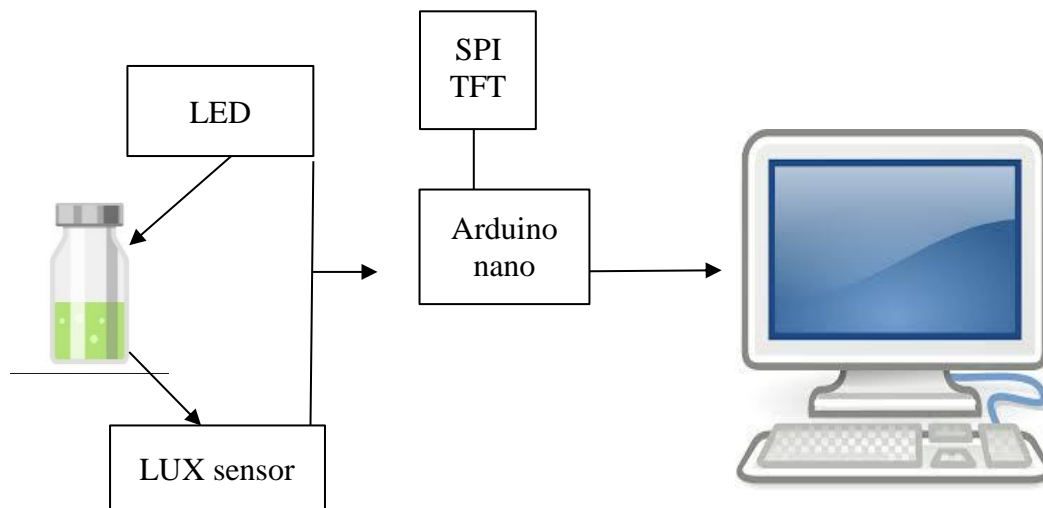
Fig 6.1 Diagram of the bioreactor – first version

6.4   Methodology

6.4.1 Biological experiment set up

To ensure the performance of the bioreactor, four different preliminary biological experiments were conducted. The first was run over 1180 mins (0.8 day), the second ran for 4430 mins (3.07 days), the third ran over 7080 mins (4.9 days), the final run was 3650 mins (2.5 days). At the end of each run, the bacterial growth curve was plotted. Experimental designs are shown in Table 6.1.

Table 6-1 Experiment designs for the examination of the bioreactor.

No. of run	Type of treatment
First	Consist of 10 mL of bacterial suspension (Inocula level) plus 190 mL MSM containing 5 g L^{-1} glucose.
Second	Consist of 15 mL of bacterial suspension (Inocula level) plus 185 mL MSM containing 5 g L^{-1} glucose.
Third	Consist of 20 mL of bacterial suspension (Inocula level) plus 180 mL MSM containing 5 g L^{-1} glucose.
Fourth	Consist of 25 mL of bacterial suspension (Inocula level) plus 175 mL MSM containing 5 g L^{-1} glucose.

6.4.2 Comparison with spectrophotometry experiment set up

To compare the data of the automated fluidic system that was calculated via CoolTerm software and the OD of the spectrophotometer, 170 mL plus 30 mL bacterial culture, and 200 mg L^{-1} DEMP plus 5 g L^{-1} glucose was used in the bioreactor. 1 mL of bacterial culture was withdrawn from the bioreactor to calculate the bacterial population using the spectrophotometer at 600 nm over 7 days. The data from the CoolTerm software and the OD were plotted together.

6.5   Results and Discussion

Fig 6.2 illustrates the bacterial growth during different periods. These intervals ranged from 0.8-4.9 days. The plots show that the automated fluidic system functions satisfactorily. Thus, we can see the direction of bacterial growth going down over time owing to the increase of bacterial turbidity. This represents the increasing bacterial population in the medium, which means the capability of bacterial growth resulting from the abundance of two sources of carbon, in particular 200 mg L^{-1} DEMP and 5 g L^{-1} glucose.
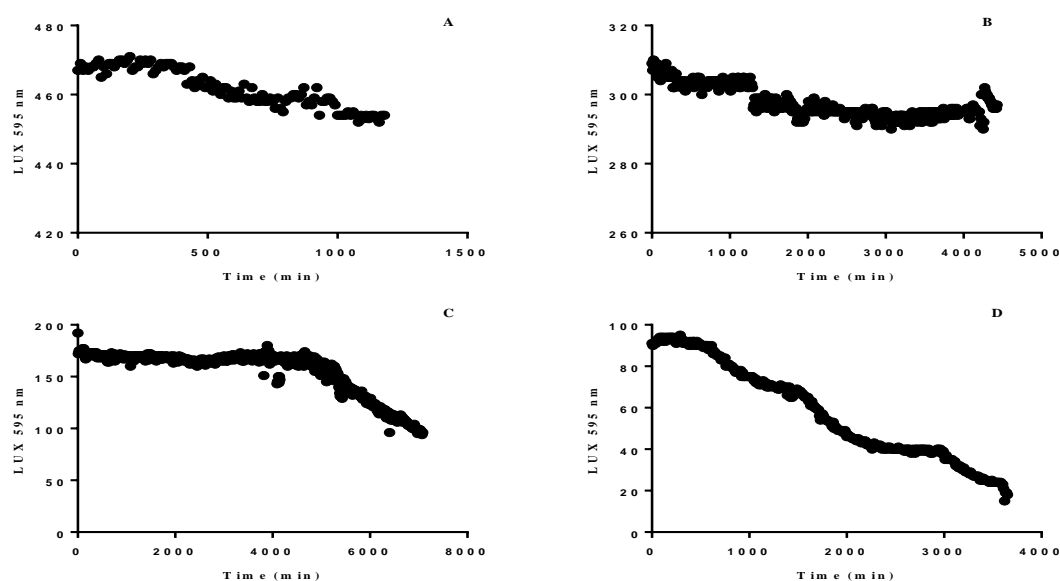
Fig 6.2 The growth curves of *B. cereus* by an automated fluidic system at various periods. Where A) during 0.8 day, B) 3.0 days, C) 4.5 days, and D) 2.5 days.

However, a new run was carried out using the bioreactor to compare the efficiency of the CoolTerm software with the OD. Therefore, Fig 6.3 shows the positive relationship between the decreasing of LUX in the bioreactor and the increasing of an OD in the spectrophotometer. Consequently, the bioreactor can be used in further development, to include the automatic fluids constant system.

In conclusion, the first version of the bioreactor system was valid in terms of its accuracy in monitoring bacterial growth. The results obtained induced us to improve it. Hence, the next version will be developed to include extra units, aiming to be an automated continuously fluidic system device.
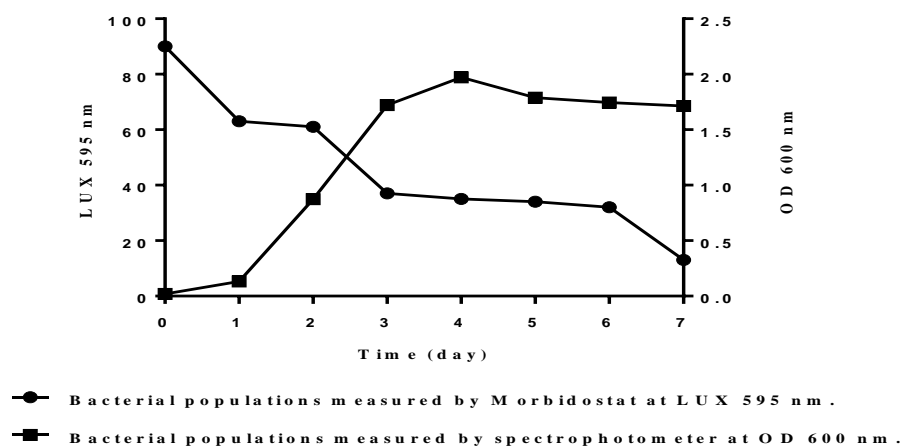
Fig 6.3 Comparison between *B. cereus* growths in an automated system versus the spectrophotometer.

6.6   The second version design

6.6.1 Overview of the procedure and their components

This version was designed based on the first and the protocol mentioned by [7]. The new design is called an automated fluidic continuously system device. The components it includes are detailed below.

6.6.1.1   Construction of peristaltic pumps

The main unit of this device is peristaltic pumps, which are considered the carrier part of the bacterial culture, substrate and medium.

The function of these pumps is transporting the liquid into the bioreactor. The first pump transfers bacterial cultures into the bioreactor, the second one provides the bioreactor with the MSM media containing DEMP, and the final pump removes the waste from the bioreactor. All these parts work together automatically.

This system allows pumps to start every 24 hrs. The pumps' test was carried out using a power supply to estimate the suitable volume of bacterial culture and MSM which contains DEMP. Different volumes of solutions should transfer from media vial and culture vial into the

bioreactor vial simultaneously and remove the same amount from the bioreactor vial. The test was performed with three different volumes 10, 20, 30 ml under 10 and 12 voltages.

The preliminary results are presented in Appendix (8). Pumps were similar in terms of their function, which means the operating system will work precisely [8].

6.6.1.2 Using of air valve connector

The Aquarium Air Valve Connector is a white plastic Inline Tubing, 3-Way T & Straight. This package included 20 T-connectors, 10 straight connectors, 10 Elbow connectors, and 10 Y-connectors [9]. It is made from a plastic material for long terms use. Healthy and non-toxic, it can be used to connect 0.5cm aquarium tubing airline.

6.6.1.3 Using of microcontroller ESP-32 Development Board

The current version also contains the Espressif system (ESP32), which is a series of low-power systems used with a chip microcontroller with integrated Wi-Fi and dual-mode Bluetooth, low-cost [10].

6.6.1.4 Using of the Real time clock (RTC)

This is one of the most important units in the device. The function is to maintain the RTC seconds, minutes, hours, day, date, month, and year information [11].

6.6.1.5 Using the MCP23017-E/SP

This is a 16-Bit Remote Bidirectional I/O Port that can be used for polarity selection, input and output. With this, the master system allows for inputs and outputs via the I/OS configuration bits (IODIRA/B). The most significant aspect is the registers can keep data and it is read by the master system [12].

6.6.1.6 Using the DC-DC converter

This is a DaoRier DC 5V-32V to1.25V-35V automatic boost, buck Converter 4A 12V for Car Regulated power supply with a Solar LED driver adjustable power supply module [13].

6.6.1.7 Use of 5 meters clear airline

These are suitable for all types of aquarium air pump with a 4mm outlet cut from a roll where a 6mm outer and 4mm inner clear airline can be used with the current pumps [14].

6.6.1.8 Using of Power Supply AC to DC

This is an individual model, output of power supply includes input voltage: 220V-240V, Output voltage: DC 12V [15].

6.6.1.9 Using the prototyping board

It is an epoxy glass, synthesis, and single-sided photoresist. It is characterized by a high resolution positive. Photoresist contains a dye to aid inspection during developing, it is coated with a photosensitive layer on one side, and is ideal for prototyping with flexible laminate or for repairs where existing material is replaced [16].

6.6.1.10 Using the pin headers

This part is widely applied in the computer and breadboards. It is suitable for Arduino, Raspberry and other electronic projects [17].

6.6.1.11 Using of the 4-pin mini micro momentary switcher and 4-Pin DIN Chassis Socket

A 20 PCS Demarkt 4-Pin Mini Micro [18]. 4-Pin DIN chassis socket [19].

6.6.1.12 Using the Nickel Standard DIN Plug

These are an 8 Pin Standard Nickel DIN Plug [20] and an 8 Pin Chassis Socket [21].

6.6.1.13 Using a Vertical, Square Pin

Two vertical square pins are 0.1- 6 Way [22], and 0.1- 4 Way used in this device. Both are important parts. They could be used for polarising back walls, signal and power applications (KK 254 and KK 396 connector-system) [23].

6.6.1.14 Use of header vertical

Two header verticals 2.54mm 10 Way [24] and header vertical, 2.54mm 8 Way [25]. These are boxes containing phosphor bronze contact and a glass-reinforced thermoplastic insulator.

6.6.1.15 Use of XLR USB

This is a USB   2.0 A to B Horizontal Feed through Panel Mount Connector [26].

6.6.1.16 Use of Single Transistor Darlington

This is an NPN Plastic medium-power complementary silicon transistor designed for general-purpose amplifier and low-speed switching applications. This transistor features a monolithic construction with built-in base-emitter shunt resistors [27].

6.6.1.17 Use of Pluggable Terminal Block

This is a 2-position pluggable terminal block with a screw connection. This terminal block comes with 5.08mm pitch spacing and is suitable for wire size ranging from 24AWG to 12AWG [28].

6.6.1.18 Use of Terminal Block, Header

This are 2-position terminal block headers with 5.08mm pitch spacing. They are 5.08mm, 2 Ways, 12 A, 250 V [29].

6.6.1.19 Use of Socket, IDC, Strain Relief

This is an 8-way 2-row IDC Socket with flash gold-plated phosphor bronze contacts, 2.54mm pitch spacing, IDC/IDT termination with strain relief, glass-reinforce thermoplastic [30].

6.6.1.20 Using of Two Resistors

Two Resistors, 0.5W 5% 1K and 0.25W 5% 1K can be used in this device [31].

6.6.1.21 Using of Electrolytic Capacitor

This is a crucial automotive grade type A. The capacitor's characteristic is that it has a radial aluminium electrolytic polarized. Therefore, it is considered an ideal solution for many different applications that depend on low cost. Despite it being a very small part, it can be used in a mounting frame for a long time, moreover, it is characterized by the high ripple. The value ranges of its capacity are 2.2 µF to 22000 µF and from 1µF to 470µF. It could be used in portable devices, consumer electronics, and power management [32].
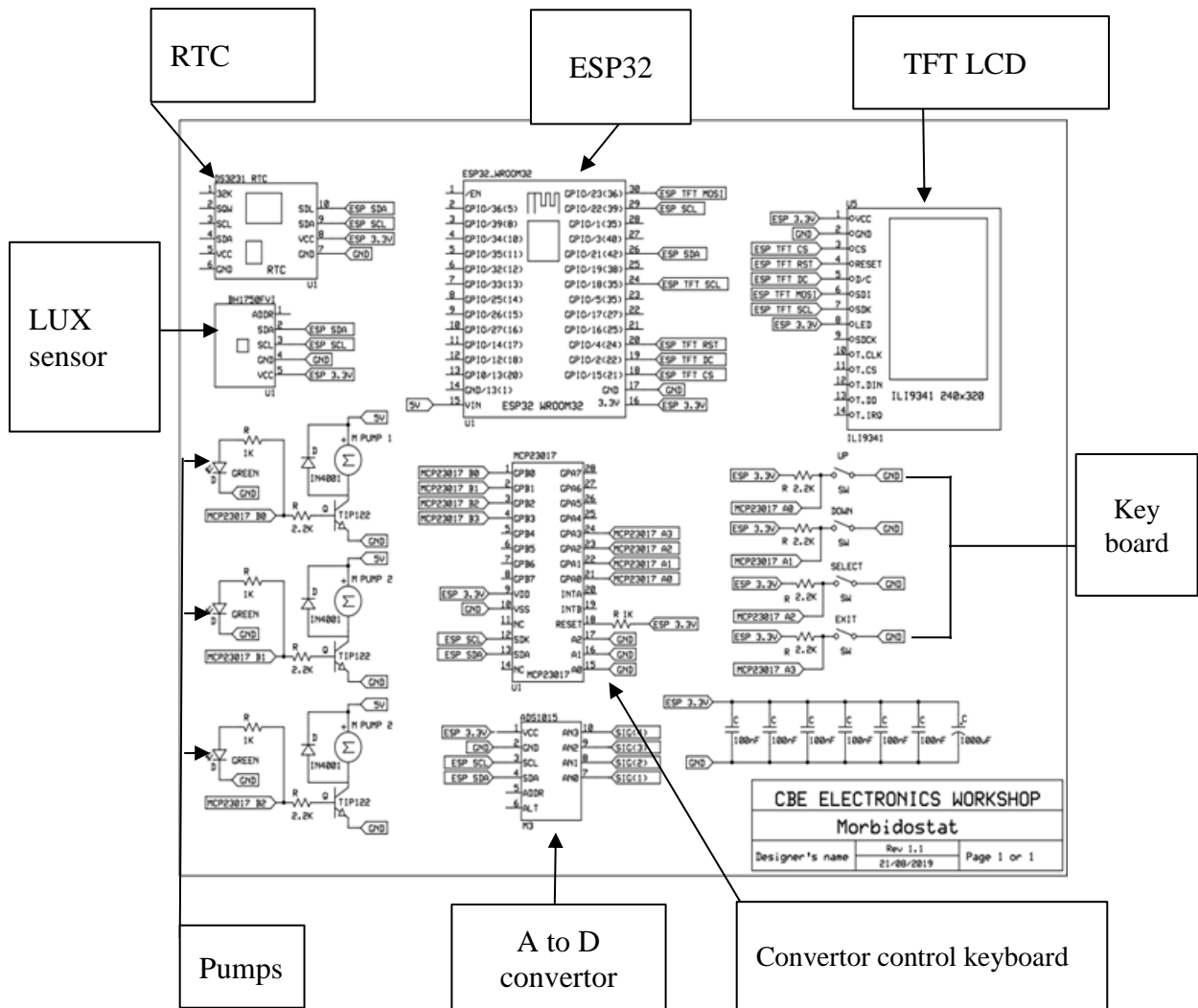
Fig 6.4 New electronic diagram of the automated fluidic system device.

6.6.2 Software sequencer manual bioreactor (Software flow chart)

Power up menu:

After powering up the first menu 1 of 4 functions can be selected.

1. Process trigger time. This routine enables changing the trigger time, which consists of hours 24 minutes 60 seconds 60. The trigger time is the time required for the process to

start based on the real time clock. Using the UP, DOWN and enter keys will change these 3 variables.

2. Pump process time. This routine enables changing the pump ON time where the time is in hours. This function is only triggered when the process time = the real time clock. Using the UP, DOWN and enter keys will change these 3 variables.

3. Real time routine. This routine enable the real time clock to be altered; 3 variables are hours 24 minutes 60 seconds 60. The real time clock is always running in the background. Even when power is lost a lithium battery is used to keep time. Using the UP, DOWN and enter keys will change these 3 variables.

4. Run process routine. This function is activated by pressing by pressing the UP button, which starts the process and counts the timer down from the real time until it equals the trigger time. The function samples of the LUX sensor output the data to the screen every 10 minutes. When the trigger time is reached the pumps are switched on to depending upon the stored process time.
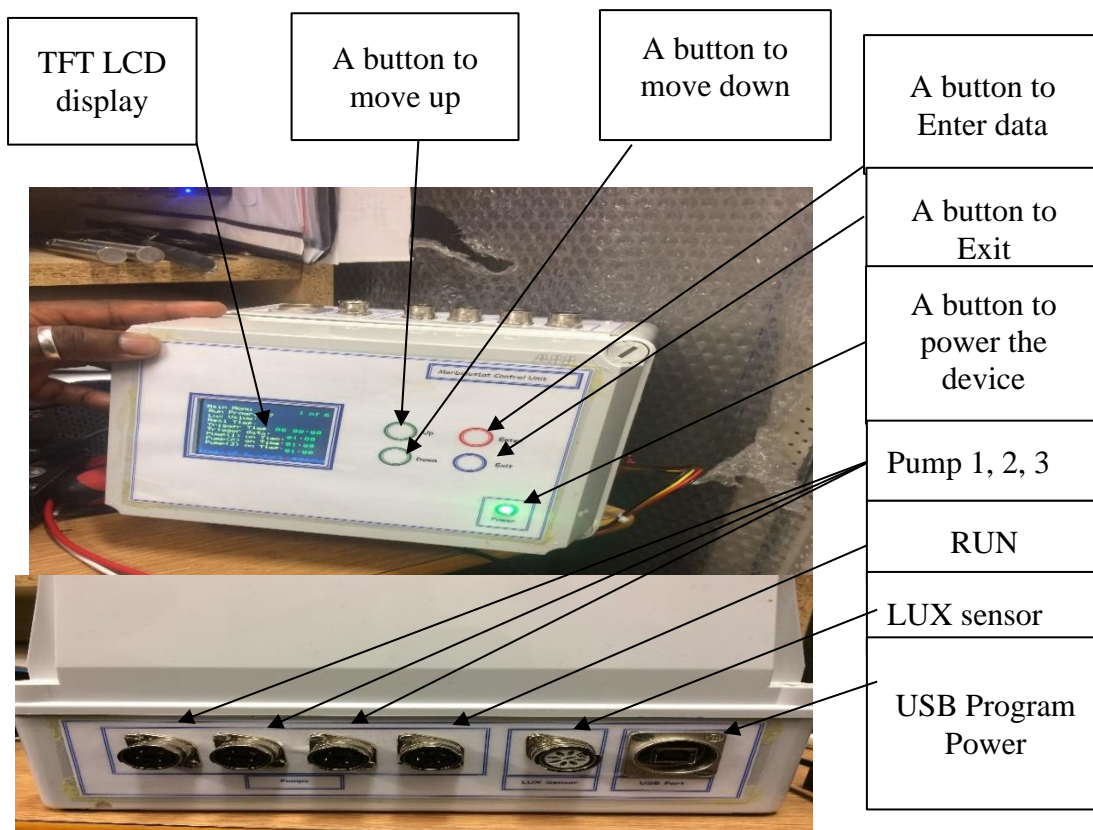
Fig. 6-5 Bioreactor operating system.
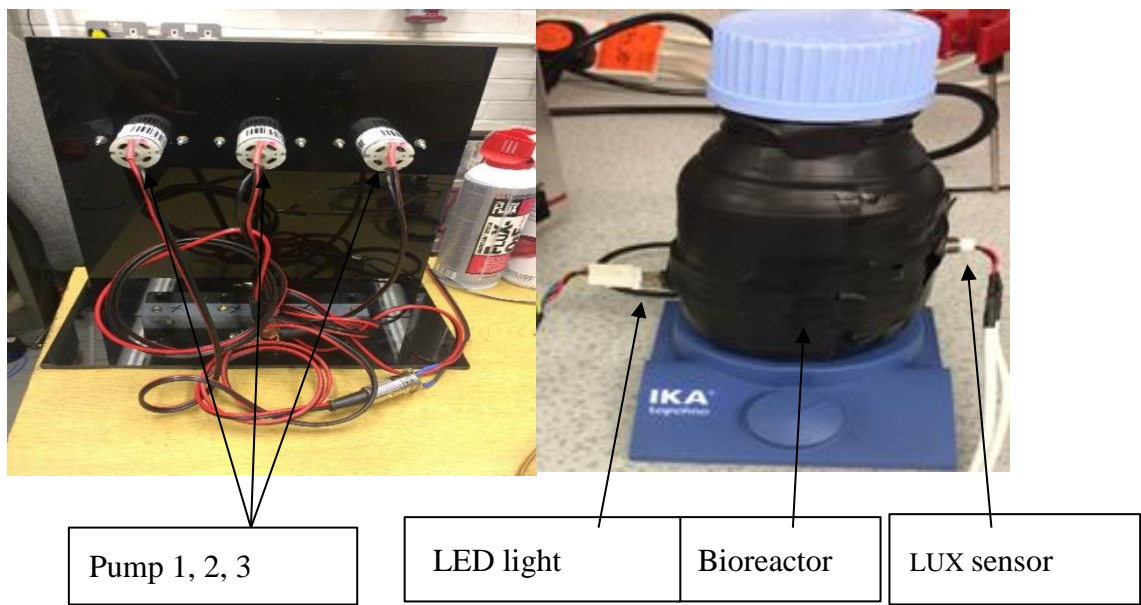
Fig. 6-6 Pumps and bioreactor used in an automated fluidic device assembling.

Fig. 6-7 Complete bioreactor unit

6.7 Conclusions

The aim of this chapter was to design and build an automated continuous cultivation device to help increase the rate of generating adaptively evolved bacterial consortia and strains. The design was undertaken through two different stages. The first stage depends on using CoolTerm software, a computer, bioreactor, LED, and LUX sensor to measure light transmittance as a proxy for bacterial growth, and track increased growth rate whilst using a novel substrate, for example, DEMP. The results of various preliminary tests of the first version of the device confirmed that bioreactor has good monitoring efficiency and measuring accuracy for bacterial growth compared spectrophotometric measurements. The first version was developed into an automated fluidic continuous system, by using extra electronic boards and pumps, an operating system and software which were determined to be appropriate for use with the device.

6.8 Reference

[1] Toprak E, Veres A, Michel JB, Chait R, Hartl DL, Kishony R. Evolutionary paths to antibiotic resistance under dynamically sustained drug selection. *Nat Genet*. 2011; 44(1):101-105. Published 2011 Dec 18. doi:10.1038/ng.1034.

[2] https://www.hotmcu.com/arduino-nano-v30-atmega328p-p-11.html. Last updated 04 June 2020. Last access 04 June 2020.

[3] http://www.ebay.co.uk/itm/DIY-White-Blue-84-48-Nokia-5110-LCD-Display-Screen-Module-Module-for-Arduino-/292041394228?var=&hash=item43ff060834:m:mSydK6nptVgrLDUbJnWRSig). Last access 04 June 2020.

[4] https://www.ebay.co.uk/itm/BH1750FVI-Digital-Light-intensity-Sensor-Module-For-AVR-Arduino-3V-5V-power-AM/253060676349?epid=1789180001&hash=item3aeb977afd:g:aYQAAOSwg55ZdWSG). Last access 04 June 2020.

[5] https://www.ebay.co.uk/p/520014642?iid=172592832354. Last access 04 June 2020.

[6] https://www.amazon.co.uk/Diode-Assorted-Emitting-Diodes-Yellow/dp/B00UWBJM0Q. Last access 04 June 2020.

[7] Toprak, E., Veres, A., Yildiz, S., Pedraza, M. J, Chait, R., Paulsson, J. & Kishony, R. (2013) 'Building a Morbidostat: An automated continuous-culture device for studying bacterial drug resistance under dynamically sustained drug inhibition', Nature Protocols. Nature Publishing Group, 8(3), pp. 555–567.

[8] https://www.amazon.co.uk/Yosoo-Peristaltic-Chemical-19-100ml-Analytical/dp/B017NFFLMG?ref_=fsclp_pl_dp_1. Last access 04 June 2020.

[9] https://www.amazon.co.uk/Uniclife-Aquarium-Airline-Connectors-40-Piece/dp/B07Q9Q9C8Y/ref=asc_df_B07Q9Q9C8Y/?tag=googshopuk-21&linkCode=df0&hvadid=255524372546&hvpos=1o1&hvnetw=g&hvrand=14042489565370453820&hvpone=&hvptwo=&hvqmt=&hvdev=c&hvdvcmdl=&hvlocint=&hvlocphy=1007064&hvtargid=pla-715796864798&psc=1. Last access 04 June 2020.

[10] https://www.espressif.com/en/products/hardware/development-boards. Last access 04 June 2020.

[11] https://siratek.net/index.php/product/rtc-real-time-clock-module-ds3231. Last access 04 June 2020.

[12] https://uk.farnell.com/microchip/mcp23017-e-sp/ic-io-expander-16bit-i2c-28dip/dp/1332088?st=MCP23017. Last access 04 June 2020.

[13] https://www.amazon.co.uk/DaoRier-1-25V-35V-Automatic-Converter-Adjustable/dp/B06VWN1WS9. Last access 04 June 2020.

[14] https://www.amazon.co.uk/Meter-Clear-Aquarium-Hose-Pipe/dp/B00KBM5YLM. Last access 04 June 2020.

[15] https://www.vieep.com/index.php/ac-110v-220v-240v-to-12v-1a-dc-power-supply-transformer-adapter.html. Last access 04 June 2020.

[16] https://uk.farnell.com/mega/3204935/pcb-fr4-233-4x160-ss/dp/3204935?ost=3204935&ICID=redirect-Y&CMP=os-geobanner-google&ddkey=https%3ASearch. Last access 04 June 2020.

[17] https://www.amazon.co.uk/Headers-Breakaway-Connector-Arduino-Prototype/dp/B07CC4V9ZY/ref=pd_day0_hl_263_5?_encoding=UTF8&pd_rd_i=B07CC4V9ZY&pd_rd_r=f010ac35-c7e6-11e8-a31f-795951fa6819&pd_rd_w=TXqxj&pd_rd_wg=mWvSP&pf_rd_i=desktop-dp-sims&pf_rd_m=A3P5ROKL5A1OLE&pf_rd_p=f6359d5f-11a6-4577-a43b-58b9bb222f57&pf_rd_r=NWXKEGMQ9MHE27CR1ZXV&pf_rd_s=desktop-dp-sims&pf_rd_t=40701&psc=1&refRID=NWXKEGMQ9MHE27CR1ZXV. Last access 04 June 2020.

[18] https://www.amazon.co.uk/Momentary-Tactile-Button-Switch-6x6x5mm/dp/B089LWMD9V/ref=sr_1_2?dchild=1&keywords=4-pin+mini+micro+momentary+switches&qid=1591277005&s=electronics&sr=1-2. Last access 04 June 2020.

[19] https://www.amazon.co.uk/PIN-CHASSIS-SOCKET-71206-040-PREHKEYTEC/dp/B0118JDBC0/ref=sr_1_11?dchild=1&keywords=4-Pin+DIN+Chassis+Socket&qid=1591277111&s=electronics&sr=1-1. Last access 04 June 2020.

[20] https://cpc.farnell.com/deltron-enclosures/610-0800/8-pin-standard-nickle-din-plug/dp/CN00041?st=8%20Pin%20Nickel%20Standard%20DIN%20Plug. Last access 04 June 2020.

[21] https://www.reichelt.com/gb/en/8-pin-din-chassis-socket-screw-coupling-270-dio-80sn-ems-p46282.html?PROVID=2788&gclid=EAIaIQobChMIy9vI5oul5wIVyLTtCh0WKwEREAQYASABEgItN_D_BwE&&r=1. Last access 04 June 2020.

[22] https://cpc.farnell.com/molex/22-29-2061/header-vertical-sq-pin-0-1-6way/dp/CN18466?st=0.**1%**20inch%20molex%20connector%20-%206%20way. Last access 04 June 2020.

[23] https://cpc.farnell.com/molex/22-29-2041/header-vertical-sq-pin-0-1-4way/dp/CN18464?ost=Header%2C+Vertical%2C+Square+Pin%2C+0.1%22%2C+4+Way&ddkey=https%3Aen-CPC%2FCPC_United_Kingdom%2Fsearch. Last access 04 June 2020.

[24] https://cpc.farnell.com/amphenol/t821110a1s100ceu/header-vertical-2-54mm-10way/dp/CN16426. Last access 04 June 2020.

[25] https://cpc.farnell.com/multicomp/mc-254-08-00-st-dip/connector-header-8pos-2row-2-54mm/dp/CN21916?st=Header,%20Vertical,%202.54mm,%208%20Way%20-%20%20T821110A1S100CEU. Last access 04 June 2020.

[26] https://www.reichelt.com/gb/en/neutrik-usb-built-in-through-connector-black-neutrik-nausb-wb-p63206.html?PROVID=2788&gclid=EAIaIQobChMIxN7jvY6l5wIVRojVCh10zAfvEAQYCCABEgICWvD_BwE&&r=1. Last access 04 June 2020.

[27] https://uk.farnell.com/on-semiconductor/tip122g/darlington-transistor-to-220/dp/9557881?st=DARLINGTON%20TRANSISTOR,%20TO-220%20-%20%20TIP122. Last access 04 June 2020.

[28] https://uk.farnell.com/phoenix-contact/1757019/terminal-block-pluggable-2pos/dp/3705353. Last access 04 June 2020.

[29])(https://uk.farnell.com/phoenix-contact/mstba-2-5-2-g-5-08-lr/terminal-block-header-2pos-th/dp/2315182. Last access 04 June 2020.

[30] https://cpc.farnell.com/amphenol/t812108a101ceu/socket-idc-s-relief-2-54mm-8way/dp/CN16373?ost=221-5246&ddkey=https%3Aen-CPC%2FCPC_United_Kingdom%2Fsearch. Last access 04 June 2020.

[31] https://cpc.farnell.com/unbranded/mcf-0-25w-1k/resistor-0-25w-5-1k-pk-100/dp/RE03803?st=resistors%201k. Last access 04 June 2020.

[32] https://cpc.farnell.com/panasonic/eca1cm221/capacitor-220uf-16v/dp/CA07278?st=capacitor%20200nF%20electrolytic. Last access 04 June 2020.

Chapter VII

Concluding remarks and future research work

Chapter Seven provides insights to the full conclusions of this work and will suggest the most important future directions for research work.

7.1 Overview

This thesis is a collection of experiments undertaken to demonstrate a feasible bioremediation strategy for OP compounds. Due to the toxic nature of OPs, an exemplar compound DEMP was chosen.

Initial chemical degradation experiments in Chapter 3 showed that although DEMP was susceptible to hydrolysis and thereby degradation, the rates were slow, especially in relevant environmental conditions. This justified a bio-related approach for sustainable remediation.

In Chapter 4, environmental soil samples were selected which had been exposed to OP use as fertilisers for several decades. An enrichment was undertaken to create a microbial consortium able to use DEMP as both a carbon and phosphorus substrate. Once growth rates and DEMP degradation rates (through DEMP and ethanol measurements and FTIR characterisations) were identified, a strategy was developed to improve these. Firstly, adaptive laboratory evolution was performed over several time periods on the total consortia (Hottes et al., 2013). Following this, strains were isolated, identified and characterised individually, and in synthetic consortia. Improved rates of DEMP bioremediation were observed.

In Chapter 5, random mutagenesis, using a combined chemical and physical approach, together with a full tested selection approach, further improved DEMP degradation rates. The resulting *B. cereus* strain was tested for DEMP degradation in soils as well as media. Unexpectedly, this strain was also tested with different OP compounds, TBP and TEPO, and degradation was again observed, demonstrating the versatility of our strain

In Chapter 6, the aim was to design a method to improve DEMP degradation using a continuous ALE approach. Although a bioreactor was constructed for this purpose in two stages, only the first stage was tested fully. The actual experiment to improve the strain characteristics was not undertaken due to time constraints.

7.2 Future work

Challenges remain for in situ bioremediation, most notably, reduced efficiency when applying bacteria to the environment due to competition from native microbes. Although testing the stability long term in the environment was beyond the scope of this thesis, soil studies did indicate reduced degradation rates. An enrichment, adaptation and engineering strategy for bacterial consortia that work together to reduce DEMP in situ would be required to achieve this. The foundations for this work are provided in this thesis. The three mutant strains identified to harbour DEMP degradation capability could be further characterised using full genome sequencing and compared to WT strains. This would help identify which attributes in the cells' genome had contributed to increased degradation and therefore direct future genome engineering methodologies. With time permitting, the automated, continuous ALE device could also be used to create much more effective bioremediation-able strains and consortia, and should be a focus of future work.

7.3 References

Hottes, A. K., Freddolino, P. L., Khare, A., Donnell, Z. N., Liu, J. C., Tavazoie, S.(2013). Bacterial Adaptation through Loss of Function. PLOS Genetics | www.plosgenetics.org PLoS Genet. 9(7):1:13.

Appendix (1)

Standard curve of DEMP, Ethanol, TBP, and TEPO

Fig. 1 shows the standard curves of DEMP, Ethanol, TBP, and TEPO after injection the serial concentrations in GC-FID. The chromatography analysis demonstrated that the retention time of DEMP, Ethanol, TBP, and TEPO peak were 5.2, 1.6, 8.1 and 10.4 minutes respectively after the injection into GC-FID (Fig. 2).
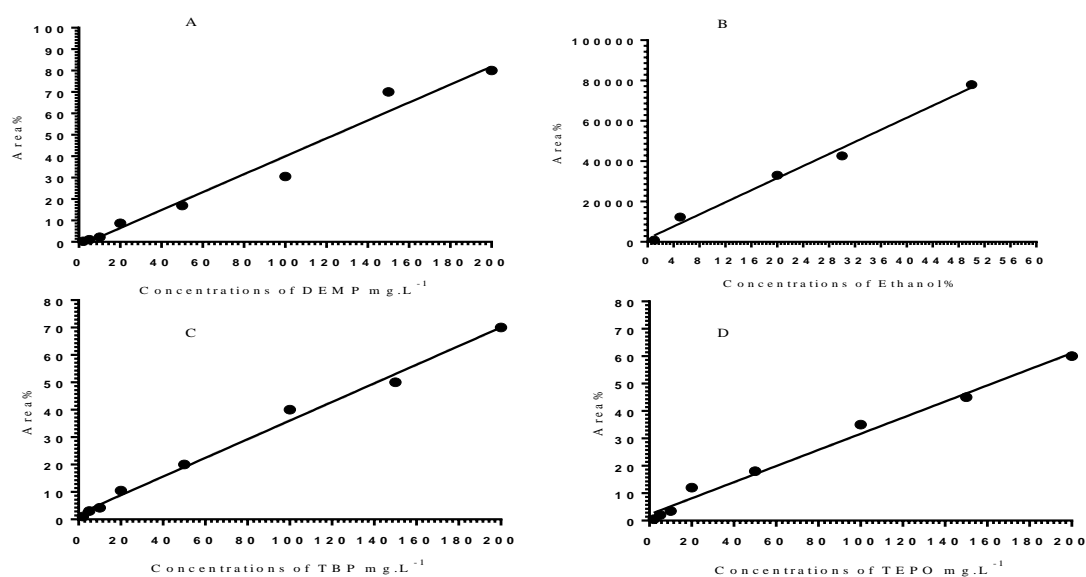
Fig. 1. Standard curves of cheimical compounds used in thesis. A) DEMP, B) Ethanol, C) TBP, D) TEPO.
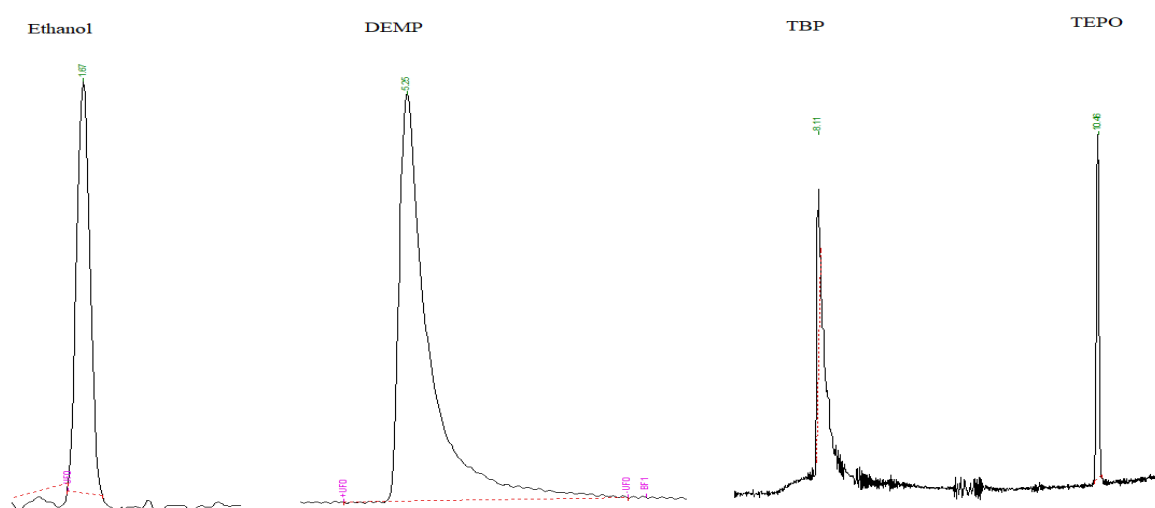
Fig. 2. The chromatography run and the retention time of Ethanol, DEMP, TBP, and TEPO peak.

Appendix (2)

Shows the efficiency of the extraction method used.

Table 1 Fortified recovery% for DEMP in soil (n=3)

Chemical compound	Efficiency %	SD
DEMP	88.3	1.8
TBP	86.6	2.3
TEPO	86.3	2.6

- Each value is the mean of three replications.

Recovery efficiency is a parameter used to calculate the concentrations of chemicals recurved to the known amount used as a percentage. This experiment was carried out to determine the efficiency of the extraction of DEMP, TBP, and TEPO from the bacterial culture MSM and soil.

Appendix (3)

Physiochemical characteristic measurements of Soils

The soil used in this study was collected from Wise Warren at Spen Farm, Tadcaster, England (longitude 1°20'32.9" W, latitude 53°51'40.7" N). Physiochemical characteristic of soil was calculated. The moisture of soil was measured through taking 5 gm of each soil was air-dried for 24 hours in order to measure the moisture content. This experiment was replicated three times. The moisture was calculated by the equation:

$$MC\% = \frac{(wi - wf)}{wf} \times 100.$$

Where: -

MC% is the moisture content; Wi is the initial weight and Wf is the final weight.

While the pH of soils was measured after taking the ratio 1:1 of the air-dried soil to the distilled water (20g). The soil was thoroughly mixed with the distilled water. The magnetic stirrer was used to create a homogeneous solution. After one hour, all the samples were measured by the digital pH meter. This experiment was replicated three times. Also, the elements C, H, N, and Sulfur were measured by applying the NC Analyzer device (Flash 2000 Organic Elemental Analyzer) after the soil is air-dried for 24 hours. Regarding the available Phosphorus, it was extracted and measured via the sodium bicarbonate by using the Colorimetric method (Koralage et al., 2015)*.

Table 2 Physical and chemical characteristics of untreated soil.

Type of Soil	pH	Moisture%	C mg/kg	N mg/kg	H mg/kg	S mg/kg	P available mg/ kg
Agriculture field	6.1	10	3.36	0.33	2.11	0	1.0

*Koralage, I.S.A., Weerasinghe, P. & Silva, N.R.N., 2015. The Determination of Available Phosphorus in Soil : A Quick and Simple Method. , 8, pp.1–17.

Appendix (4)

Preparation of Buffered Solutions

The pH 6.0 buffered solutions were prepared by mixing 100 ml of 0.1 mol. L^{-1} KH_2PO_4 with 11.2 ml of 0.1 mol. L^{-1} NaOH, while the pH 7.0 was prepared by mixing 100 ml from 0.1 mol. L^{-1} KH_2PO_4 with 58.2 ml of 0.1 mol. L^{-1} NaOH. However, the pH 10.0 was prepared by mixing 100 ml of 0.05 M $NaHCO_3$. $10H_2O$ with 21.4 mls of 0.1 M NaOH and the 0.02 M $CaCl_2$ buffered solutions was prepared to investigate DEMP hydrolysis at 30°C (http://delloyd.50megs.com/moreinfo/buffers2.html).

Appendix (5)

Detection of the gene of DEMP-degrading in *Bacillus cereus* and *Micrococcus luteus*.

The detection of a gene responsible for the degradation of organophosphorus compounds was carried out following the protocol given by Pérez-Pérez and Hanson (2002), which modified the one from Ali et al., (2002). Bacterial colonies were picked by a sterile wooden toothpick then put into a PCR tube containing 10 μl nucleus free water. Bacterial cell disruption was performed by a thermocycler at 99°C, heating for 3 minutes. A 5 μl aliquot was used to prepare a DNA template of PCR amplification. In order for DEMP-degrading genes' detection, three different primers were designed according to the conserve regions previously reported. The primers were *opda*, *opd*, and mpd genes tabulated in Table 3. These primers were supplied by Integrated DNA Technologies (www.idtdna.com). A 50 μl total volume of PCR mixture templet was used for PCR amplification. This mixture consisted of 1 μl of cell suspension, 5 μl of 10 × green reaction buffer, 5μl dNTPs, 1 μl of each F primer and R primer, and 1μl polymers. The program for PCR amplification was run at 95°C for 5 min. The denaturation of the sample was carried out via 30 cycles at 90°C for 0.5 min, followed by annealing at 55°C for 1 min, extension at 72°C for 0.5 min, and a final extension at 72°C for 5 mins.

An amplification of bacterial DNA was carried out to investigate the organophosphorus-gene degrading in two different strains: *B. cereus* and *M. luteus*. Fig. 3 shows the DNA electrophoresis analysis of *B. cereus* using 1% agarose gel. By using Ultraviolet, a band of the mpd gene in *B. cereus* strains only was revealed at the molecular weight 547 bp. This is explains why *B. cereus* strain can use DEMP. In contrast, the *opd* and *opda* are not found in the bacterial strains. However, this is the first study to detect the mpd gene in *B. cereus* after a one-year adaptation with 100 mg L^{-1} DEMP.

Table 3. Primers for the detection of organophosphate degrading genes.

Gene	Primer	Sequence	Amplication size (bp)
OpdA	Opda-F	5' tgttccggtaaccactcaca 3'	412
	Opdaa-R	5' cactctcagagggacgaagg 3'	
Opd	Opd-F	5' agggttgtgctcaagtctgc 3'	327
	Opd-R	5' caataaactgacgtcgcgac 3'	
mpd	Mpd-F	5' agcaggtcgacgagatctac 3'	547
	Mpd-R	5' ttgacgaccgagtagttcac 3'	

*Ali, M., Naqvi, T.A., K, Kanwal, M., Rasheed, F., Hameed, A., Ahmed, S. (2012). Detection of the organophosphate degrading gene opdA in the newly isolated bacterial strain Bacillus pumilus W1.Ann Microbiol: 62:233–239.

* Pérez-Pérez FJ, Hanson ND (2002) Detection of plasmid-mediated AmpC beta-lactamase genes in clinical isolates by using multiplex PCR. J Clin Microbiol 40:2153–2162.
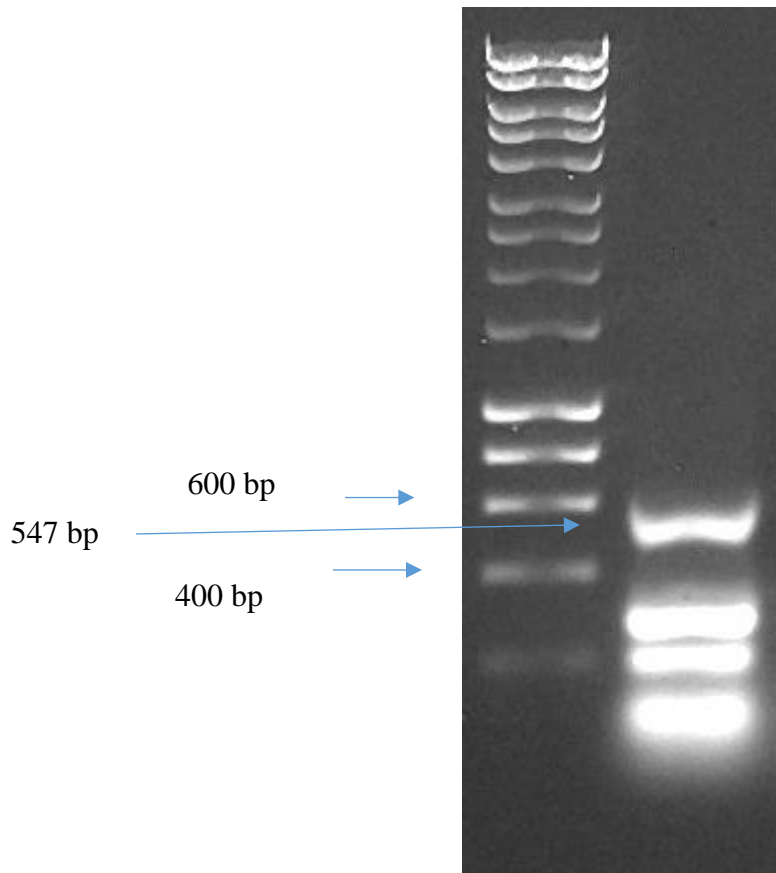
Fig. 3 Electrophoretic analysis of gene-degrading DEMP for *B. cereus* using 1% agarose.

Appendix (6)

Colterm software

CoolTerm is a simple serial port terminal application. It can be used to communicate and exchange data with hardware connected to serial ports, such as servo controllers, robotic kits, Global Positioning System (GPS) receivers, and microcontrollers. This software has many features including:

1. Capability of multiple concurrent connections if multiple serial ports are available
2. Display of received data in plain text or hexadecimal format
3. Sending data via keypresses as well as a "Send String" dialog that supports data entry in plain text or hexadecimal format
4. Sending data via copy-paste of text into the terminal window
5. Sending of text files
6. Capability to capture received data to text files
7. Local echo of transmitted data
8. Local echo of received data (loop back to sender)
9. Software flow control
10. Capability to manually toggle line states of certain handshaking signals when hardware flow control is disabled,
11. Ability to save and retrieve connection options.

Data of bacterial growth has been documented as a text document (.txt) file. This software can be installed under Windows 7 or even 10 versions via this URL http://freeware.the-meiers.org. It is produced by Roger Meier Company 2007-2017.

How CoolTerm works?

Once installed, run the software by clicking on the connection. Then, the text file to create a file will contain the bioreactor data. Finally, click connect to allow your computer to access the documented data. The file can be grabbed after opening Microsoft Excel and importing it through data, then from text, select a file. A new window will appear and be ready to use.

Appendix (7)

Shows Gram stain of *Bacillus cereus* and *Micrococcus luteus.*

Gram stain

A colony was isolated from R2A agar treated with 100 mg L^{-1} DEMP. Placed and resuspended separately in approximately 20 µL of sterile distilled water by sterilised lop on a glass slide by the needle with a rotary movement. The bacteria were fixed by the heat on the slide. The slide was placed on the staining rack and the smear was covered with a crystal violate for 1 min; the slide was then washed gently with tap water. The smear was covered by Iodine for 1 min, and then washed with tap water by tilting the slide and pouring water on the smear. The smear was then decolorized with ethanol for about 10-15 seconds or until the amounts of purple colour could no longer be washed out; they were then immediately washed with tap water. The smear is covered with safranine for 30 seconds, and then it was washed with water and dried. After that, the samples were examined via oil immersion; the objective was to determine gram differentiation (Cappuccino and Sherman, 2014)*. On the other hand, Microscope set up was performed through the light microscope (Olympus, Japan) that works by a magnifying power of100X/1.30 oil Iris. It is connected to Camera ProgRes C5 pro 2.6 (JENOPTIK laser, optical, systems GmbH). After cell staining, the microorganisms were imaged. The camera image resolution capture was 2580×1944 and lives 644×490 VGA. There is also an option called Crop. It could be used to take the image for microbes after selecting the microbes closely.

*Cappuccino, J. and Sherman, N. (2014). Microbiology A laboratory Manual. Pearson IN. 10th Eddition.565p.

Appendix (8)

Shows the efficiency of pumps used.

Table 4. shows the efficiency of the pumps used. Two different voltages (10 and 12) voltage were tested to transfer three various volumes of liquid solutions (10, 20, and 30) milliliters using a power supply.

Table 4. The efficacy of pumps used.

Pump 1						
Voltage	Volume	R1	R2	R3	Average	SD
12 V	10 ml	11.61	11.58	11.69	11.62667	0.046428
12 V	20 ml	22.07	22.71	22.98	22.58667	0.381605
12 V	30 ml	32.91	32.68	32.51	32.7	0.163911
10 V	10 ml	14.03	14.61	14.2	14.28	0.243447
10 V	20 ml	28.7	28.38	28.15	28.41	0.225536
10 V	30 ml	41.41	40.5	39.9	40.60333	0.62077
Pump 2						
Voltage	Volume	R1	R2	R3	Average	SD
12 V	10 ml	11.25	11.21	11.42	11.29333	0.091043
12 V	20 ml	21.01	20.46	21.28	20.91667	0.341207
12 V	30 ml	31.9	31.64	31.08	31.54	0.34215
10 V	10 ml	14.31	13.95	14.1	14.12	0.147648
10 V	20 ml	26.48	26.14	26.37	26.33	0.141657
10 V	30 ml	40.36	39.81	38.81	39.66	0.641613
Pump 3						
Voltage	Volume	R1	R2	R3	Average	SD
12 V	10 ml	11.58	11.77	11.61	11.65333	0.0834
12 V	20 ml	22.41	23.01	22.95	22.79	0.269815
12 V	30 ml	33.71	32.68	33.84	33.41	0.518909
10 V	10 ml	14.46	14.98	14.37	14.60333	0.268866
10 V	20 ml	27.88	27.81	27.97	27.88667	0.06549
10 V	30 ml	40.57	40	40.25	40.27333	0.233286

Appendix (9)

Software program which used in 'Morbidostat'

- Software library TFT_eSPI.h this library can be found in the sketch / add library in arduino

- When using the TFT_eSPI.h you must edit the User_Setup file.h file which is within the library folder. you must enable these lines to make it work with the esp32 then save the file

- #define TFT_MISO 19

- #define TFT_MOSI 23

- #define TFT_SCLK 18

- #define TFT_CS   15 // Chip select control pin

- #define TFT_DC   2 // Data Command control pin

- #define TFT_RST   4 // Reset pin (could connect to RST pin)

- //#define TFT_RST -1 // Set TFT_RST to -1 if display RESET is connected to ESP32 board RST

- //#define TFT_BL   32 // LED back-light (only for ST7789 with backlight control pin).

Appendix (10)

Table 5 illustrated the different components that used in the construction of an automated fluidic system continuously. This table shows the name of the components, their package prices, and the size of the package, the name of the supplier, the website, and the description of these items.

Item	name	pack price	pack size	quant	supplier	url	long description
microcontroller	ESP32 Development Board	£6	1	1	Amazon	https://www.amazon.co.uk/Wildlead-Development-Bluetooth-Antenna-Ultra-Low/dp/B079G6VFLT/ref=sr_1_1?ie=UTF8&qid=1538659779&sr=8-1&keywords=ESP-32S+ESP32+Development+Board	ESP-32 Development Board WiFi+Bluetooth 2-In-1 Dual Core 2.4 GHz Antenna Module Ultra-Low Power ESP32 ESP-32S
screen	2.8" 240x320 SPI TFT LCD	£5.03	1	1	Amazon	https://www.amazon.co.uk/Display-240x320-ILI9341-Compatible-Interface/dp/B07QFLFGFW/ref=sr_1_fkmr1_1?keywords=240X320+Resolution+2.8%22+SPI+TFT+LCD+Display+Touch+Panel+ILI9341+With+PCB+5V%2F3.3V+STM32&qid=1567076980&s=gateway&sr=8-1-fkmr1	Display Module Kit, 2.8" 240x320 SPI TFT LCD Shield Touch Panel With PCB ILI9341 5V/3.3V Compatible with 5110 Interface. 5V Compatible
real time clock	DS3231 AT24C32 IIC Precision RTC	£1.99	1	1	Amazon	https://www.amazon.co.uk/Fornateu-Arduino-DS3231-AT24C32-Precision/dp/B07VGL4PPX/ref=sr_1_7?keywords=DS3231+AT24C32+IIC+Precision+RTC&qid=1567076728&s=gateway&sr=8-7	Fornateu For Arduino DS3231 ZS042 AT24C32 IIC Module Precision RTC Real Time Clock Memory New
light sensor	Bh1750fvi Light Intensity Sensor	£1.85	1	1	Amazon	https://www.amazon.co.uk/SODIAL-BH1750FVI-Digital-intensity-Arduino/dp/B07BWB6DBL/ref=sr_1_4?keywor	SODIAL BH1750FVI Digital Light intensity Sensor Module For AVR Arduino 3V-5V power

						ds=BH1750FVI&qid=1567076411&s=gateway&sr=8-4	
MCP23017-E/SP		£1	1	1	Farnell	https://uk.farnell.com/microchip/mcp23017-e-sp/ic-io-expander-16bit-i2c-28dip/dp/1332088?st=MCP23017	MCP23017-E/SP - I/O Expander, 16bit, 1.7 MHz, I2C, Serial, 1.8 V, 5.5 V, DIP
pump	12V DC Pump Dosing Peristaltic	£6.50	1		Amazon	https://www.amazon.co.uk/Water-pumps-Peristaltic-Aquarium-Analytical/dp/B01MTJ2N23/ref=sr_1_4?ie=UTF8&qid=1530018709&sr=8-4&keywords=peristaltic+pump	12V DC Dosing Pump Peristaltic Dosing Head For Lab Analytical
pump	6V DC Peristaltic Dosing Pump	£9.77	1		Amazon	https://www.amazon.co.uk/zjchao-Dosing-Peristaltic-Aquarium-Analytical/dp/B00N3KZVHG/ref=sr_1_2_sspa?keywords=6V+DC+Peristaltic+Dosing+Pump&qid=1567076155&s=gateway&sr=8-2-spons&psc=1&spLa=ZW5jcnlwdGVkUXVhbGlmaWVyPUEyWUsyTUFMR0RJQ1c0JmVuY3J5cHRlZElkPUEwNDI5NzM5Uk1GTE9USU82N05ZJmVuY3J5cHRlZEFkSWQ9QTEwNDM5OTEyNDY3V0Y0QkM0UjImd2lkZ2V0TmFtZT1zcF9hdGYmYWN0aW9uPWNsaWNrUmVkaXJlY3QmZG9Ob3RMb2dDbGljaz10cnVl	6V DC DIY Peristaltic Pump Dosing Head Automatic Doser Pump Connector
air valve connectors	Air Valve Connector	£4.59	40		Amazon	https://www.amazon.co.uk/Uniclife-40-Piece-Aquarium-Connector-Straight/dp/B07796RL3S/ref=all_spx_3?_encod	40-Piece Aquarium Air Valve Connector White Plastic Inline Tubing, 3-Way T & Straight

						ing=UTF8&pd_rd_i=B07796RL3S&pd_rd_r=e91bb677-c7dc-11e8-9aa7-031f4d2ad831&pd_rd_w=cNVFj&pd_rd_wg=ZlihA&pf_rd_i=desktop-dp-sims&pf_rd_m=A3P5ROKL5A1OLE&pf_rd_p=83f4248b-0733-4500-a557-e145ce3214a1&pf_rd_r=DX3EQ5GEDAVGHKGDP3G8&pf_rd_s=desktop-dp-sims&pf_rd_t=40701&psc=1&refRID=DX3EQ5GEDAVGHKGDP3G8	
airline	5 metres airline	£2.69	1		Amazon	https://www.amazon.co.uk/dp/B003ZII5TC/ref=twister_B06X9Q5HYG?_encoding=UTF8&th=1	5 METRES OF 6MM OUTER AND 4MM INNER CLEAR AIR LINE
PCB	PCB 1.6mm, 100mm x 220mm	£12.36	1		Farnell	https://uk.farnell.com/mega/3204923/pcb-fr4-220x100-ss/dp/3204923?st=Photoresist,%20Epoxy%20Glass%20Composite,%201.6mm,%20100mm%20x%20220mm	Prototyping Board, FR4, Epoxy Glass Composite, 1.6mm, 100mm x 220mm
pin headers	2.54mm Pin Headers	£7.99	40		Amazon	https://www.amazon.co.uk/Headers-Breakaway-Connector-Arduino-Prototype/dp/B07CC4V9ZY/ref=pd_day0_hl_263_5?_encoding=UTF8&pd_rd_i=B07CC4V9ZY&pd_rd_r=f010ac35-c7e6-11e8-a31f-795951fa6819&pd_rd_w=TXqxj&pd_rd_wg=mWvSP&pf_rd_i=desktop-dp-sims&pf_rd_m=A3P5ROKL5A1OLE&pf_rd_p	40 Piece 2.54mm Pin Headers 40 Pin Breakaway PCB Board Single Row Male and Female Pin Header Connector Kit for Arduino Prototype Shield (20pcs male header, 20pcs female header)

					=f6359d5f-11a6-4577-a43b-58b9bb222f57&pf_rd_r=NWXKEGMQ9MHE27CR1ZXV&pf_rd_s=desktop-dp-sims&pf_rd_t=40701&psc=1&refRID=NWXKEGMQ9MHE27CR1ZXV	
switch	4-Pin Mini Micro Momentary switcher	£1.81	20		Amazon	https://www.amazon.co.uk/Demarkt-Momentary-Tactile-Arduino-Breadboards/dp/B071RBCRVH/ref=pd_sbs_147_5?_encoding=UTF8&pd_rd_i=B071RBCRVH&pd_rd_r=42b8bacb-c7e9-11e8-81cf-4387fc18cc21&pd_rd_w=QcsBW&pd_rd_wg=BX95C&pf_rd_i=desktop-dp-sims&pf_rd_m=A3P5ROKL5A1OLE&pf_rd_p=85d62760-2a0e-407d-aa36-f3c03afc01c3&pf_rd_r=5ZC94YGM8Q1RQPK5FTX4&pf_rd_s=desktop-dp-sims&pf_rd_t=40701&psc=1&refRID=5ZC94YGM8Q1RQPK5FTX4	20 Pcs Demarkt 4-Pin Mini Micro Momentary Tactile Push Button Switch for Arduino / Breadboards (6*6*5mm)
4 pin DIN socket	4 Pin DIN Chassis Socket	£1.81	1		Farnell	https://cpc.farnell.com/prehkeytec/71206-040/4-pin-din-chassis-socket/dp/CN00761?mckv=sQ3W3F6wQ_dc|pcrid|224645161149|kword||match||plid||slid||product|CN00761|pgrid|45968746254|ptaid|pla-524516827571|&CMP=KNC-GUK-CPC-SHOPPING&gclid=EAIaIQobChMIj73dk9en5	4 Pin DIN Chassis Socket - 71206-040

						AIV2eF3Ch2-wgQfEAQYBSABEgKRvPD_BwE	
4 pin DIN plug	4 Pin Nickel Standard DIN Plug - 610-0400	£1.75	1		Farnell	https://cpc.farnell.com/deltron-enclosures/610-0400/4-pin-nickel-standard-din-plug/dp/CN00035?MER=sy-me-pd-mi-alte	4 pin DIN plug
8 pin DIN plug	8 Pin Standard Nickel DIN Plug - 610-0800	£2.40	1		Amazon	https://cpc.farnell.com/deltron-enclosures/610-0800/8-pin-standard-nickle-din-plug/dp/CN00041?st=8%20Pin%20Nickel%20Standard%20DIN%20Plug	8 pin DIN plug
8 pin DIN socket	8 Pin Chassis Socket - 71206-080	£2.37	1		Farnell	https://cpc.farnell.com/prehkeytec/71206-080/8-pin-chassis-socket/dp/CN00765?CMP=CPC-ebooks-BIGBOOK2019	8 pin DIN socket
white - molex - 6 way	Header, Vertical, Square Pin, 0.1", 6 Way - 22-29-2061	£4.00	5		Farnell	https://cpc.farnell.com/molex/22-29-2061/header-vertical-sq-pin-0-1-6way/dp/CN18466?st=0.1%20inch%20molex%20connector%20-%206%20way	white - molex - 6 way
white - molex - 4 way	Header, Vertical, Square Pin, 0.1", 4 Way - 22-29-2041	£2.50	5		Farnell	https://cpc.farnell.com/molex/22-29-2041/header-vertical-sq-pin-0-1-4way/dp/CN18464?ost=Header%2C+Vertical%2C+Square+Pin%2C+0.1%22%2C+4+Way&ddkey=https%3Aen-CPC%2FCPC_United_Kingdom%2Fsearch	white - molex - 4 way

USB socket	XLR USB 2.0 A to B	£3.05	1		Farnell	https://cpc.farnell.com/cliff-electronic-components/cp30110/gender-changer-xlr-shell-usb-a/dp/CN19601?st=xlr%20usb%20connector	USB 2.0 A to B Horizontal Feedthrough Panel Mount Connector,
transistor	Single Transistor, Darlington, NPN, 100 V, 65 W, 5 A, 1000 hFE	£0.61	1		Farnell	https://uk.farnell.com/on-semiconductor/tip122g/darlington-transistor-to-220/dp/9557881?st=DARLINGTON%20TRANSISTOR,%20TO-220%20-%20%20TIP122	transistor
green terminal	Pluggable Terminal Block, 5.08 mm, 2 Ways	£1.47	1		Farnell	https://uk.farnell.com/phoenix-contact/1757019/terminal-block-pluggable-2pos/dp/3705353?st=5.08mm%20Pitch%202%20Pin%20Screw%20Pluggable	Pluggable Terminal Block, 5.08 mm, 2 Ways, 24AWG to 12AWG, 2.5 mm², Screw, 12 A
green terminal	Terminal Block, Header, 5.08 mm, 2 Ways	£4.64	10		Farnell	https://uk.farnell.com/phoenix-contact/1755736/header-vertical-5-08mm-2way/dp/3705262?MER=bn_level5_5NP_EngagementRecSingleItem_3	Terminal Block, Header, 5.08 mm, 2 Ways, 12 A, 250 V, Through Hole Vertical
black - IDC socket - 8 way	Socket, IDC, Strain Relief, 2.54mm, 8 Way - T812108A101 CEU	£0.22	1		Farnell	https://cpc.farnell.com/amphenol/t812108a101ceu/socket-idc-s-relief-2-54mm-8way/dp/CN16373?ost=221-5246&ddkey=https%3Aen-CPC%2FCPC_United_Kingdom%2Fsearch	black - IDC socket - 8 way
black - IDC header - 10 way	Header, Vertical, 2.54mm, 10 Way - T821110A1S 100CEU	£0.46	1		Farnell	https://cpc.farnell.com/amphenol/t821110a1s100ceu/header-vertical-2-54mm-10way/dp/CN16426?MER=sy-me-pd-mi-alte	black - IDC header - 10 way

black - IDC header - 8 way	Header, Vertical, 2.54mm, 8 Way - T821108A1S 100CEU	£0.44	1		Farnell	https://cpc.farnell.com/amphenol/t821108a1s100ceu/header-vertical-2-54mm-8way/dp/CN16425?st=Header,%20Vertical,%202.54mm,%208%20Way	black - IDC header - 8 way
black - IDC socket - 10 way	Socket, IDC, Strain Relief, 2.54mm, 10 Way - T812110A101CEU	£0.24	1		Farnell	https://cpc.farnell.com/amphenol/t812110a101ceu/socket-idc-s-relief-2-54mm-10way/dp/CN16374?MER=sy-me-pd-mi-alte	black - IDC socket - 10 way
LED - CO-RODE pack	LED Diode Kit, 3mm LED 5mm LED, pack of 300	£20.12	300		Amazon	https://www.amazon.co.uk/Diode-Assorted-Emitting-Diodes-Yellow/dp/B00UWBJM0Q/ref=sr_1_1?keywords=CO-RODE+LED+300&qid=1567073241&s=gateway&sr=8-1	LED Diode Kit, 3mm LED 5mm LED Assorted Clear Light Emitting Diodes LEDs with White Red Blue Green Yellow Pack of 300
resistor 1k	Resistor, 0.25W 5% 1K, 100 Pack - MCF 0.25W 1K	£0.55	100		Farnell	https://cpc.farnell.com/unbranded/mcf-0-25w-1k/resistor-0-25w-5-1k-pk-100/dp/RE03803?st=resistors%201k	resistor 1k
resistor 470R	Resistor, 0.25W 5% 470R, 100 Pack - MCF 0.25W 470R	£0.55	100		Farnell	https://cpc.farnell.com/unbranded/mcf-0-25w-470r/resistor-0-25w-5-470r-pk-100/dp/RE03799?st=resistors%20470%20ohms	resistor 470R
capacitor 100nF	Capacitor, 100nF 50V - MCRR25104X7RK0050	£0.40	5		Farnell	https://cpc.farnell.com/unbranded/mcrr25104x7rk0050/capacitor-100nf-50v/dp/CA05514?st=capacitor%20100nF	capacitor 100nF

| capacitor 220uF electrolytic 16V | Electrolytic Capacitor, 220 µF, 16 V | £0.55 | 5 | | Farnell | https://cpc.farnell.com/panasonic/eca1cm221/capacitor-220uf-16v/dp/CA07278?st=capacitor%20200nF%20electrolytic | Electrolytic Capacitor, 220 µF, 16 V, M Series, ± 20%, Radial Leaded, 6.3 mm - ECA1CM221 |